

**CHARACTERIZATION OF A NOVEL COMPONENT OF WNT
SIGNALING PATHWAY USING ZEBRAFISH AS
A MODEL ORGANISM**

A Dissertation
Submitted to
the Temple University Graduate Board

In Partial Fulfillment
of the Requirements for the Degree
DOCTOR OF PHILOSOPHY
Department of Biological Sciences

By Noopur Mandrekar
July 2016

Examining Committee Members:

Dr. Raymond Habas, Advisory Chair, Biology
Dr. Allen Nicholson, Examining Chair, Biology
Dr. Darius Balciunas, Biology
Dr. Alana O'Reilly, External Member, Medical Genetics and Molecular Biochemistry

COPYRIGHT

CHARACTERIZATION OF A NOVEL COMPONENT OF WNT SIGNALING PATHWAY

USING ZEBRAFISH AS A MODEL ORGANISM

By

Noopur Mandrekar

2016

®All rights reserved

Abstract

Wnt signaling plays important role in many aspects of embryogenesis such as cell proliferation, cell fate specification, cell polarity and organogenesis (Clevers 2006, van Amerongen and Nusse 2009). Wnt ligands have been shown to activate several intra-cellular signaling cascades, including the canonical or Wnt/ β -catenin dependent pathway and the non-canonical or β -catenin independent pathway. Dishevelled (Dvl) occupies a key position at crossroads of all branches of Wnt signaling cascade. To understand, how Dishevelled (Dvl) may channel signaling into the downstream branches, we sought to identify novel effectors for Dishevelled (Dvl) using a yeast-two hybrid screen. In this study, we used the PDZ domain of Dishevelled (Dvl) as a bait and from this screen, we identified a new binding protein of Dishevelled (Dvl)-termed as Custos.

To characterize the functional role of Custos in Wnt signaling pathway, we used mammalian cell culture and zebrafish as a model vertebrate organism. We confirmed the interaction between Custos and Dvl using co-immunoprecipitation and GST pull-down. Custos also interacted with β -catenin *in vivo* and this interaction was positively regulated by Wnt stimulation. Immunofluorescence experiments in mammalian cells showed that Custos co-localizes with the nuclear envelope marker, lamin and inhibits translocation of β -catenin to the nucleus. In zebrafish embryos, Custos is a maternal gene and expressed throughout development. Spatial *in situ* hybridization studies showed that Custos was expressed in the dorsal region of the embryo at early stages and in the nervous system in zebrafish at 24hpf. To delineate the biological role of Custos during embryogenesis, we conducted a gain of function

and loss of function studies. Overexpression of exogenous Custos and morpholino knockdown of Custos revealed that Custos is critical for embryonic patterning. Knockout of Custos in zebrafish revealed that Custos delays embryonic development and exhibits defects in pigmentation suggesting a plausible role in neural crest development.

Taken together, our studies demonstrate that Custos is a novel component of canonical Wnt signaling and required for β -catenin translocation into the nucleus and important for embryonic patterning.

Acknowledgements

Graduate school, what a roller coaster ride! It has been an exciting and fascinating journey for me and I am thankful to many people who have guided me and helped me during this time. First of all, I would like to thank my advisor, Dr. Raymond Habas for giving me an opportunity to work under his mentorship. His endless support, patience and guidance have been instrumental in shaping me into an independent and diligent scientist. I am grateful for his advice and will always look up to him for any guidance in future.

I would like to thank all my committee members for their guidance and support along the way. Namely, I would like to thank Dr. Allen Nicholson for his helpful comments and guidance during the course of my research. I would also like to thank Dr. Darius Balciunas for his countless advice and constructive criticism on my thesis. Special thanks to Dr. Alana O'Reilly for agreeing to serve as an external expert on my thesis committee.

I must extend my thanks to all the members of the Habas lab, past and present for their help throughout my time in the lab. Special thanks to Dr. Yuko Komiya for her guidance during the initial years of my P.hD. I would also like to thank my labmates Courtney, Rick, Baihao, Enping, Kaushik, Carlee and Salina for all the fun times we had in and outside the lab.

I would like to thank all the teaching faculty and administrative staff at the Biology department, namely, Dr. Dan Spaeth, Dr. Sheryl Love, Dr. Seema Freer, Toni Matthews, Regee Neely and Brenda Mims for being so helpful.

I want to thank my family and friends for their constant love and support during these years. I am forever grateful to my parents, Sheetal and Suresh Mandrekar. I would also like to thank my uncle, Madhukar Kulkarni who is a big part of my upbringing. Many thanks to my in-laws, Nandini and Arun Padgaonkar for all their love and support. Special thanks to the US Padgaonkar family for being a constant source of stress relief throughout the years and were a great mental vacation from the scientific world. I would like to thank my friends Deepa, Sabyasachi, Priyanka, Priyam and Ninoshka who kept my sanity intact when I was out of the lab. I would like to thank my best-friend and my beloved husband, Amol who has always been an inspiration to me. Without his endless love, patience and encouragement, I wouldn't have achieved this milestone in my life. Finally, I thank God for letting me through all the difficult times and also for all the good times.

TABLE OF CONTENTS

ABSTRACT.....	iii
ACKNOWLEDGMENTS.....	v
LIST OF TABLES.....	x
LIST OF FIGURES.....	xi
CHAPTER	
1. INTRODUCTION.....	1
History of Wnt signaling.....	2
Biology of Wnt signaling.....	2
Wnt signaling cascade	12
Dishevelled.....	21
Dishevelled interacting proteins.....	25
Mesoderm development.....	27
Maternal Wnt pathways	29
Zebrafish as a model organism.....	30
Zebrafish early development	35
CHAPTER	
2. MATERIALS AND METHODS.....	40
CHAPTER	
3. RESULTS.....	55
Custos interacts with Dishevelled.....	56

Dishevelled promotes dephosphorylation of Custos.....	56
Custos- β -catenin interaction increases with Wnt treatment.....	57
Subcellular localization of Myc-Custos.....	65
Custos colocalizes with nuclear envelope marker.....	68
Subcellular localization of truncated constructs of Myc-Custos.....	70
Custos does not colocalize with Dishevelled.....	73
Custos inhibits canonical Wnt signaling.....	75
Temporal and spatial expression of Custos.....	77
Custos is critical for anterior development.....	79
Knockdown of Custos does not have effect on mesodermal induction.....	84
Design and synthesis of CRISPR/Cas9.....	86
Custos gene disruption in F0 embryos.....	86
Heritable Custos gene modification induced by the CRISPR/Cas9 system.....	90
F0 progeny fish homozygous for frameshift mutation.....	92
Knockout of Custos gene.....	94
Endogenous V5 epitope tagging of Custos using CRISPR/Cas9 system.....	96
Characterization of mutants using molecular markers.....	100
Custos morpholino effects on mutants.....	102

CHAPTER

4. DISCUSSION.....	105
The Custos protein.....	106
Custos interacts with Dishevelled.....	106

Dishevelled promotes dephosphorylation of Custos.....	109
Custos strongly binds to β -catenin.....	109
Subcellular localization of Custos.....	110
Custos does not co-localize with Dishevelled.....	111
Custos inhibits β -catenin transcriptional activity and modulates canonical Wnt signaling.....	111
Custos co-localizes with lamin.....	112
Expression pattern of Custos.....	113
Custos is required for anterior development.....	113
Genetic modifications to create Custos knockout.....	114
SUMMARY AND CONCLUSION.....	120
BIBLIOGRAPHY.....	121

List of Tables

Table 1: List of Dishevelled interacting proteins.....	27
Table 2: List of primers used for indicated experiments	42
Table 3: Morpholinos used for knockdown of Custos in zebrafish.....	48
Table 4: CRISPR/cas9 target sites for knockout of Custos.....	51
Table 5: Primers for synthesizing sgRNA.....	52
Table 6: Primers for genotyping zebrafish embryos, tail-clipped genomic DNA and nested primers for V5 tag.....	53

List of Figures

Figure 1: Wnt processing, secretion and reception.....	8
Figure 2: Canonical Wnt signaling cascade.....	17
Figure 3: Schematic representation of non-canonical Wnt signaling cascade.....	19
Figure 4: Schematic representation of Wnt-Ca ²⁺ signaling cascade.....	21
Figure 5: Schematic representation of Dishevelled domain structure.....	23
Figure 6: Mesoderm formation in vertebrates.....	
Figure 7: Zebrafish embryogenesis.....	38
Figure 8: Schematic diagram of the PDZ domain region within Dishevelled that was used as a bait in the yeast two-hybrid screen.....	58
Figure 9: Schematic diagram of Dishevelled and Custos.....	59
Figure 10: Custos interacts with Dishevelled.....	60
Figure 11: GST pull down for Custos.....	61
Figure 12: Custos binds to Dishevelled in response of Wnt treatment.....	62
Figure 13: Custos binds to β -catenin in response of Wnt treatment.....	63
Figure 14: Dephosphorylation of Custos.....	64
Figure 15: Subcellular localization of Myc-Custos and effect of overexpression of Myc-Custos on Wnt signaling.....	68
Figure 16: Myc-Custos colocalizes with lamin.....	69
Figure 17: Subcellular localization of Flag-Custos and its fragments and effect of overexpression of Flag-Custos and its fragments on Wnt signaling.....	71

Figure 18: Quantification of nuclear localization of β -catenin in untransfected and Myc-Custos and its truncated constructs transfected cells in response to Wnt stimulation.....72

Figure 19: Myc-Custos does not colocalize with Flag-Dvl.....74

Figure 20: TOPflash luciferase assay.....76

Figure 21: Expression pattern of Custos during zebrafish development.....78

Figure 22: Overexpression of Custos interferes with anterior development.....81

Figure 23: Knockdown of Custos causes ventralization defects.....82

Figure 24: Knockdown of Custos using a second Custos morpholino produces ventralization defects.....83

Figure 25: Effect of Custos knockdown on mesodermal induction.....85

Figure 26: CRISPR/Cas9 gene editing of Custos at target site SG11.....88

Figure 27: CRISPR/Cas9 gene editing of Custos at target site SG12 and SG13.....89

Figure 28: Mutagenesis in F1 fish via Sanger sequencing.....91

Figure 29: F0 generation is heterozygous.....93

Figure 30: RT-PCR analysis of wildtype, heterozygous and homozygous fish embryos.....95

Figure 31: Endogenous V5 tagging of Custos.....98

Figure 32: Heterozygous incrosses and genotyping analysis.....99

Figure 33: Characterization of homozygous embryos using molecular markers....101

Figure 34: Quantification of Custos morpholino microinjection in mutant embryos.....103

Figure 35: Multiple Sequence alignment of Custos among different vertebrate species.....108

Figure 36: Schematic model of how Custos is involved in the canonical Wnt signaling pathway.....119

CHAPTER 1
INTRODUCTION

History of Wnt signaling

Wnt was first identified in 1982 as a mouse proto-oncogene, Int-1, which was activated by integration of MMTV pro-viral DNA in virally induced mammary gland tumors (Nusse and Varmus 1982). It was then found to be homologous to the Wingless gene in *Drosophila* which was a segment polarity gene involved in the body axis formation during embryonic development (Rijsewijk, Schuermann et al. 1987). The origin of the word “Wnt” was a portmanteau of Wg and Int-1. The first study of Wnt pathway in vertebrates was performed in 1989 by injecting mouse Int-1 RNA into early stages of *Xenopus* embryos that led to duplication of axis (McMahon and Moon 1989).

Biology of Wnt signaling

An intricate interplay between various signaling pathways is involved in the development of an embryo from a fertilized egg into a multicellular organism. These signaling pathways are important in coordinating cell growth, patterning and inducing cell fate specification (Willert and Jones 2006). Wnt signaling is one of the critical pathways implicated in all of the above processes (Yamaguchi 2001).

Wnt ligand biogenesis and secretion

Wnts belong to a family of secreted glycoproteins that function as ligands to activate a receptor mediated signal transduction cascade. These play a

vital role in multiple developmental processes during embryogenesis including cell fate specification, cell differentiation and morphogenesis (Cadigan and Nusse 1997, Komiya and Habas 2008). Humans and mice harbor 19 Wnts genes highlighting the complexity of the outputs of this pathway. Wnts are approximately 350-400 amino acids long and contain conserved cysteine residues (Tanaka, Kitagawa et al. 2002). These cysteine residues participate in inter- and intra-molecular disulphide bond formation that are involved in Wnt folding and multimerization (Tanaka, Kitagawa et al. 2002). Despite containing multiple charged residues, Wnt proteins are hydrophobic in nature, which raises a question as to how these hydrophobic molecules spread or diffuse in the aqueous extracellular environment. Wnt proteins possess an amino terminal hydrophobic sequence that is required for targeting them to the ER. When the immature Wnts reach the ER, here they undergo two major post-translational modifications: lipidation and N-glycosylation. Addition of N-glycans to the Wnt peptide backbone simplifies the Wnt secretion process, but the function of these N-glycans remain unclear as mutations in the N-glycosylation sites does not impair signaling (Komekado, Yamamoto et al. 2007, Kurayoshi, Yamamoto et al. 2007, Doubravska, Krausova et al. 2011). The second post-translational modification occurs when a palmitate group is added to the amino terminal part of the Wnt protein. This was observed during purification of Wnt3a in cell culture medium and also for the Wnt family member, Wingless (Wg) gene in *Drosophila* (Willert, Brown et al. 2003, Zhai, Chaturvedi et al. 2004).

Unlike the first modification, lipidation is critical for Wnt signaling, as an absence of palmitoylation impairs function of the Wnt3a protein in cell culture medium studies (Willert, Brown et al. 2003).

Genetic studies suggest that an ER based protein, *Porcupine*, member of membrane-bound O-acyl transferase family is responsible for the acylation of Wingless in *Drosophila* (Zhai, Chaturvedi et al. 2004). Mutations in the *porcupine* gene prevent the release of Wingless from the producing cell, thus playing a role in exit of Wnt from the ER and entry in the secretory pathway (Zhai, Chaturvedi et al. 2004).

Once the Wnts proteins are lipid modified and glycosylated in the ER, they move to the trans-Golgi network. This trafficking is facilitated by the p24 cargo adaptor family members. As evidenced by RNA interference studies, knockdown of the p24 family members, Opossum, Emp24 and Éclair, reduces secretion of Wingless in *Drosophila* (Port, Hausmann et al. 2011). From here, the Wnt proteins move through subcellular compartments before being released into the secretory pathway. In *Drosophila* Wingless producing cells, a small pool of Wingless has been found in the endosomal compartment that is later on directed to the plasma membrane (Gonzalez, Swales et al. 1991, Pfeiffer, Ricardo et al. 2002). The transport of Wnt to the plasma membrane was shown to be mediated by another protein, Wntless. In *Drosophila*, loss of Wntless results in retention of Wingless within its producing cells thereby disrupting Wingless signaling (Banziger, Soldini et al. 2006, Bartscherer, Pelte et al. 2006). This role of Wntless is specific to

Wingless signaling as a loss of Wntless did not affect the secretion of the lipid related morphogen, Hedgehog (Banziger, Soldini et al. 2006). Wntless physically binds to Wingless in co-immunoprecipitation experiments and this interaction requires Porcupine and conserved lipid modified cysteine residues in Wnt proteins including Ser209 in Wnt3a and Ser239 in Wingless indicating that the lipid modification at this position is critical for interaction of Wntless with Wnt (Banziger, Soldini et al. 2006, Coombs, Yu et al. 2010, Herr and Basler 2012). Localization of endogenous and fluorescently tagged Wntless revealed that Wntless is localized to the Golgi network, endosomes and the plasma membrane suggesting that it may function to facilitate trafficking of Wnt from Golgi apparatus to the plasma membrane for release into the extracellular space (Belenkaya, Wu et al. 2008, Franch-Marro, Wendler et al. 2008, Yang, Lorenowicz et al. 2008). Once it reaches the cell surface, Wntless is recycled back to the Golgi apparatus to participate in further rounds of Wnt secretion. The recycling of the Wntless is initiated by internalization of the plasma membrane, which is mediated through clathrin and AP2 adaptin based endocytosis (Yang, Lorenowicz et al. 2008, Gasnereau, Herr et al. 2011). Next, Wntless is recovered from the endosomes and is transported back to the Golgi apparatus via the retromer dependent trafficking pathway (Belenkaya, Wu et al. 2008, Franch-Marro, Wendler et al. 2008, Yang, Lorenowicz et al. 2008). The role of the retromer complex in Wnt signaling was first discovered in *C. elegans*. The retromer complex consists of the cargo selective sub-complex that includes the subunits, which associate

with a membrane bound coat formed by the sorting nexins. Mutations in the cargo selective subunits in *C.elegans* abrogate Wnt signaling (Coudreuse, Roel et al. 2006, Prasad and Clark 2006). It was shown that the subunit trimer, Vps26, Vps29 and Vps35 interacts with Wntless and loss of retromer function interferes with Wnt signaling in *Drosophila*, mammalian cells and *Xenopus* suggesting an evolutionary conserved role of the retromer complex in Wnt signaling (Belenkaya, Wu et al. 2008, Franch-Marro, Wendler et al. 2008, Port, Kuster et al. 2008).

Once the Wnt proteins reach the plasma membrane, there are different mechanisms proposed for how they transported through the plasma membrane to the extracellular space. Secretion of Wnt from its producing cell is initiated by dissociation of Wntless from Wnt. Binding of Heparan sulphate proteoglycans (HSPGs) on the surface of the Wnt producing cell, enables spreading of Wnt in the tissue to mediate long range concentration gradient. This may also involve direct interaction of Wnt and lipoprotein particles or joint internalization of Wnt and lipoprotein particles, suggested by Wingless-Lipoporphin colocalization in *Drosophila* (Panakova, Sprong et al. 2005). Wnts also undergo deacylation by the enzyme Notum, which enzymatically removes the lipid from the Wnt (Giraldez, Copley et al. 2002). Wnt signal turns on expression of Notum for negative feedback regulation by intrinsically limiting its own activity (Kakugawa, Langton et al. 2015). Another plausible mechanism is that dissociation of Wnt and Wntless occurs due to vacuolar acidification of the secretory vesicles that can transport the

Wnt-Wntless complex to the plasma membrane and the acidic environment stimulates the release of Wnt (Coombs, Yu et al. 2010).

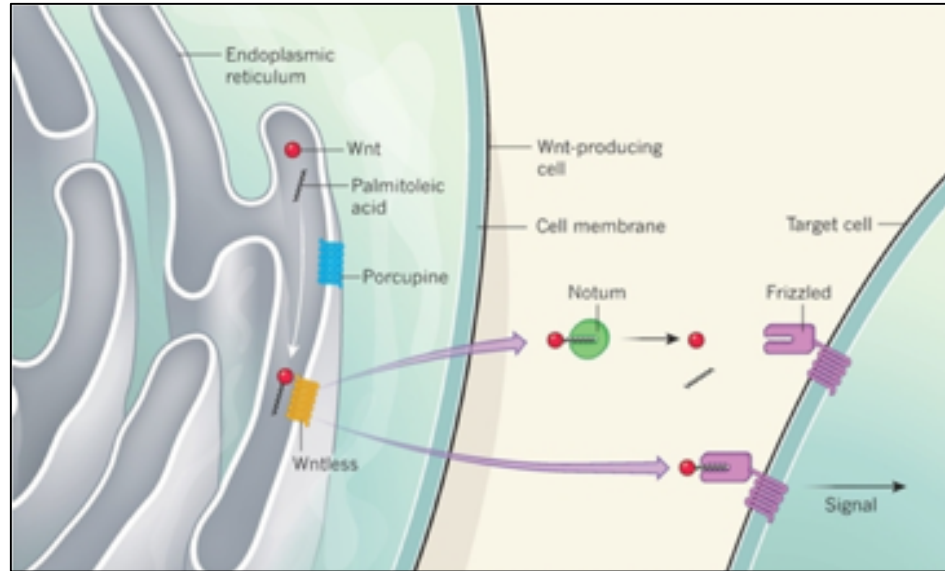


Figure 1: Wnt processing, secretion and reception. In Wnt producing cells, Wnt becomes palmitoylated in the ER. Transport and secretion of Wnt out of the cell is then controlled by the multi-pass transmembrane protein Wntless. Wnt protein then binds to its receptor on the receiving cell, Frizzled to mediate signal transduction. This Wnt-Frizzled interaction is regulated by enzyme Notum which removes acyl group from Wnt (Nusse 2015).

Wnt as morphogens

The first step to analyze whether a molecule is a “morphogen” is to know if it induces a cellular response in a concentration dependent manner. Much data in the past two decades support the idea that Wnts can mediate signal in a short-range as well as a long-range, thus serving as bonafide-secreted morphogens. Short range signaling occurs when cells produce Wnt signal directly to its adjacent receiving cell via direct cell-cell contact. This kind of cell communication is observed in the crypts of small intestine where Paneth cells secrete Wnt3 to sustain adjacent stem cells (Sato, van Es et al. 2011). Long range signaling is observed during embryonic development where concentration gradients are formed that provide positional information to cells to mediate tissue pattern formation. In *Drosophila*, loss of function of the membrane microdomain protein, Reggie-1/flotillin-2 reduces the spreading of Wnt, thus suggesting its importance for long range signaling (Katanaev, Solis et al. 2008). Another protein, Secreted Wingless interacting molecule (SWIM) was shown to promote long range Wnt signaling and act as co-receptors in *Drosophila*. SWIM, when complexed with Wnt, maintains extracellular Wnt in soluble form complex by shielding its lipid tail. Once, the complex reaches the target cell, it transfers the lipid tail to a groove in the Frizzled extracellular domain for Wnt activation (Janda, Waghray et al. 2012). Two glypicans from the HSPG family, *Dally* and *Dally-like* further act as co-receptors and facilitate the binding of Wingless to Frizzled receptors in *Drosophila*. This leads to activation of Wingless signaling and degradation of

the complex, thus playing an important role in Wingless morphogen concentration (Lin 2004).

Receptors and co-receptors

Two families of membrane receptors are required for Wnt signal transduction: Frizzled (Fz) receptor and low-density lipoprotein receptor-related protein (LRP5/6) (Bhanot, Brink et al. 1996, Pinson, Brennan et al. 2000). Frizzled (Fz) is a seven-pass transmembrane protein consisting of an amino terminal cysteine rich domain (CRD) that is required for interaction with Wnt (Bhanot, Brink et al. 1996, Yang-Snyder, Miller et al. 1996). Frizzled gene has been found in diverse metazoans including five in *Drosophila*, three in *C.elegans* and ten in humans. Frizzled proteins are found to be localized on the plasma membrane of the Wnt responsive cells and function in all the three signaling pathways. Frizzled receptor on its own cannot transduce Wnt signaling but requires a co-receptor, LRP5/6 to mediate Wnt signal (Tolwinski, Wehrli et al. 2003, Cong, Schweizer et al. 2004). LRP5 and 6 co-receptors consist of conserved cytoplasmic domain with five PPPSPXS motifs that are essential for activation and recruitment of the destruction complex in the canonical Wnt signaling pathway (Mao, Wang et al. 2001, Tamai, Zeng et al. 2004). The canonical Wnt signaling pathway is activated when Wnt ligand binds to the Frizzled (Fz)-LRP5/6 complex together with Dishevelled (Dvl). This interaction recruits the destruction complex to the plasma membrane through the DIX domain of both Dishevelled and Axin. This is then

thought to initiate the phosphorylation of LRP6 and stabilize β -catenin in the cytoplasm (Zeng, Huang et al. 2008)

Destruction complex

The destruction complex plays an important role in regulating the Wnt signaling pathway. This task is carried out of by the members of the destruction complex. It comprises of a group of proteins: Adenomatous polyposis coli(APC), protein kinases: Casein kinase 1 (CK1) and Glycogen synthase kinase (GSK3), Axin and E3 ligase β -transducin repeat containing protein (β -TrCP). In absence of Wnt, the destruction complex binds to β -catenin and targets it for degradation via the proteosomal machinery.

Axin is the most flexible protein of the destruction complex as it possesses binding sites for all of the other members of the complex. The Axin protein contains a regulator of G-protein signaling (RGS) domain that interacts with APC and essential for phosphorylation of APC and degradation of β -catenin (Peterson-Nedry, Erdeniz et al. 2008). Axin binds to GSK-3, CK1 and β -catenin in close proximity and the closeness of the binding sites increases the enzyme-substrate concentration. The proximity of CK1 and GSK3 on Axin is known to enhance the phosphorylation of β -catenin (Sobrado, Jedlicki et al. 2005) (Dajani, Fraser et al. 2003)

APC is a 310 kDa protein that contains of binding sites for β -catenin and Axin (Stamos and Weis 2013). The carboxyl terminal of APC contains a microtubule interaction region dispensable for β -catenin degradation

(McCartney and Nathke 2008). The main function of APC in the destruction complex is to bind to Axin via serine-alanine-methionine-proline(SAMP) repeats and contribute to β -catenin destruction as seen in mammalian cells(Behrens, Jerchow et al. 1998, Hart, de los Santos et al. 1998, Stamos and Weis 2013). Elimination all of the SAMP repeats converts this protein into an oncogenic form (Kohler, Brauburger et al. 2010). APC proteins consist of multiple β -catenin binding sites, comprising of repeats of either 15 or 20 amino acids (Eklof Spink, Fridman et al. 2001). Phosphorylation of these 20mer repeats by GSK3 and CK1 increases the binding affinity for β -catenin (Ikeda, Kishida et al. 2000). The amino terminal of APC contains an armadillo domain which interacts with a number of cytoskeletal regulators and the carboxyl terminal region of APC that contains a microtubule interacting domain (Kawasaki, Senda et al. 2000, Breitman, Zilberberg et al. 2008, McCartney and Nathke 2008).

Casein kinase 1(CK1) proteins have many isoforms, six found in humans, α , δ , ϵ , γ 1, γ 2, γ 3. These are ubiquitously expressed and share a high homology within the kinase domain (Cheong and Virshup 2011). CK1 α , δ and ϵ are localized in the cytoplasm and nucleus, whereas, CK1 γ is anchored to the cell surface via carboxyl terminal lipid modification (Davidson, Wu et al. 2005).Members of the CK1 family play both positive and negative role in canonical Wnt signaling. CK1 α isoform is responsible for initiation of β -catenin phosphorylation and degradation in the β -catenin-destruction complex. In the absence of Wnt signaling, CK1 α phosphorylates β -catenin at

serine 45 and primes β -catenin for phosphorylation by GSK3 at threonine 41, serine 37 and serine 33 (Stamos and Weis 2013). CK1 phosphorylates Tcf3, Dapper1a, p120-catenin and E-cadherin to activate Wnt signaling. CK1 ϵ phosphorylates Tcf3 to promote β -catenin-Tcf3 binding (Lee, Salic et al. 2001). Phosphorylation of Dapper1a by CK1 δ abrogates Dishevelled-Dapper1a interaction and derepress its Wnt inhibitory activity (Teran, Branscomb et al. 2009). Upon activation of Wnt pathway, phosphorylation of β -catenin at S268 and S269 and E-cadherin at serine rich C-terminal by CK1 α is important for β -catenin transcriptional activity (Casagolda, Del Valle-Perez et al. 2010).

GSK3 exists in two isoforms in mammals, GSK3 α and GSK3 β , both playing a role in phosphorylation of β -catenin. GSK3 typically is unable to phosphorylate a protein without a priming phosphate that targets it to the protein (Marin, Bustos et al. 2003). Priming phosphorylation at serine 45 of β -catenin leads to GSK3 phosphorylation at threonine 41, serine 33 and serine 37, thus targeting β -catenin for degradation (Yost, Torres et al. 1996, Aberle, Bauer et al. 1997).

Wnt signaling cascades

Wnt signaling pathway is comprised of two major intracellular signaling branches, the canonical or Wnt/ β -catenin dependent pathway (Figure1) and non-canonical Wnt signaling pathway or Wnt/ β -catenin independent pathway (Figure2 and 3). Mutations in the Wnt signaling cascade are often linked to numerous human hereditary disorders, cancer and developmental defects (Clevers 2006).

β -catenin-dependent pathway

In the absence of Wnt, any β -catenin protein within the cytoplasm is degraded by a protein complex termed the destruction complex, which comprises of Glycogen synthase kinase (GSK3), adenomatous polyposis coli(APC) and casein kinase I (CK1). GSK3 and CK1 phosphorylate the amino terminal region of β -catenin, resulting in recognition by β -TrCP leading to its subsequent ubiquitination and proteosomal degradation (Komiya and Habas 2008). The canonical Wnt signaling pathway is activated when Wnt ligand binds to the Frizzled (Fz)-LRP5/6 receptor and co-receptor complex. This binding induces the interaction of Dishevelled (Dvl) with Frizzled (Fz) and also results in recruitment of Axin to a conserved sequence in the cytoplasmic tail of LRP5/6 that is catalyzed via phosphorylation of LRP5/6, mediated by CK1 or GSK3. This results in disruption of the destruction complex leading to accumulation of β -catenin in the cytoplasm, which then translocates into the nucleus to form complexes with TCF/LEF family of

transcription factors and activate transcription of target genes involved in cell fate determination, cell polarity, neural patterning and organogenesis (Figure 1) such as *Siamois* and *Twin*, genes required for Spemann organizer formation in *Xenopus* and *Dharma/bozozok* in zebrafish. Mutations in genes encoding the components of this pathway can lead to detrimental effects on vertebrate development. Mutations in Tcf4 in mouse leads to intestinal stem cell loss and tissue breakdown (Korinek, Barker et al. 1998). Gene inactivation of Tcf3 and Axin resulted in the *headless (hdl)* and *masterblind (mbl)* mutants in zebrafish exhibiting lack of forebrain and telencephalon respectively (Kim, Oda et al. 2000, Heisenberg, Houart et al. 2001). Mutations in the Frizzled (Fz4) gene in humans results in cerebellar and auditory defects along with Familial exudative vitreoretinopathy (FEVR) (Wang, Huso et al. 2001, Toomes, Bottomley et al. 2004).

β-catenin-independent pathways

The non-canonical or β-catenin-independent pathway further can be separated into the Planar Cell Polarity and the Wnt/Ca²⁺ pathway (Semenov, Habas et al. 2007, Komiya and Habas 2008). This Wnt signaling cascade functions independently of transcription and has been shown to regulate the actin cytoskeleton and directed migration (Komiya and Habas 2008). In vertebrates, this pathway was found to regulate cell polarity and dorsal mesodermal cells during convergent extension in *Xenopus* and zebrafish (Wallingford, Fraser et al. 2002, Jessen 2012).

The Planar Cell Polarity pathway was first identified in genetic studies performed in *Drosophila* in which mutations in Frizzled and Dishevelled randomized epithelial structures including cuticle, hair and sensory bristles (Seifert and Mlodzik 2007). The core components of this pathway include Frizzled, Dishevelled, Strabismus, Flamingo, Prickle and Diego. These core proteins co-ordinate the polarity between adjacent cells on the subcellular level across a tissue. Initially these components are recruited to the apical cell membranes followed by asymmetric distribution in the polarized epithelia (Gray, Roszko et al. 2011). Some of these components such as Prickle and Strabismus are localized in the proximal part of the polarized cell membrane of the *Drosophila* wing cells whereas proteins such as Frizzled, Dishevelled and Diego accumulate in the distal region of the cell membrane (Axelrod 2001, Strutt 2001, Tree, Shulman et al. 2002). During vertebrate gastrulation, the cells of the mesoderm and ectoderm intercalate on the future dorsal side resulting in convergence and extension to form the embryonic axis. Such alignment of cell behaviors requires proper re-organization of the cytoskeleton (Tada and Heisenberg 2012). The non-canonical Wnt pathway is known to regulate the movement of the dorsal mesodermal cells and cell polarity during this process (Komiya and Habas 2008).

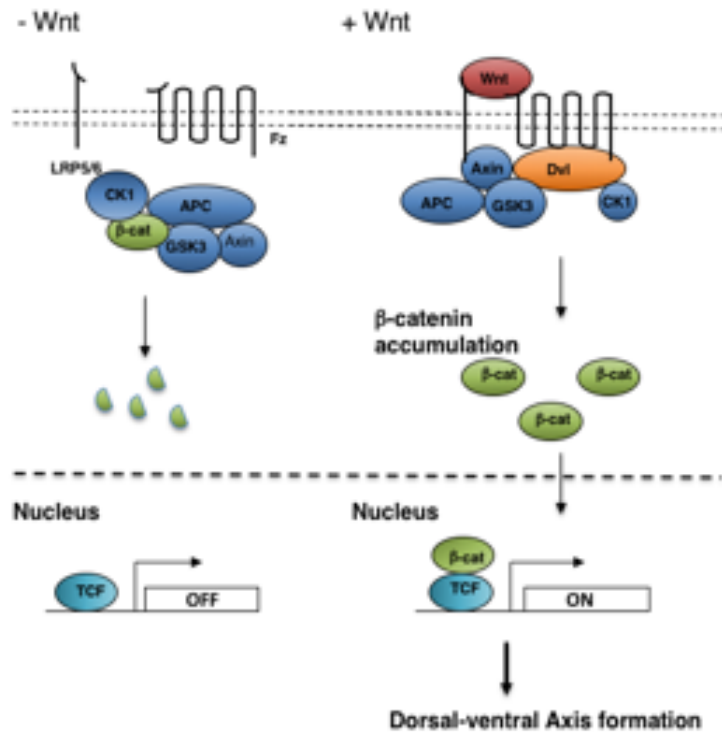


Figure 2. Canonical Wnt signaling cascade. Frizzled binds to an extracellular Wnt ligand, and transduces the signal to dishevelled that leads to the stabilization of β-catenin in the nucleus to regulate transcription of several important Wnt target genes.

In the non-canonical Wnt pathway; the Wnt signal is also mediated through the Frizzled (Fz) receptor in absence of the Lrp5/6 co-receptor but there have been some conflicting studies suggesting role of Lrp5/6 in regulation of convergent extension (He, Semenov et al. 2004, Tahinci, Thorne et al. 2007). However, there are some other putative candidates for co-receptors such as NRH1, Ryk, PTK7 and ROR2 that been identified to play a role in this pathway (Lu, Yamamoto et al. 2004, Lu, Borchers et al. 2004, Sasai, Nakazawa et al. 2004, Nishita, Yoo et al. 2006). The signal is then transduced to the cytoplasmic protein Dishevelled (Dvl). At the level of Dishevelled, the PDZ and DEP domains of Dishevelled activate two parallel pathways. The PDZ domain leads to activation of the small GTPases Rho and Rac. The activation of Rho occurs when DAAM1 interacts with the PDZ domain of Dishevelled. Activated small GTPase Rho then activates the Rho-associated kinase ROCK, ultimately leading to modification of actin cytoskeleton and cytoskeletal rearrangement (figure 2) (Habas, Kato et al. 2001, Marlow, Topczewski et al. 2002). The second pathway activates Rac GTPases to stimulate c-Jun N-terminal Kinase (JNK) activity via the DEP domain of Dishevelled, which plays critical role in modulation of the actin cytoskeleton (Li, Yuan et al. 1999, Keller, Davidson et al. 2003)

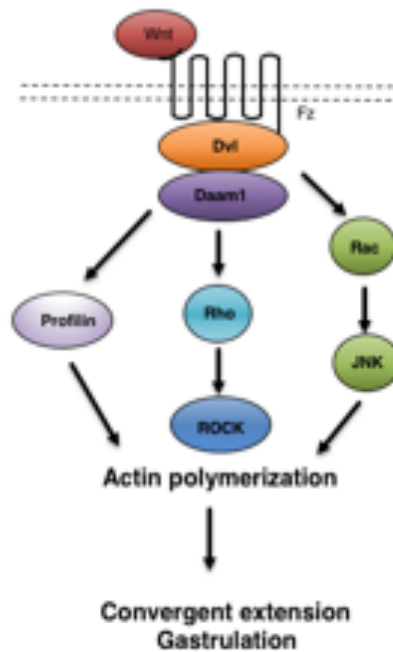


Figure 3: Schematic representation of non-canonical Wnt signaling cascade. In the non-canonical signaling pathway, Wnt signal is received by the Frizzled receptor (Fz) and transduced via Dishevelled to both Rho and Rac via Daam1 which then activate more downstream targets to modulate changes to the actin cytoskeleton.

The second branch of β -catenin independent pathway termed as Wnt/ Ca^{+2} is involved in regulation of calcium release from the endoplasmic reticulum. When the Wnt ligand binds to the frizzled receptor, the signal is transduced via the PDZ and DEP domain of Disheveled. Unlike the canonical Wnt pathway, here the Frizzled receptor interacts directly with trimeric G-protein leading to activation of downstream component, phospholipase C (PLC). Activation of PLC leads to cleavage of phosphatidylinositol 4,5 biphosphate (PIP₂) producing Diacylglycerol (DAG) and inositol-1,4,5-trisphosphate (IP₃). IP₃ diffuses through the cytosol and binds to its receptor on ER resulting in release of calcium in the cell. The released calcium then activates calcium dependent enzymes including calcium/calmodulin-dependant kinase II (CaMK II), calcineurin and PKC. CaMKII activation further induces activation of nuclear factor of activated T cells (NFAT), which is involved in cell migration. Increased calcium also activates small GTPase Cdc42 via PKC, which is involved in ventral patterning. Calcineurin activation can in turn lead to activation of NLK kinase, which can inhibit the canonical Wnt signaling pathway (figure 3). Ca^{+2} also controls the process of tissue separation during gastrulation via activation of the small GTPase Cdc42 as shown in *Xenopus* (Winklbauer, Medina et al. 2001, Winklbauer and Luu 2008).

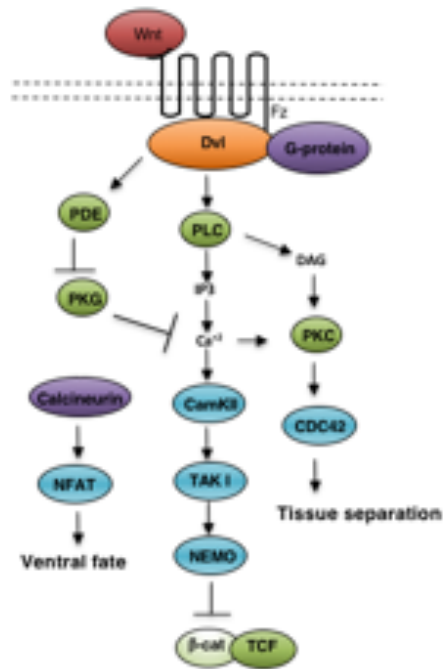


Figure 4. Schematic representation of Wnt-Ca²⁺ signaling cascade The Wnt-Ca²⁺ pathway is activated by the Wnt signal through the Fz receptor in a G protein coupled fashion, ultimately leading to the activation of PKC and CamK2 for many different downstream functions.

Dishevelled

The Dishevelled gene was first identified in *Drosophila*, as a mutation in this gene produced disorientation in hair and bristle polarity (Fahmy and Fahmy 1959). Its role in the canonical Wnt signaling was first established due its influence on segment polarity in the early embryonic development. Later on, it was also known to be involved in the epithelial planar polarity, thus defining its role in non-canonical Wnt signaling pathway. Dishevelled is considered as a central branch point for regulating all branches of Wnt signaling cascades. Dishevelled is highly conserved between *Drosophila*, *Xenopus laevis* and humans. These modular proteins are made up of 500-750 amino acids comprising of three highly conserved domains, Dishevelled/Axin (DIX) domain, Post synaptic density protein, *Drosophila* disc large tumor suppressor and zonula occludens (PDZ) domain and Dishevelled, EGL-10 Pleckstrin (DEP) domain (Wallingford and Habas 2005).

There are several characteristics features of the conserved domains of Dishevelled. During the canonical Wnt signaling, DIX and PDZ domains are utilized to induce the stabilization of cytosolic β -catenin and its subsequent translocation into the nucleus to activate transcription of various Wnt target genes. The non-canonical Wnt signaling cascade acts via the PDZ and DEP domains of Dishevelled. Two independent pathways lead to activation of small GTPases Rho and Rac via the PDZ and DEP domain respectively. The formin homology protein, Daam1 interacts with the PDZ domain to activate

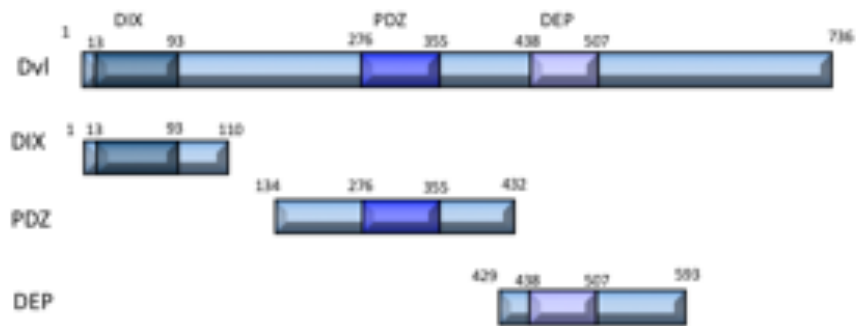


Figure 5: Schematic representation of Dishevelled domain structure. DIX: Dishevelled Axin domain; PDZ: Post synaptic density protein, *Drosophila* disc large tumor suppressor and zonula occludens; DEP: Dishevelled, Egl-10, Pleckstrin. Numbers indicate amino acid positions.

the Rho-associated Kinase, ROCK, which leads to activation of Rho. Rac activation utilizes the DEP domain of Dishevelled and activates Jun kinase (JNK) activity. The subcellular localization of Dishevelled also influences the specificity of the signaling pathway. Subcellular localization of Dishevelled in the cytoplasm suggests its role in the canonical Wnt signaling pathway whereas its localization on the membrane indicates its role in the non-canonical signaling cascade (Axelrod, Miller et al. 1998, Wu, Klein et al. 2004). When overexpressed, dishevelled localizes to cytoplasmic puncta, which was shown, to be protein aggregates. DIX domain plays a critical role in polymerization of Dishevelled in head to tail manner (Schwarz-Romond, Fiedler et al. 2007). This puncta is known to consist of different signaling components of the β -catenin dependent pathway (Bilic, Huang et al. 2007). Dvl has also been known to shuttle between the nucleus and cytoplasm due to presence of nuclear localization signal (NLS) and nuclear export signal (NES) between the DIX and PDZ domain (Boutros and Mlodzik 1999). In the nucleus, Dvl interacts with β -catenin and C-Jun followed by the formation of a stable β -catenin/TCF complex and transcriptional activation of Wnt target genes (Gan, Wang et al. 2008). Hence, it is likely that there are two pools of Dvl: a small pool which translocates to the nucleus that activates canonical Wnt signaling and other larger pool moves to the plasma membrane to mediate both canonical and non-canonical Wnt signaling

In *Drosophila*, mutation of the DEP domain of Dishevelled disrupts the polarity of bristles and wing hair (Wong and Adler 1993, Theisen, Purcell et

al. 1994). This mechanism is also conserved in vertebrates; the dominant negative form of Dishevelled disrupts the cell division polarity in zebrafish embryonic development during gastrulation (Gong, Mo et al. 2004). Mouse mutants with disruption in Dvl1 and Dvl2 cause neural tube closure defects thus indicating its critical role during gastrulation (Hamblet, Lijam et al. 2002). Dvl1 null mouse mutants exhibit defects in social behavior, whisker trimming and nest building (Lijam, Paylor et al. 1997). It was postulated that it is also known to play a major role in later stages of development especially during neuronal development in vertebrates (Fan, Ramirez et al. 2004, Kishida, Yamamoto et al. 2004). Overall, Dishevelled is critical for both canonical as well as non-canonical Wnt signaling, but the mechanism by which it channels signaling into both these pathways is still unclear. It is worthy to investigate Dishevelled interacting molecules, which will help us to unravel the highly complex mechanism of Dishevelled during vertebrate development.

Dishevelled interacting proteins

Dishevelled is known to be a “scaffolding” protein and regulates the intracellular Wnt signaling cascades by binding to other proteins into a multiprotein complex (Table1). Previous studies have shown that each domain of Dishevelled acts as a docking site for a large number of proteins and suggest a dynamic spatial localization for Dishevelled. The DIX domain of Dishevelled as the name suggest dimerizes with Axin in a multiprotein complex regulating the intracellular concentration of β -catenin (Wharton 2003, Luo and Lin 2004). Another protein Dapper was also identified as a Dishevelled-interacting protein binding to the DIX domain involved in canonical Wnt signaling and critical for notochord formation during embryogenesis (Cheyette, Waxman et al. 2002). Thus, DIX domain interacting proteins plays a major role in canonical Wnt signaling. The PDZ domain acts as a major docking site for interacting partners involved in both Canonical as well as non-canonical Wnt signaling. Activation of these pathways is determined in part by the proteins interacting with Dishevelled. Dishevelled interacts with frizzled via its PDZ domain (Wong, Bourdelas et al. 2003). A number of kinases, phosphatases and adaptor molecules interact with the PDZ domain of Dishevelled to relay intracellular signaling. CKI and CKII family of proteins bind to the PDZ domain and act as positive regulators of Wnt signaling. Daple is another regulator of the non-canonical Wnt pathway affecting cell migration (Ishida-Takagishi, Enomoto et al. 2012). The DEP domain of Dishevelled enables proteins like DAAM1 to interact with it and

Component	Dishevelled interacting domain	Cellular localization
Axin	DIX	cytoplasmic
Frizzled	PDZ	membrane
Casein kinase I	PDZ	cytoplasmic
Casein kinase II	PDZ	cytoplasmic
Dapper/dact1	PDZ	cytoplasmic
IDAX	PDZ	cytoplasmic
Naked cuticle	PDZ	cytoplasmic
Strabismus	PDZ	membrane
EPS8	PDZ	cytoplasmic
PAR I	PDZ	cytoplasmic
DAAM1	PDZ	Cytoplasmic
	DEP	membrane
MuSK	DEP	cytoplasmic
DDIP	DEP	unknown

Table 1 List of Dishevelled interacting proteins. List of Dishevelled interacting proteins including the disheveled interacting domain and sub-cellular localization of each protein {modified from (Wallingford and Habas 2005)}

regulate gastrulation during vertebrate development (Habas, Kato et al. 2001). Due to this versatile nature of Dishevelled, it is likely that there are number of unidentified Dishevelled interacting proteins that exist and play modulatory roles in transducing Wnt signal.

Formation of the mesoderm

During vertebrate embryogenesis, formation of mesoderm and dorsoventral axis specification are the most critical processes for establishing an organized body plan. In vertebrates, the mesoderm cells arise prior to gastrulation at the marginal zone (equator) of the embryo. In zebrafish, these mesodermal cells sit on the top of yolk syncytial layer (YSL) whereas in *Xenopus*, all the cells in the early gastrula contribute to the final embryos. Three types of cell movements occur during gastrulation. The mesoderm around the marginal zone from the outermost layer, epiblast moves into the inner layer, hypoblast, thus internalizing the mesoderm inside the ectoderm. These mesodermal cells later on undergo convergent extension by moving the mesodermal cells on the dorsal side of the embryo. By the end of gastrulation, the precursors of these mesodermal cells give rise to axial mesoderm, the paraxial mesoderm and lateral plate mesoderm. Peter Nieuwkoop first established the study of mesoderm formation in amphibians in the 1960s. He showed that the tissue explanted from the vegetal cap region could convert potential ectodermal cells obtained from the animal cap region into mesodermal tissue indicating that the mesoderm is formed by a

mechanism called 'induction' (Weyer, Nieuwkoop et al. 1977). Induction refers to a process in which extracellular signals bring about a change from one cell fate to another in a group of cells (Kimelman 2006). This study suggested that mesoderm inducing signals are localized to the vegetal hemisphere in *Xenopus* embryo. During fertilization, VegT transcripts from that encode T box transcription factor are released from the vegetal pole of the egg and slowly diffuse upwards. At the start of zygotic transcription, VegT activates transcription of *Xenopus nodal related* (Xnr) genes which then initiates mesoderm formation (Zhang, Houston et al. 1998, Clements, Friday et al. 1999, Hyde and Old 2000). In zebrafish, the nodal genes *squint* and *cyclops* initiate mesoderm formation, but their transcription is activated by unknown signal and not by an orthologue of VegT, as the orthologue of zebrafish VegT is not maternal (Griffin, Amacher et al. 1998, Schier and Talbot 2005). Apart from Nodal signaling, Wnt signaling also plays an important role in mesoderm induction. It was shown that maternal β -catenin is required for activation of MAPK and expression of mesodermal genes during *Xenopus* development (Schohl and Fagotto 2003).

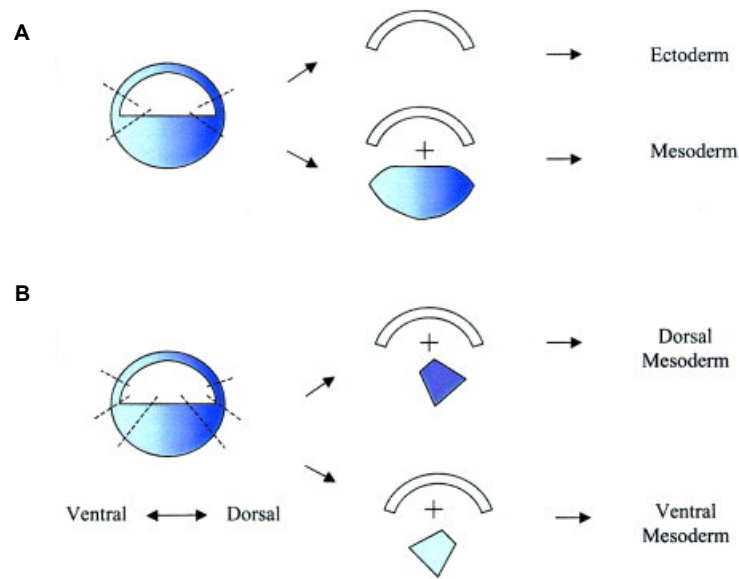


Figure 6: Nieuwkoop mesoderm induction experiment. **A.** Animal cap cells when combined to vegetal cells gave rise to mesoderm instead of ectoderm. **B.** The position of the vegetal cells influences the type of mesoderm induced along the dorsal ventral axis of the embryo (Weng and Stemple 2003).

Maternal Wnt pathways involved in dorsal patterning in zebrafish

In zebrafish, there is an interaction between two maternal pathways to determine the dorsal patterning of the zebrafish embryo at the blastula stage: Wnt/ β -catenin pathway and Wnt/ Ca^{+2} pathway.

Asymmetric translocation of a dorsal determinant, localized at the vegetal pole of the egg to the marginal blastomeres via microtubules establishes the dorsal side of the zebrafish embryo (Jesuthasan and Stahle 1997). This translocation of the dorsal determinant results in local activation of Wnt/ β -catenin signaling on the future dorsal side of the embryo. Nuclear accumulation of β -catenin leads to activation of target genes required for dorsal organizer formation such as *bozozok*, *chordin* and *gooseoid* (Stachel, Grunwald et al. 1993, Schulte-Merker, Lee et al. 1997, Melby, Beach et al. 2000). There are two maternally expressed β -catenin genes in zebrafish, β -catenin 1 and β -catenin 2 (Bellipanni, Varga et al. 2006). In absence of β -catenin 2, the mutant *Ichabod* displays a ventralized phenotype (Kelly, Chin et al. 2000, Bellipanni, Varga et al. 2006). The role of the Wnt/ Ca^{+2} pathway in dorsoventral patterning is to downregulate the dorsal cell fates induced Wnt/ β -catenin signaling ventrally (Slusarski and Pelegri 2007). Co-expression of Wnt5 and Wnt8 in zebrafish embryos blocks the ability of Wnt8 to activate Wnt/ β -catenin pathway and increase in intracellular Ca^{+2} levels by ectopic expression of serotonic receptor also inhibited Wnt/ β -catenin signaling (Slusarski, Yang-Snyder et al. 1997).

Zebrafish as a model organism

The teleost fish, *Danio rerio* in latin, also commonly called as zebrafish is a native to East India. This tropical fish is an excellent genetic model to study early embryonic development, especially to bridge the gap between fly/worm and mouse/human (Mandrekar and Thakur 2009). The adult zebrafish is approximately 2cm to 4cm long, males slender and torpedo shaped whereas females are usually fat with eggs in their belly. Zebrafish have a short generation time of 2-3 months enabling faster generation of desired mutant. Zebrafish can produce 100-200 embryos each week, providing significant statistical data for each experiment. The embryos fertilize externally and are optically transparent thus enabling direct visualization of early developmental processes.

Understanding the role of a particular gene during development and its role in a signaling pathway is essential to illuminate the mechanisms of various human diseases. Forward genetics in zebrafish gained prominence in the 1990s when the first large-scale genetic screen was performed leading to the discovery of number of novel genes fundamental to vertebrate development (Driever, Solnica-Krezel et al. 1996, Haffter, Granato et al. 1996). In zebrafish, several different approaches were used to create mutants. Earlier researchers used gamma radiation to induce mutagenic lesions that gave rise to large deletions and chromosomal aberrations in the genome leading to gross embryonic mutant phenotypes(Chakrabarti, Streisinger et al. 1983). Hence, identifying genes responsible for these

phenotypes was difficult. Later on, chemical mutagenesis approach was used as a standard method that applied N-ethyl-N-nitrosourea (ENU) to mutagenize zebrafish (Mullins, Hammerschmidt et al. 1994). This was used as a standard technique in forward genetics for a long time in vertebrates. Recent technological advancement, including sequencing and assembly of the whole zebrafish genome, anti-sense morpholino approach, transgenesis and CRISPR/Cas9 technology paved way to fully exploit the zebrafish model to unravel the role of various genes in vertebrate development.

Knockdown of a particular gene of interest is the most common reverse genetics strategy used to study genes involved in embryogenesis. Antisense RNAi technology was widely used to knockdown a desired gene in the mammalian system, but did not have much success with frogs and zebrafish embryos. Use of anti-sense oligonucleotides called as “morpholinos” to knockdown specific gene expression was widely used in frog and zebrafish embryos (Nasevicius and Ekker 2000). Morpholinos are chemically synthesized oligonucleotides with a morpholine ring instead of a ribose ring. These oligonucleotides are resistant to nucleases thus much more stable than the conventional oligonucleotides. There are two types of morpholinos that can be used to study gene function: translation blocking morpholino and splice inhibiting morpholino. Morpholinos are designed to bind to the start codon to block the initiation of translation of the protein of interest or to splice acceptor sequences to cause aberrant splicing of mRNA.

Morpholinos can be directly injected into zebrafish embryos at one cell stage and scored for phenotypes up to 5 dpf (Bill, Petzold et al. 2009). High fecundity enables injection of varying concentration of morpholino in several hundreds of fish embryos thus providing a statistically significant read out. The disadvantage of this particular technique is the plausible “off target” effects such as the morpholino can lead to artifacts by non-specifically binding to unintended target gene instead of the desired gene. The recent literature consists of several examples wherein morphants of *sox18*, *nr2f1a* and *prox1a/b* show defects in the lymphatic vasculature but the mutant phenotypes are normal (van Impel, Zhao et al. 2014). It is important to address these issues by performing a number of experiments. Firstly, the optimization of the injection dose should be done using a mutant. Secondly, co-injection of the targeted RNA that lacks the morpholino binding site and the morpholino should be used. Rescue of the morphant phenotype will indicate the specificity of the morpholino.

With the advent of TILLING, TALENS and zinc finger nucleases (ZFNs), the field of reverse genetics was revolutionized. Identifying an inexpensive method to study gene function in reverse genetics has been challenging. Targeted induced local lesions in genomes (TILLING) utilize a combination of both forward as well as reverse genetics. Here, fish are mutagenized using ENU and sequencing the target region from the genome identifies mutations (Moens, Donn et al. 2008). This method requires large scale screening of individual fish and hence cannot be used as a routine technique in the lab.

Zinc finger nucleases (ZFNs) are artificial endonucleases that consist of zinc finger motif that recognizes specific sequence in the genomic DNA and a restriction enzyme, FokI that cleaves the double stranded DNA. The repair machinery then repairs the double strand breaks via homologous recombination or non-homologous end joining (NHEJ) creating indels at the site of lesion. But this approach yielded a lot of non-specific phenotypes due to off target effects(Kim, Lee et al. 2009, Lawson and Wolfe 2011). Later, TALENs emerged as an efficient method for targeted mutagenesis and worked on the same principle as ZFNs. Transcription activator like effector nucleases (TALENs) are artificial restriction enzymes made up of TAL effector DNA-binding domain fused to a DNA cleavage domain. These induce double strand breaks at a specific sequence, cells respond to with repair mechanism. TALENs are more specific than ZFNs with less off target effects had hence been increasingly used as an easily available reverse genetic screening strategy in many laboratories.

The next game changer in the field of reverse genetics was CRISPR/Cas9 technology. CRISPR is a simple method that allows site-specific genomic modification in a wide range of species. This method uses engineered nucleases that target specific sequences in a genome leading to DNA double strand breaks. The non-homologous end joining (NHEJ) pathway then repair these double strands breaks giving rise to mutations in the genome(Sander and Joungh 2014).

CRISPR system was first identified in bacteria as a defense mechanism against exogenous DNA (Horvath and Barrangou 2010). CRISPR system consists of small RNAs and CRISPR associated proteins (Cas) proteins that work together to target the foreign DNA and cleave it. There are six families of CRISPR/Cas system: CRISPR system I-III are the best studied whereas IV-VI are recently identified (Makarova, Haft et al. 2011, Makarova, Wolf et al. 2015). In type II system, CRISPR RNA (crRNA) function with a transactivating RNA(tracrRNA) to localize Cas9 nuclease to the target DNA sequence and cleave it(Jinek, Chylinski et al. 2012). The same methodology is used for inactivating a gene in different species. CRISPR/Cas9 can be easily delivered in a broad range of cell types. Electroporation and lipofectamine mediated transfection can easily be used to transiently express Cas9 in mammalian cells. In zebrafish, Cas9 RNA and sgRNA can be easily microinjected at once cell stage to induce efficient genome editing (Jao, Wente et al. 2013).

Zebrafish early development

The precise co-ordination of cell divisions and extensive cellular rearrangements along with proper regulation of different signaling pathways is required for establishment of the vertebrate body plan. The zebrafish egg is telolecithal and undergoes meroblastic cleavage. Following 3hpf, rapid and synchronous cleavage divisions occur within the blastodisc marking the blastula stage of the embryo.(Kimmel, Ballard et al. 1995) (Schier and Talbot 2005)The mid-blastula transition (MBT) begins at around 3hpf (512-cell

stage), which is also when the zygotic transcription initiates. The cells at the blastoderm margin collapse into the yolk giving rise to the yolk syncytial layer, a multinucleated layer at the interface of the yolk and blastoderm. Beginning in the late blastula stage, cells rearrange to reshape the blastoderm such that the cells intercalate radially and spread over the yolk- a process called as epiboly. When the embryo reaches 50% epiboly stage, a thickened marginal region appears around the blastoderm rim that marks the onset of gastrulation. Within this thickened margin, there are two germ layers, epiblast, which later gives rise to the ectoderm and hypoblast which forms the endoderm and mesoderm. By 6hpf, convergent and extension movements initiate, resulting in dorsal accumulation of cells moving from ventral and lateral regions of the blastoderm. Simultaneously, dorsal blastomeres also intercalate with these converging cells, leading to extension of the anterior-posterior axis. Convergence of cells towards the dorsal side marks the shield stage, thickening of dorsal blastomeres equivalent to Spemann-Mangold organizer in *Xenopus laevis*. Following epiboly, the rudiments of the primary organs become more prominent as the tail bud forms, elongating the embryo. The early somites become visible anteriorly marking the start of segmentation period and the neural tube forms via secondary neurulation. The lumen of the neural tube, neurocoel forms by a process called as cavitation. By the end of segmentation period, the

cardiovascular system starts to develop and by 24hpf, the zebrafish embryo develops into an organized larva with majority of the organs formed.

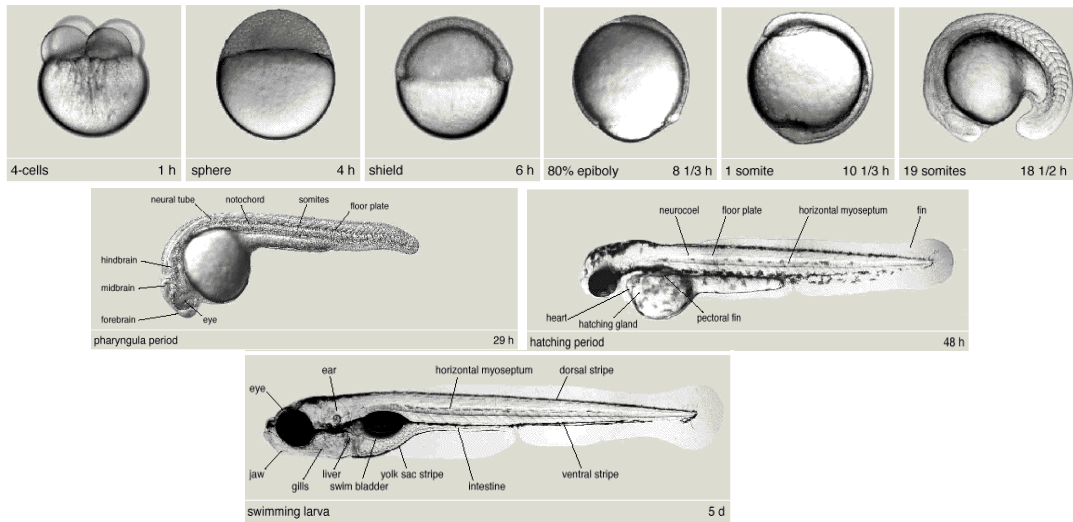


Figure 7: Zebrafish embryogenesis. Representation of first 24 hours of development indicating time of development and different structures formed during embryogenesis {adapted from (Haffter, Granato et al. 1996)}

CHAPTER 2
MATERIALS AND METHODS

MATERIALS AND METHODS

Yeast two-hybrid screen

A yeast two-hybrid screen was previously performed using a rat brain cDNA library (Clontech, Mountain View, CA) wherein PDZ domain spanning a fragment of Dishevelled, about 238-430 amino acids was used as bait and screened 3.9 million independent clones. 24 positives were obtained in this screen, of which Custos was found 22 times.

Cloning

NCBI BLAST was used to find the zebrafish homolog of the rat sequence of Custos obtained from the yeast two-hybrid screen. Primers were designed to amplify Custos based on sequence obtained from NCBI database. Custos fragment was isolated from a 24hpf zebrafish cDNA using an RT-PCR approach and Custos was sub-cloned into pCS2-GFP-N3, pCS2-Flag and pCS2+MT_(Myc-tagged) vector using restriction enzymes, Stu1 and Xho1. The truncates of Custos were generated using a PCR approach and subcloned into pCS2Myc and pCS2Flag vectors. Dishevelled (Dvl) and truncates of Dvl were previously generated by restriction digestion or PCR approach and subcloned into pCS2-Myc and pCS2-Flag vectors. *In situ* constructs were amplified by PCR and cloned into the pCS2-Myc Vector. For all our experiments we used mouse Dishevelled 2 (mDvl2) and zebrafish Custos.

Primers and PCR conditions

Below is a table of primers and conditions used for the indicated experiments for Custos and suitable control constructs (Table 1). All primers were ordered from Integrated DNA Technologies (Coralville, IA) and optimized according to primer melting temperatures and length of each construct. PCR cycles were performed in general as follows: 95° for 5 minutes; 25-30 cycles of 95° for 30 seconds, 50-55° for 30 seconds.

Experiment	Gene	Primer Sequence (5'-3')
RT-PCR	Custos	FOR:CGCCTACCGAATTTGATGAT REV:ATGTGCTGCATGTGGAAAAA
pCS2-Myc-Custos	Custos	FOR:GCCAATTCAAGGCCTATGTCTGAA REV:TAGAGGCTCGAGTCATTCATCGCC
Truncates	N-Custos	FOR:GAATTCAAGGCCTATGTCTG REV:AGGCTCGAGTCAAAGTGATTG
	C-Custos	FOR:GAATTCAAGGCCTATGACTTC REV:TAGAGGCTCGAGTCATTCATCT
	ΔNLS	FOR:GAATTCAAGGCCTATGTCTG REV:TAGAGGCTCGAGTCATGTGCT
	ΔNLS1	FOR:AAGAGACAGAGGATACAGTCACAACCTCCAGTGAG REV:CTCACTGGAGGTTGTGACTGTATCCTCTGTCTCTT
	ΔNLS2	FOR:GCTGGAGAGAGATTGAAAAAGAAAAGGAAAAAGT TGGAGGAG REV:CTCCTCCAACTTTTTCCTTTTCTTTTCAATCTCTC TCCAGC
	NLS12	FOR:AGGCCTGAGACAGAGGATACAG REV:AGGCCTCTCCTCCACCTCC
Heat Shock	Custos	FOR:GGATCCATGTCTGAAAGCAGCA REV:GGGGATCCTCATTCATCTTC

Table 2. List of primers used for indicated experiments. FOR: forward primer, REV: reverse primer.

RT-PCR

RNA was extracted from zebrafish embryos, ranging from 1hpf to 24hpf, homogenized in homogenization buffer (1M Tris pH 7.5, 5M NaCl, 0.5M EDTA pH 8, 10% SDS, 400 µg/ml Proteinase K) using traditional methods of RNA isolation. RNA was purified using phenol/chloroform extraction and 8M LiCl or TRIZOL method. Reverse transcription was performed using iScript cDNA Synthesis Kit. (Bio-Rad, Hercules, CA).

Antibodies and Immunoblot

Rabbit polyclonal-Flag antibody (Santa Cruz A-14, sc-789) was used for co-IP, while mouse monoclonal-Flag antibody (Sigma #F3165) was used for detection of Flag-tagged constructs in co-IP and immunofluorescence studies. Monoclonal Myc antibody (SantaCruz) was used for both IP and detection of Myc-tagged constructs via Western blot. Monoclonal β -catenin antibody (BD Transduction Labs #610154) was used for detection of β -catenin in Co-IP studies, immunofluorescence and immunoblotting. Actin (SantaCruz #C-2: sc-8432) was used as an internal control for all the immunoblots. All antibodies were used at optimized dilutions for each technique, with appropriate secondary antibodies accordingly.

Co-Immunoprecipitation Studies

For co-immunoprecipitation studies (Co-IPs) to determine Dishevelled interaction with Custos, Myc-tagged Custos was co-transfected with Flag-Dvl into HEK-293T cells (ATCC, Manassas, VA). HEK-293T cells were grown to ~70% confluence and counted for plating at a density of 1.2×10^6 cells/plate in 60 mm dishes containing DMEM supplemented with 10% Fetal Bovine Serum and 1X Penicillin/StreptoMycin and then returned to incubators overnight. A total of 2 μ g of DNA was dissolved in DMEM (without serum/antibiotics) to a total volume of 150 μ l, and 40 μ l of PolyFect Transfection Reagent was added to the DNA solution.. This was mixed and incubated for 10 minutes at room temperature to allow complex formation. While complex formation was taking place, the media was changed on the cell culture plates to fresh 293T-CM. After the 10-minute incubation, 1 ml of cell growth medium (containing serum and antibiotics) was added to the reaction mixture. The reaction was immediately transferred to the 60 mm dishes and gently swirled. Myc-tagged Custos and Flag-Dvl DNA alone were used as a negative control. Cells were then incubated for 24 hours at 37C. Following 24 hours of treatment, cells were washed with cold PBS and centrifuged for 10 minutes at 15000 RPM at 4°C. Supernatant was aspirated and cell pellet was lysed in pre-chilled 0.5%NP40 buffer (containing 1X protease and phosphatase inhibitor cocktail) on ice for 20 mins. Lysates were then centrifuged at 13,000 RPM, 4°C for 20 minutes. The supernatant was collected in a fresh tube and 20 μ l was subjected for western analysis.

For co-immunoprecipitation assays, 180 μ l of the cell lysate was added to 40 μ l of pre-washed Protein G-PLUS-Agarose beads (sc-2002, Santa Cruz, Santa Cruz, CA) (washed three times with lysis buffer) for 30 minutes at 4° on a nutator. After pre-clearing, the supernatant was divided into two tubes, and lysis buffer was added to reach a total of 500 μ l volume. Three μ l of antibody (either Myc or Flag) was added to each tube, and rotated overnight at 4°C on a nutator. The next morning, the lysate-antibody mixture was added to another set of pre-washed beads, and incubated for one hour at 4°C. Following this, the samples were spun down at 3000 rpm, and washed three times with lysis buffer. After the final wash, 30 μ l of 2XSDS buffer was added. Ten percent β -mercaptoethanol (BME) was added to whole cell lysate and IP samples, and the samples were boiled for 5 minutes at 98° on a hot plate, and immediately put on ice. Samples were then subjected to Western blotting, as described below.

In brief, 10% SDS-PAGE gels were made, and samples were loaded to each lane in the appropriate amount, and run at 120 volts. Gels were then transferred for 1 hour at 90 volts onto nitrocellulose membranes. Membranes were then blocked for 30 minutes in 10% nonfat dried milk in 1XPBST, and briefly washed with 1XPBST followed by incubation with the appropriate antibodies in sealed bags overnight at 4°C on a nutator. The following morning, blots were washed 3 times for five minutes each with 2% milk and incubated with the appropriate secondary antibody in 2% milk for one hour at room temperature. Blots were then washed 3 times with 2% milk for five

minutes each, and 1XPSBT 3 times for five minutes each. Blots were then added to an equal mixture of Solutions A and B of homemade ECL reagent, and developed using standard methods.

GST pull-down Assays

GST pull-down assay was performed using cell lysates of HEK293T cells transfected with full length Flag-Custos and purified GST or GST-PDZ. GST-PDZ construct was previously made, and transformed in BL21-DE3 bacterial cells for production of GST proteins. The GST proteins were purified using GST beads and their concentration and purity were tested by coomassie staining. Purified proteins were then used for the pull-down. GST pull-down assay was performed as previously described (Habas, Kato et al. 2001).

Luciferase reporter assays

HEK293T cells were co-transfected with TOPflash reporter plasmid, pSV40-RL(Promega) plasmid, Flag-Dishevelled or GFP- β -catenin and subjected to luciferase assay using the Dual Luciferase Reporter assay system (Promega) as per the manufacturer's protocol. Firefly luciferase and Renilla luciferase activities were measured and detected by 20/20 Luminometer (Turner Biosystems).

Immunofluorescence Studies

For immunofluorescence studies, HeLa cells (ATCC) were used according to manufacturer's protocol. The day before transfection, cells were seeded to 4×10^5 cells per well on a 6-well plate containing BD BioCoat fibronectin coated coverslips (BD Biosciences) in 3 ml of 293T-CM according to the Polyfect Transfection Reagent guidelines (Qiagen, Valencia, CA). Cells were kept at 37°C and 5% CO₂ in an incubator. The cells were transfected at 20-24 hours post seeding at 70% confluency. A total of 1.5 µg of DNA was dissolved in DMEM (without serum/antibiotics) to a total volume of 100 µl, and 12 µl of PolyFect Transfection Reagent was added to the DNA solution. This was mixed by vortex and incubated for 10 minutes at room temperature (20–25°C) to allow complex formation. While complex formation was taking place, the media was changed on the cell culture plates to fresh 293T-CM. After the 10-minute incubation, 600 µl of cell growth medium (containing serum and antibiotics) was added to the reaction tube. The reaction was immediately transferred to the 6-well plate and gently swirled. Cells were then incubated for 24-48 hours, depending on the experiment. In cells that were Wnt treated, the day after transfection the media was changed to DMEM only for serum starvation conditions. Cells were then treated the following day with 250 ng/ml Wnt3A or Wnt5A, depending on the experiment, for 3 hours, in 1% BSA in DMEM, while control (non-Wnt treated cells) were changed to media containing 1% BSA in DMEM for the three hour period.

For staining, cells were washed 2 times with 1XPBS briefly, and then fixed with 4% paraformaldehyde (PFH) for 30 minutes shaking at room temperature. Cells were then washed with 1XPBS briefly and then washed 3 times for 5 minutes each in 0.1% Triton in 1XPBS. Cells were then briefly washed with 1XPBS and blocked for one hour at room temperature in 5% fetal calf serum in 1XPBS. Cells were then washed briefly with 1XPBS, and incubated in primary antibody for one hour at a dilution of 1:200 in 5% serum. Cells were then washed 3 times in 5% serum, and then incubated with secondary antibody (1 μ l/ml secondary fluorescent conjugated antibody, 0.1 μ l DAPI, and 5 μ l/ml of either Texas Red Phalloidin Oregon Green Phalloidin when appropriate) for one hour at room temperature. Cells were then washed three times for five minutes each with 5% serum, followed by 3 washes in 1XPBS. Cell were then transferred to a glass slide and mounted with Fluoro-gel (Electron Microscopy Sciences, Hatfield, PA). Cells were visualized using a Zeiss Axiovert 100 confocal microscope and imaged using MetaMorph imaging software (Molecular Devices, LLC, Sunnyvale, CA).

Morpholinos

Morpholino oligonucleotides (MOs) were designed to block the start site of translation of *Custos* for knockdown experiments in zebrafish embryos. MOs were ordered from Gene Tools, LLC (Philomath, OR). The sequences can be found below.

Gene	Morpholino Sequence
Custos morpholino I	5'- CTGCTGCTTTCAGACATATTTGAGG-3'
Custos morpholino II	5' CTTCACTGCTGCTTTCAGACATATT-3'
Zebrafish p53 morpholino	5'- GCGCCATTGCTTTGC-3'
Control morpholino	5'- CCTCTTACCTCAGTTACAATTTATA-3'

Table 3. Morpholinos used for knockdown of Custos in zebrafish

In situ hybridization

Myc-tagged Custos was linearized by digestion with BamH1 (New England BioLabs) for SP6 sense probes, and PstI for T7 antisense probes. DNA was isolated by phenol/chloroform extraction, and the respective mMessage mMachine *in vitro* transcription kit (Ambion) was used in conjunction with DIG RNA Labeling Mix (Roche Applied Science, Indianapolis, IN). The probes were purified using the phenol/chloroform purification method. The *in situ* hybridization protocol was carried out according to standard lab protocol. In brief, embryos were collected at different stages and fixed in 4%Paraformaldehyde for 30mins. Embryos were dechorionated using forceps followed by dehydration in methanol at -20°C for 2hours prior to use. Embryos were rehydrated by successive incubation in 50%Methanol/PBST, 30%Methanol/PBST and 100%PBST respectively. Embryos were then incubated in pre-hybridization buffer for 1 hour at 65°C. Probes were dissolved in 0.5 ml hybridization buffer and incubated

overnight at 65°C. Embryos were washed with different dilutions of SSC and CHAPS, washed with MAB, and blocked with blocking solution for one hour. Blocking solution was replaced by blocking solution + pre-adsorbed antidigoxigenin AP antibody (Roche) for four hours at room temperature. Embryos were washed twice with PBST for 20mins, and incubated in PBST overnight at 4°C. Following day, embryos were washed with PBST 6 times and incubated in staining buffer for 5 minutes. Further, embryos were stained using 0.5 ml of BM Purple reagent (Roche). Staining was monitored every fifteen minutes, and more often when staining began to show. The chromogenic reaction was stopped and fixed with 4%PFA. All images were taken using a Nikon SMZ800 stereomicroscope.

Overexpression, Knockdown, and Rescue Studies in zebrafish

The evening prior to embryo injection, male and female zebrafish were separated in a breeding tank using a divider. The breeding tank typically features an outer tank, inner tank with small openings, divider and lid. The next morning, at dawn, the divider was removed and the females started spawning in 15-20 minutes. Once the eggs were laid, they fell down through the small openings of the inner tank into the bottom of the outer tank preventing the fish from eating their eggs. The eggs were collected in a petridish containing embryo water.

Needles were calibrated according to length and pressure to allow for a 3 nL injection per embryo. Embryos were injected with samples (RNA,

morpholino, or RNA + morpholino) at one cell stage in the appropriate amount according to the experiment. mRNAs for injection were made via *in vitro* transcription using the sp6 mMessage mMachine kit (Ambion, Austin, TX). Post-injection, embryos were transferred to a new petridish-containing embryo medium and incubated at 28°C for 4hours. Dead embryos were removed and fresh medium was added and scored for phenotype at 24hpf. Embryos were visualized under the Nikon SMZ800 stereomicroscope.

CRISPR/Cas9 knockout

CRISPR target site was designed as per the standard guidelines. The single guide RNAs (sgRNAs) were synthesized by annealing two oligonucleotides by PCR approach. Below is the table of target sites for CRISPR and primers required for sgRNA synthesis.

sgRNA	Target site ending with PAM sequence (NGG)	Restriction sites
SG11	5'- ACAATGGTAGACA <u>AAAGTCATAGG</u> -3'	PfI
SG12	5'-GAGCATGATGGGAAT <u>GAGCTCGG</u> -3'	AvaI
SG13	5'- GAAAAAGTTAGGA <u>ACCTATTTGG</u> -3'	NlaIV

Table 4: CRISPR/Cas9 target sites for knockout of Custos

sgRNA	Primers
SG11 For	5'CGCTAGCTAATACGACTCACTATAgACAATGGTAGACAAGT CATGTTTTAGAGCTAGAAATAG 3'
SG12 For	5'CGCTAGCTAATACGACTCACTATAgGAGCATGATGGGAATGAG CTGTTTTAGAGCTAGAAATAG 3'
SG13 For	5'CGCTAGCTAATACGACTCACTATAgGAAAAAGTTAGGAACCTA TTGTTTTAGAGCTAGAAATAG 3'
sgRNA Rev	5'AAAAGCACCGACTCGGTGCCACTTTTTCAAGTTGATAACGGAC TAGCCTTATTTAACTTGCTATTTCTAGCTCTAAAAC 3'
V5 donor oligo	5'TAGAAAACAATGGTAGACAAGGCAAGCCTATCCCAAACCCTCT GCTGGGCCTGGACTCCACAAGTCATAGGTGAGTTTACTT 3'

Table 5: Primers for synthesizing sgRNA

Synthesis of sgRNA and Cas9RNA

sgRNA was synthesized for each target site using the MegashortScript RNA synthesis kit. pT3TS-nls-Cas9-nls plasmid was obtained from Balciunas lab and linearized using XbaI. Cas9 RNA was synthesized using the T3 *mMessage mMachine in vitro* transcription kit.

Microinjection of zebrafish embryos with sgRNA and Cas9RNA

A wildtype cross was set up prior to injection day. On the day of microinjection, zebrafish embryos were co-injected with 30pg of sgRNA and 150pg of zebrafish Cas9 RNA at one cell stage. Embryos were then stored in an incubator at 28C. For V5 tag injection, zebrafish embryos were co-injected with 30pg of sgRNA, 150pg of human Cas9 RNA and 100nM of V5 oligo.

Genotyping of zebrafish embryos

The embryos were lysed in DNA extraction buffer with 10ul of Proteinase K and incubated at 65°C for 1 hour. Following lysis, the genomic DNA was precipitated using 100µl of ethanol. The target region was amplified and PCR cycles were performed in general as follows: 95°C for 5 minutes; 35-40 cycles of 95°C for 30 seconds, 45-65°C for 30 seconds. The amplified fragment was then subjected to restriction fragment length polymorphism. The primers are given in the table listed below.

oligos	Genotyping primers
zDBPF105	5'- TGTATTTCTGGCTATTGCTGTG -3'
zDBPR102	5'- CCTAACTTTTTTCGCAACATGGG-3'
V5F1	5'- GGCAAGCCTATCCCAAACCCTCTG-3'
V5R1	5'- TTCAGACTGAGCAGGTTCAACAGTG-3'
V5F2	5'- TGTATTTCTGGCTATTGCTGTG -3'
V5R2	5'- TTCAGACTGAGCAGGTTCAACAGTG-3'

Table 6: Primers for genotyping zebrafish embryos, tail-clipped genomic DNA and nested primers for V5 tag.

DNA sequencing

For sequencing, the genomic targets were PCR amplified and sent for sequencing to Genewiz Inc.

CHAPTER 3

RESULTS

Results

Custos interacts with Dishevelled

As the PDZ domain region of Dishevelled protein is epistatically positioned at the branch point between canonical and non-canonical Wnt signaling, we reasoned effectors that can regulate these pathways may bind to this region. To identify such effectors, a yeast two-hybrid screen was performed and Custos was one of the 24 positives obtained from this screen (Figure 8). As yeast two-hybrid screens can yield potential false positive interactors, it was necessary to confirm the interaction outside of the yeast system. We therefore employed mammalian culture cells to verify the interaction between Custos and Dishevelled using co-immunoprecipitation assays. We generated Custos and fragments of this protein. These include an amino-terminal fragment of Custos (N-Custos), a carboxyl terminal fragment of Custos (C-Custos), a fragment lacking the nuclear localization signals (delta NLS), a fragment lacking nuclear localization signal1 (delta NLS1), a fragment lacking nuclear localization signal 2 (delta NLS2), a fragment containing both the nuclear localization signals (NLS12). Custos and the fragments were subcloned into pCS2+Myc, pCS2+Flag and pCS2+HA vectors from here on referred to as Myc-, Flag- or HA- (Figure 9). Dishevelled and its fragments were already available in the laboratory. We used zebrafish Custos and mouse Dishevelled for all our experiments.

Myc-Custos along with Flag-Dvl were co-transfected into HEK293T cells and co-immunoprecipitation assays were performed. We observed that

Myc-Custos did specifically bind to Flag-Dvl (Figure 10A and 12). After 6 hours of Wnt treatment using Wnt3A conditioned medium but not control conditioned media, co-immunoprecipitation assay revealed that of Myc-Custos strongly bound to Flag-Dvl for 3 hours and the interaction reduced at 6 hours (Figure 12). To delineate the region within Dvl that binds to Custos, we co-transfected fragments of Dvl with Custos in HEK293T cells and performed co-immunoprecipitation experiments. We found that the fragment consisting the PDZ domain of Dvl interacts with Custos, thus confirming the yeast two-hybrid experiment (Figure 10B and 10C). GST pulldown assay also confirmed a strong interaction between Dvl and the fragment of Dvl containing the PDZ domain (Figure 11). After delineating the specific domain of Dishevelled that binds to Custos, different generated fragments of Custos were used to determine its binding region with Dishevelled. Interestingly, the co-immunoprecipitation assays revealed that the carboxyl terminus of Custos, specifically the fragments containing the two nuclear localization signals (NLS12) were important for the interaction of Custos with Dishevelled (Figure 10D).

Dishevelled promotes dephosphorylation of Custos

An analysis of the amino acid sequence of Custos using protein motif comparison revealed the presence of one consensus casein kinase 1 phosphorylation site within its amino terminus (Figure 14B). When HEK293T cells were co-transfected with Flag-Custos and GFP-Dvl,

interestingly, expressed Flag-Custos protein migrated as double bands in the presence of GFP-Dvl suggesting Custos may be dephosphorylated by the expression of the Dvl protein. To confirm this possibility, lysates of Flag-Custos were treated with an antartic phosphatase enzyme for 20 minutes. This resulted in a downshifted Custos band to the same position as observed with Dvl expression (Figure14A). These studies suggest that Dvl promotes a de-phosphorylation of Custos.

Custos- β -catenin interaction increases with Wnt treatment

β -catenin is a critical component of the canonical Wnt signaling pathway and cytoplasmically stabilized downstream of Dishevelled function. Since the PDZ domain of Dishevelled functions in canonical Wnt signaling, we were interested to examine whether Custos is a potential functional component in canonical Wnt signaling pathway. HEK293T cells were transfected with Myc-Custos and immunoprecipitation was performed to examine whether Custos may interact with β -catenin. Interestingly, β -catenin was found to bind with Myc-Custos. After 6 hours of Wnt treatment using Wnt3A conditioned medium but not control conditioned media, co-immunoprecipitation assay revealed that the binding of Myc-Custos and β -catenin was positively regulated by Wnt treatment (Figure 13).

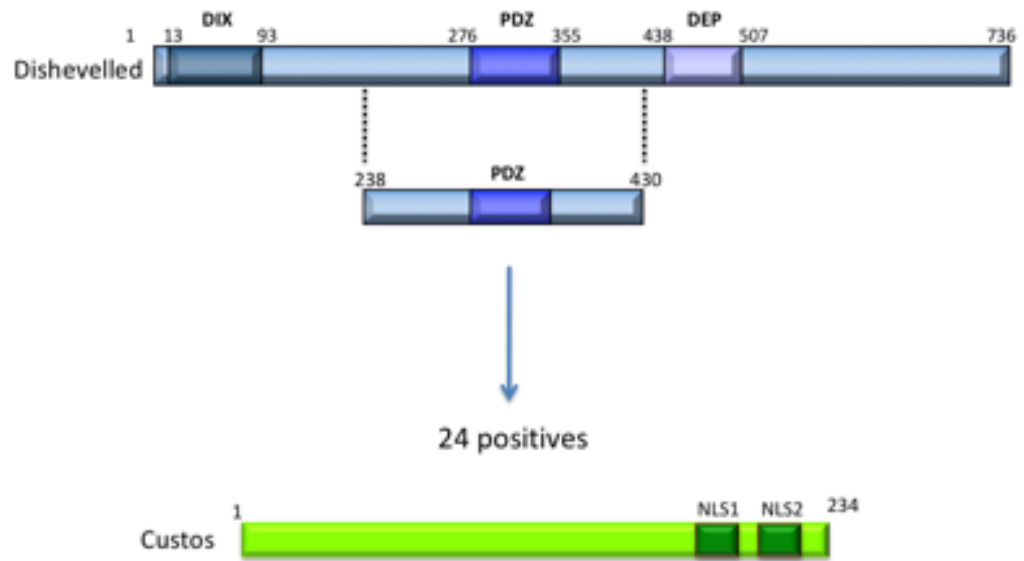


Figure 8: Schematic diagram of the PDZ domain region within Dishevelled that was used as a bait in the yeast two-hybrid screen. Out of 24 positives from this screen, Custos appeared 22 times. Protein domain structure of Custos is shown above. Numbers indicate amino acid positions. DIX: Dishevelled, Axin, PDZ: Post synaptic density 95, Discs Large, Zonula Occludens-1, DEP: Dishevelled, Egl-10, Pleckstrin. NLS1: nuclear localization signal 1, NLS2: nuclear localization signal 2.

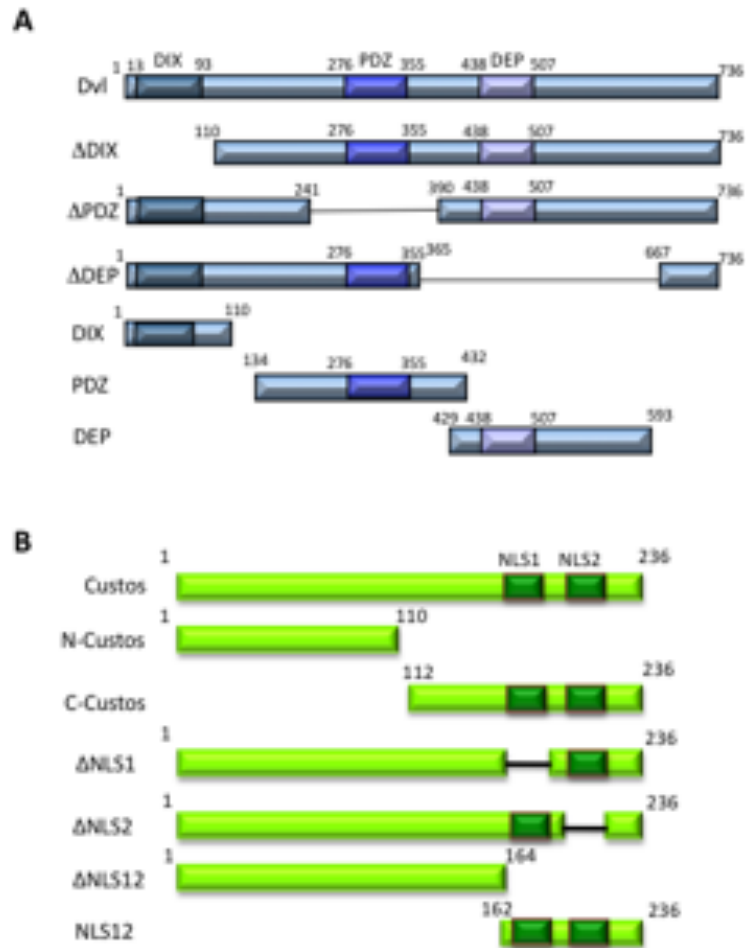


Figure 9: Schematic diagram of Dishevelled and Custos. A. Protein domain structure of Dishevelled and its truncated constructs. Numbers indicate amino acid positions. **B.** Protein domain structure of Custos and its truncated constructs. Numbers indicate amino acid positions.

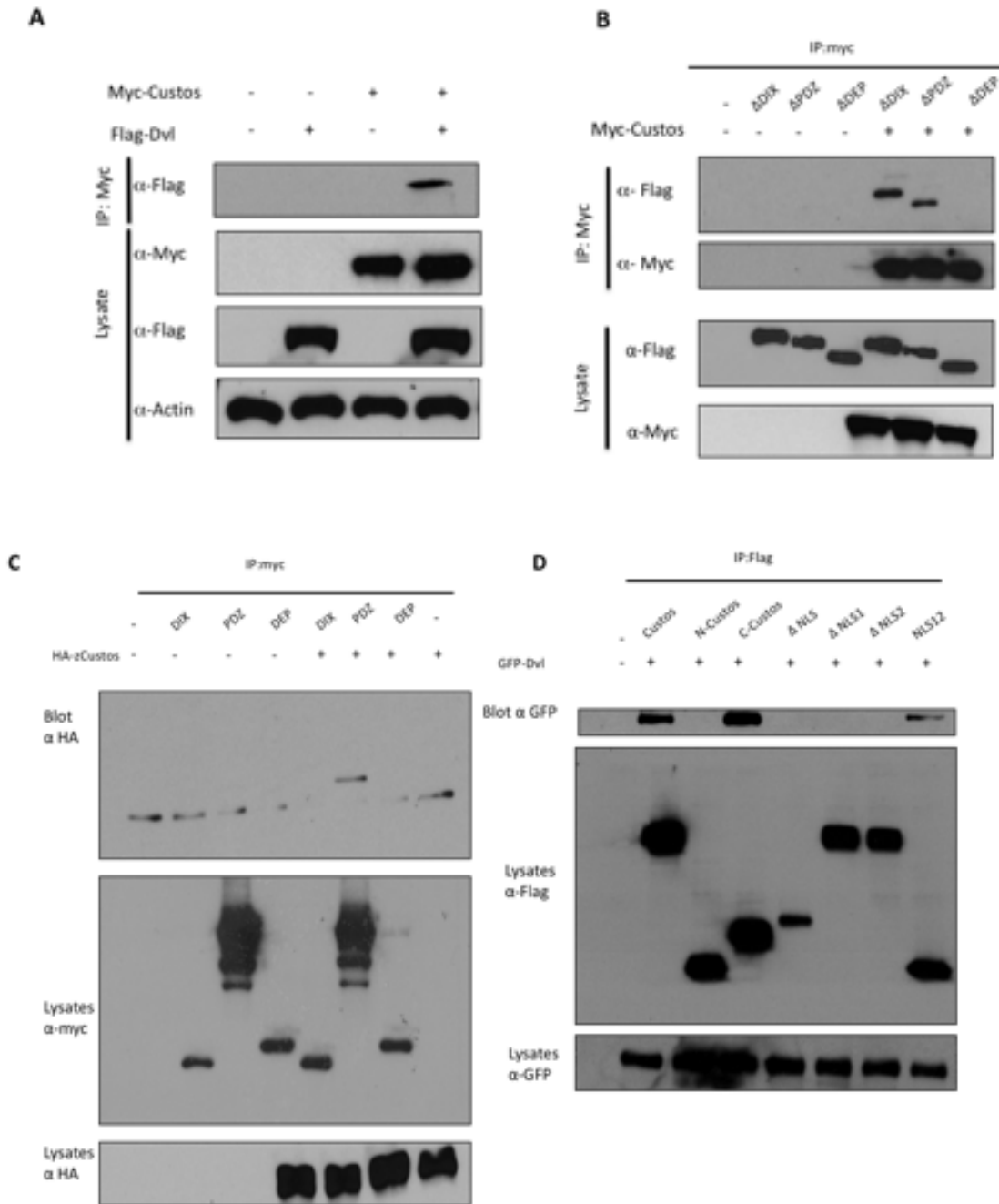


Figure 10: Custos interacts with Dishevelled **A.** Myc-Custos interacts with Flag-Dvl **B.** Myc-Custos binds to Flag-ΔDIX and Flag-ΔPDZ. **C.** HA-Custos binds to Myc-PDZ. **D.** GFP-Dvl interacts with Flag-Custos, Flag-C-Custos and Flag-NLS12.

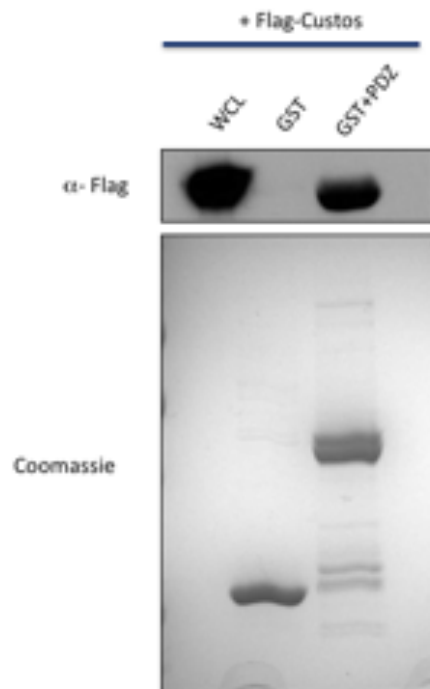


Figure 11: GST pull-down for Custos. Custos shows strong binding to the fragment containing the PDZ. The bottom panel is a Coomassie of the GST proteins to indicate a representative of the expression for each GST fusion protein.

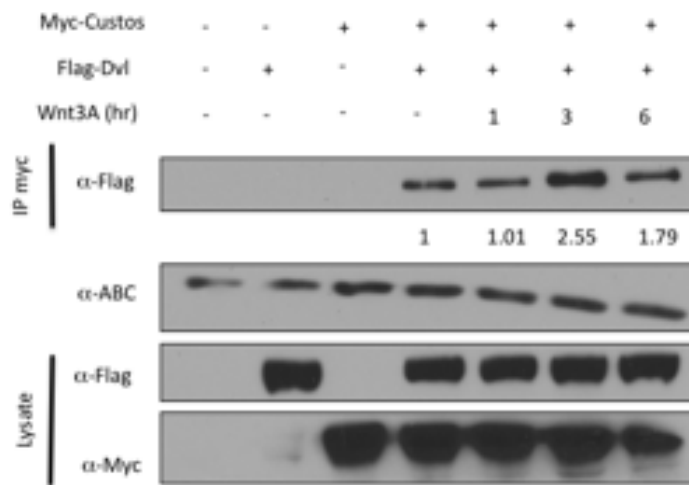


Figure 12: Custos binds to Dishevelled in response of Wnt treatment. The binding of Myc-Custos to Flag-Dvl increases with Wnt3A stimulation upto 3 hrs and decrease at 6hr.

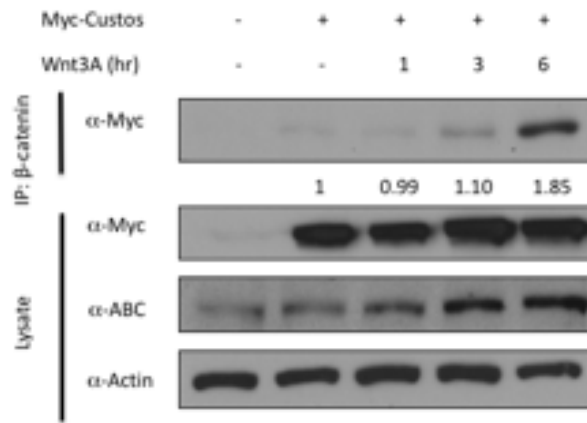


Figure 13: Custos binds to β -catenin in response to Wnt treatment. The binding of Myc-Custos to β -catenin increases with Wnt3A stimulation.

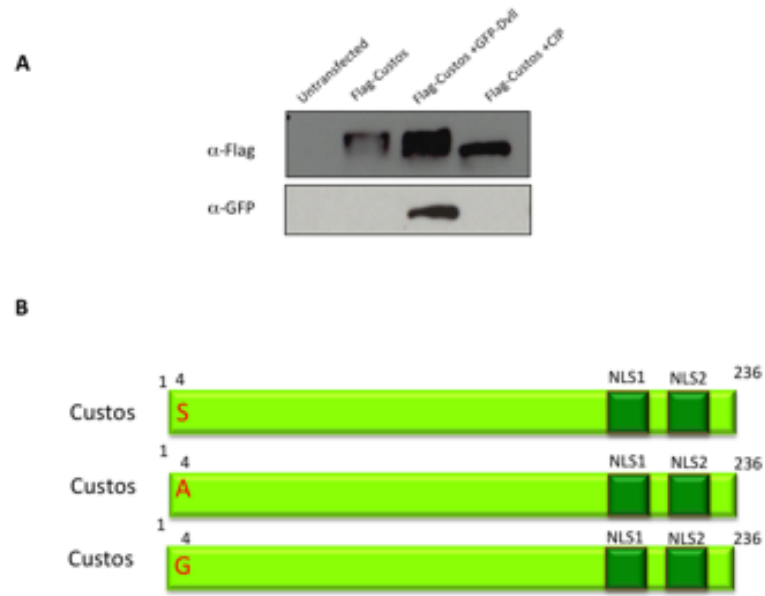


Figure 14: Dephosphorylation of Custos. **A.** Dephosphorylation of Custos in presence of Dishevelled and after treatment with calf intestinal phosphatase **B.** Putative phosphorylation sites within Custos. Protein structure of Custos with its phosphorylation site and constructs of Custos where its phosphorylation site was mutated. S: serine, A: alanine, G: glutamine. Numbers indicate amino acid positions.

Subcellular localization of Myc-Custos

As Dishevelled is localized in the cytoplasm and there are conflicting reports as to whether Dishevelled is also localized within the nucleus, we sought to determine the sub-cellular localization of Custos. As Custos has two putative nuclear localization signals, NLS1 and NLS2, this protein may be localized within the nucleus or even perinuclear region. HeLa cells were transfected with Myc-Custos and immunostaining was performed to image its sub-cellular localization in the presence or absence of Wnt stimulation. Cells were further stained with anti- β -catenin and anti-Myc antibodies and DAPI was used to stain the nucleus. This study revealed that indeed Custos was found to localize in and around the nucleus (Figure 15A, lower panel). Myc-Custos localized in and around the nucleus and interestingly Wnt3A treatment had no effect on localization of Custos (Figure 15A, lower panel).

We next sought to determine if Custos co-localized or affected the sub-cellular localization of β -catenin. HeLa cells were transfected with Myc-Custos and 24 hours post transfection, cells were serum starved for cell cycle synchronization. After 24h serum starvation, cells were treated with Wnt3A conditioned medium for 3h. We observed, β -catenin accumulated in the nucleus after Wnt3A treatment in HeLa cells, however in Myc-Custos expressing cells, β -catenin failed to accumulate in the nucleus. These results were quantified by calculating the percentage of cells that showed translocation of β -catenin in the nucleus in both un-transfected and Myc-Custos transfected cells (Figure 15B). These results indicated that expression

of Custos inhibits the nuclear translocation of β -catenin, leading to an inhibition of canonical Wnt signaling.

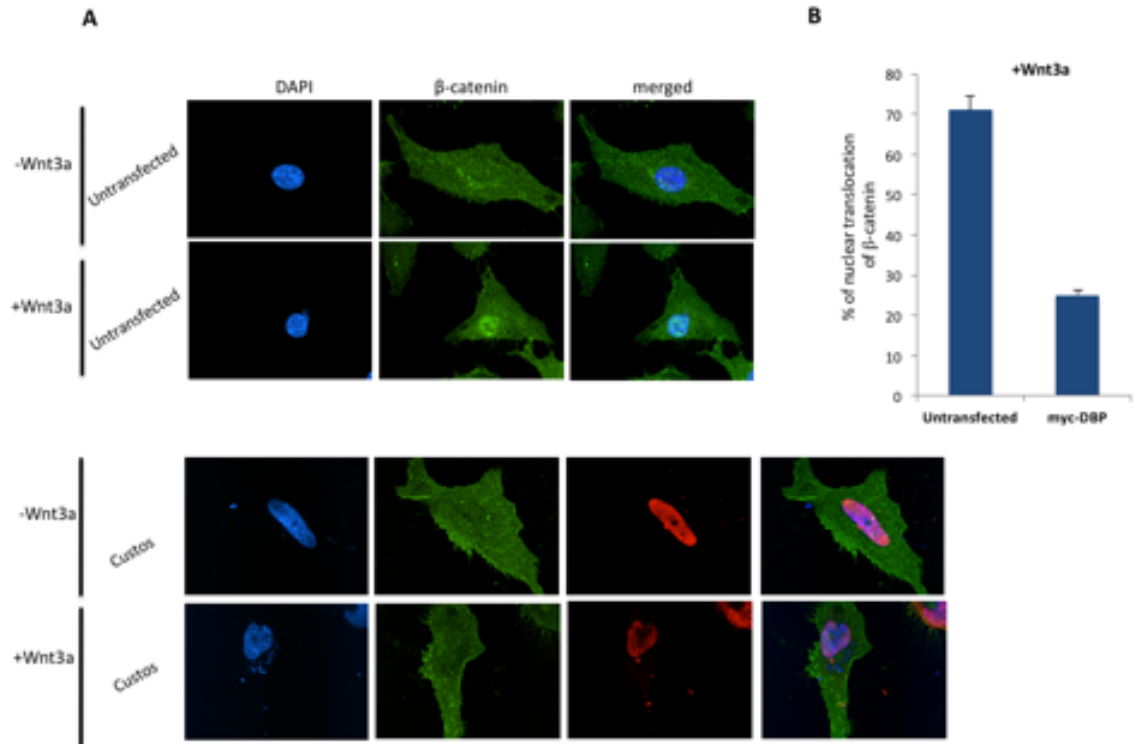


Figure 15: Subcellular localization of Myc-Custos and effect of overexpression of Myc-Custos on Wnt signaling. **A.** Untransfected HeLa cells showing the efficacy of Wnt treatment. Cells that were treated with Wnt3A show translocation of β -catenin to the nucleus. Myc-Custos is localized in and around the nucleus. With Wnt3A treatment localization of Myc-Custos did not change. The nuclear localization of β -catenin was inhibited in cells expressing Myc-Custos. **B.** Quantification of nuclear localization of β -catenin in untransfected and Myc-Custos transfected cells in response to Wnt treatment. 70% of untransfected cells show β -catenin in the nucleus whereas only 28% of Myc-Custos expressing cells show β -catenin in the nucleus.

Custos colocalizes with a nuclear envelope marker

Our previous binding studies demonstrate that β -catenin can bind to Custos. It is known that β -catenin in order to translocate from the cytoplasm into the nucleus interacts with components of nuclear pore complex. Our studies show a striking localization of Custos in and around the nucleus suggesting that Custos may be localizing to the nuclear envelope in the cell. To clarify this hypothesis, HeLa cells were transfected with Myc-Custos and immunostaining was performed. The cells were stained with anti-Myc and anti-lamin antibody; DAPI was used to stain the nuclei. Interestingly, Myc-Custos strongly colocalized with the nuclear envelope marker, lamin. When treated with Wnt3A conditioned medium, there was no change in localization of both Custos and lamin and were still co-localized on the nuclear envelope (Figure 16).

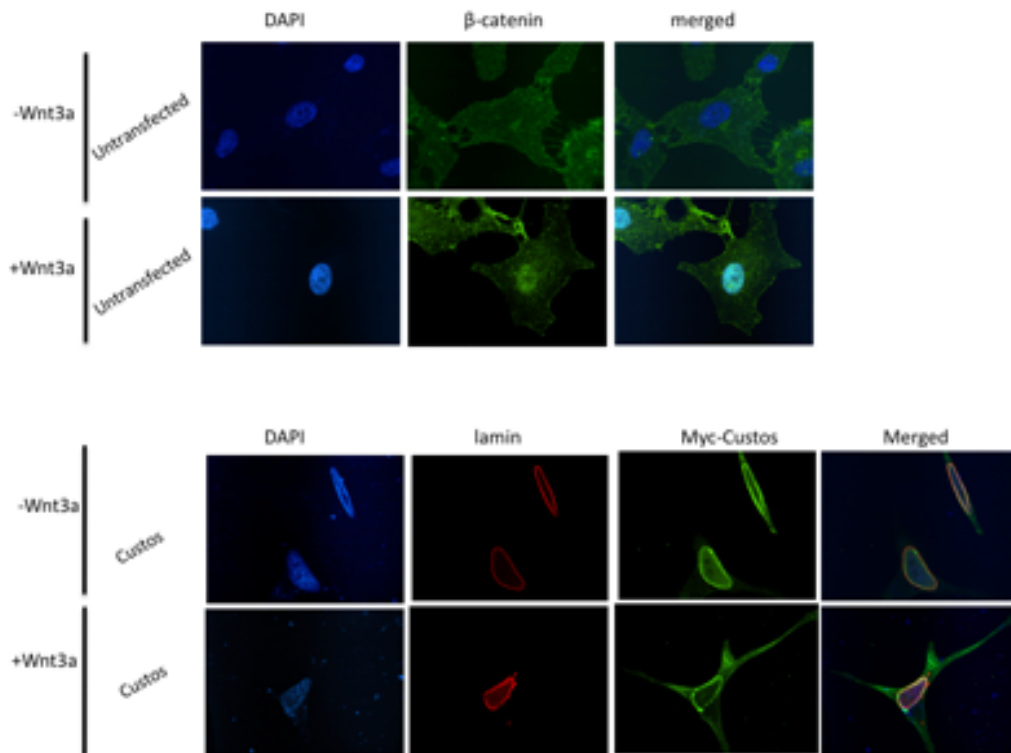


Figure 16: Myc-Custos colocalizes with lamin. In control conditions, Myc-Custos and lamin colocalize on the nuclear envelope. In Wnt-treated conditions, there was no change in the co-localization pattern of Myc-Custos and lamin.

Subcellular localization of truncated constructs of Flag-Custos

To understand the requirement(s) of the protein domains within Flag-Custos for its subcellular localization, truncated constructs of Flag-Custos were transfected in HeLa cells and their localization pattern was studied. Immunostaining experiments revealed that amino-terminus of Flag-Custos was localized in the cytoplasm unlike Flag-Custos. The carboxyl terminus of Custos was localized in and around the nucleus similar to the pattern of full length Flag-Custos localization. Δ NLS construct also lost its nuclear localization and relocated into the cytoplasm, whereas NLS1, NLS2 and NLS12 constructs were localized in and around the nucleus (Figure 17). These results were quantified by calculating the percentage of cells that showed nuclear localization of β -catenin in the nucleus in both untransfected and Myc-Custos transfected cells in response to Wnt treatment (Figure 18). These results indicated that both the nuclear localization signals, NLS1 and NLS2 of Custos play a critical role in negatively regulating Wnt signaling.

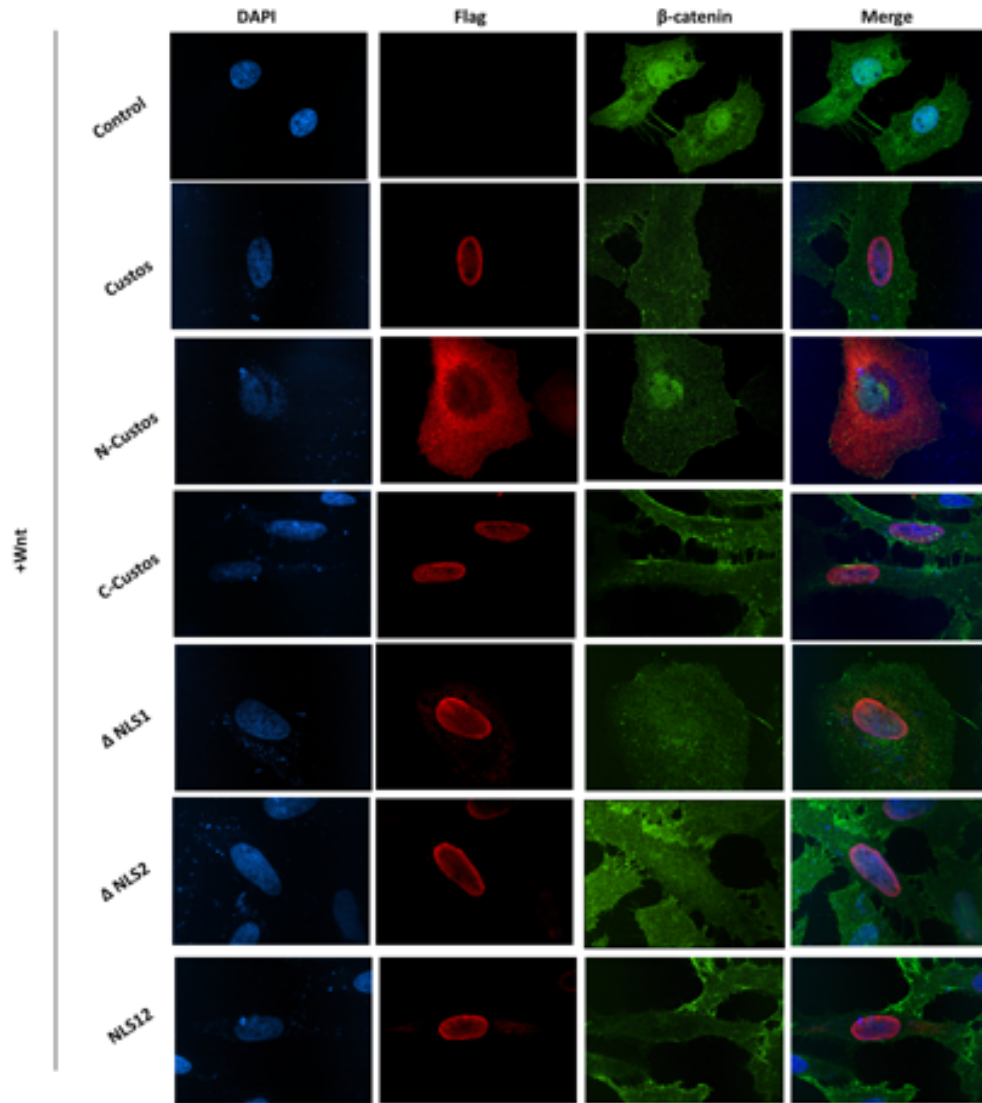


Figure 17: Subcellular localization of Flag-Custos and its fragments and effect of overexpression of Flag-Custos and its fragments on Wnt signaling. A. Control HeLa cells showing the efficacy of Wnt treatment. Cells that were treated with Wnt3A conditioned medium show translocation of β -catenin to the nucleus. Flag-Custos, C-Custos, Δ NLS1, Δ NLS2 and NLS12 are localized in and around the nucleus whereas N-Custos is localized in the cytoplasm. The nuclear localization of β -catenin was inhibited in cells expressing Flag-Custos, C-Custos, Δ NLS1, Δ NLS2 and NLS12, but was not affected in the cells expressing N-Custos.

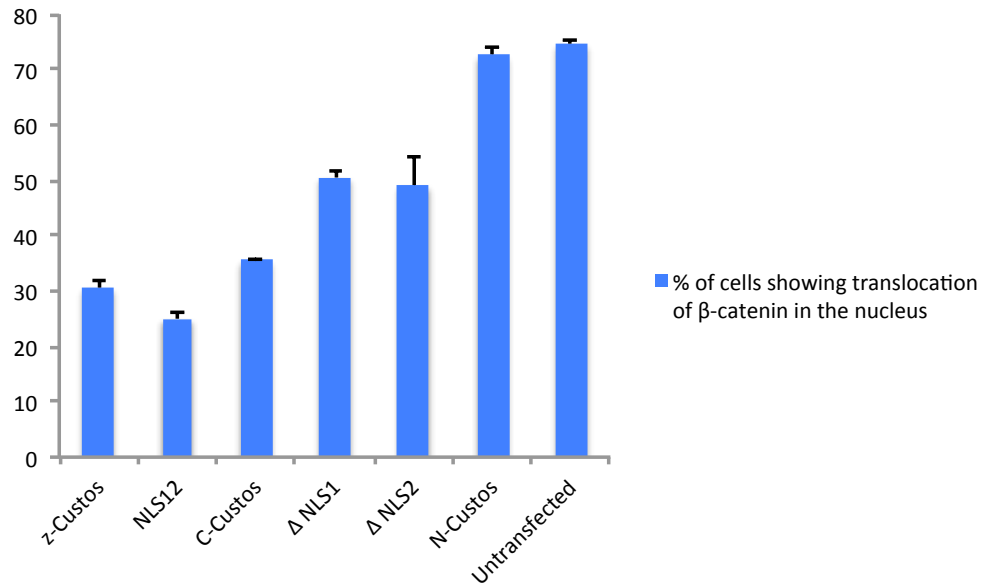


Figure 18: Quantification of nuclear localization of β -catenin in untransfected and Myc-Custos and its truncated constructs transfected cells in response to Wnt stimulation. Custos, NLS12 and C-Custos expressing cells show approximately 28-35% cells showing β -catenin in the nucleus, whereas untransfected and N-Custos show the highest percentage of cells having β -catenin in the nucleus. Δ NLS1 and Δ NLS2 show approximately 45% of cells having β -catenin in the nucleus.

Custos does not colocalize with Dishevelled

Since, Custos was found as Dishevelled interacting protein from the yeast two hybrid screen and Custos also strongly bound to Dishevelled in co-immunoprecipitation studies, we sought next sought to determine if these two proteins colocalized subcellularly. Hela cells were transfected with Myc-Custos and Flag-Dvl and 24 hours post transfection, cells were serum starved for cell cycle synchronization. After 24h serum starvation, cells were treated with Wnt3A conditioned medium for 3h. Surprisingly, I did not see any colocalization of Dishevelled and Custos in Hela cells with or without Wnt treatment (Figure 19).

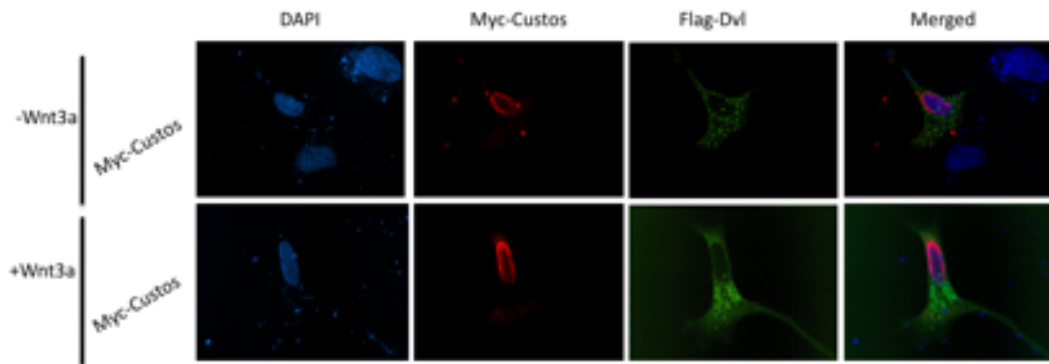


Figure 19. Myc-Custos does not colocalize with Flag-Dvl. In both control and Wnt-treated conditions, no significant colocalization is seen with Custos and Dishevelled.

Custos inhibits canonical Wnt signaling

To delineate the epistatic position of Custos in Wnt signaling pathway, we performed TOPflash assay. The TOPflash plasmid encodes a luciferase reporter downstream of six TCF binding sites. The TOPflash reporter gene is transcriptionally activated by positive canonical Wnt signaling components such as Wnt1, Dvl and β -catenin (Figure 20A). HEK293T cells were co-transfected with increasing doses of Myc-Custos along Wnt1, Dvl and β -catenin respectively. We found that Custos dose-dependently inhibited the transcriptional activation of reporter gene by Wnt1, Dvl and β -catenin (Figure 20A and B). These results implied that Custos functions downstream of Dishevelled.

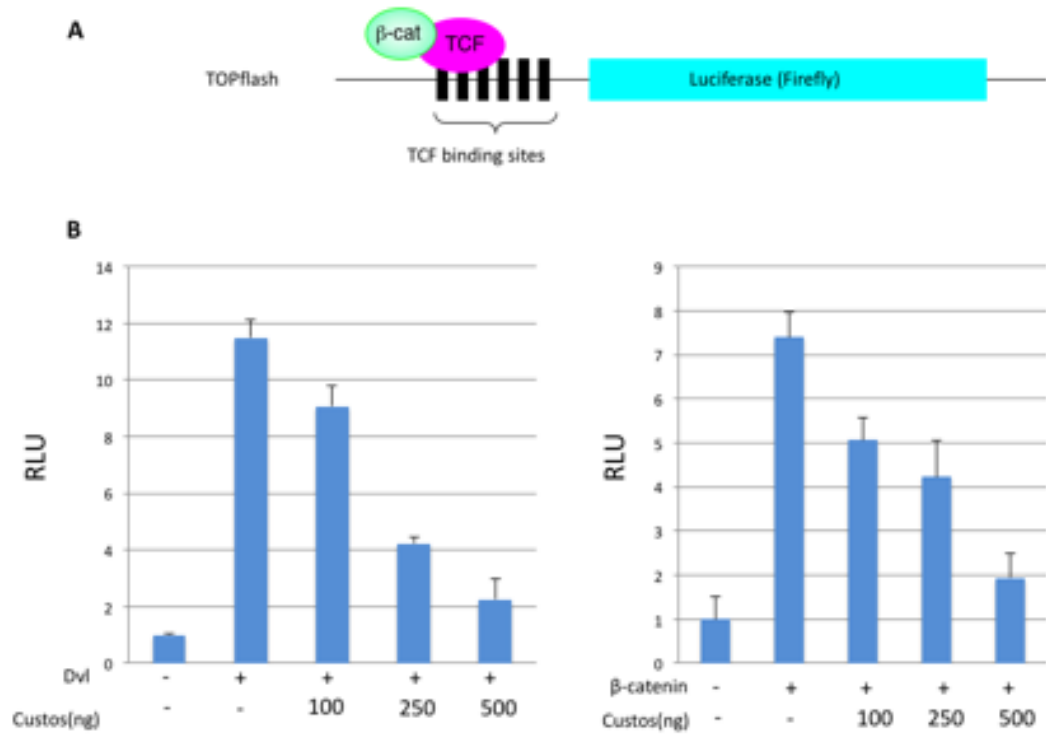


Figure 20: TOPflash luciferase assay **A.** Diagrammatic representation of a TOPflash plasmid encoding a firefly luciferase gene. TOPflash reporter gene is transcriptionally activated by canonical Wnt components that positively regulate signaling such as Dvl and β -catenin. **B.** Custos inhibits the transcriptional activation of the reporter gene by Dvl and β -catenin.

Temporal and spatial expression of Custos during early zebrafish development

Our studies thus far reveal that Custos is a Dishevelled and β -catenin binding protein that appears to negatively regulate canonical Wnt signaling. To unravel the role of Custos during zebrafish embryonic development, we first examined the temporal and spatial expression pattern of Custos. Zebrafish embryos were collected at different stages of development and subjected to RT-PCR. The temporal expression pattern revealed that Custos was a maternally expressed gene, expressed during the early stages of development especially during cleavage stage. Custos was expressed through the shield stage but the expression decreased during gastrulation and again expressed during brain development as compared to the internal control, EF1 α (Figure 21A).

Whole mount *in situ* hybridization was next performed to examine the spatial expression of Custos during early zebrafish development. During early stages of development, Custos was expressed in the blastomeres, especially in the yolk syncytial layer. By bud stage, Custos expression was detected on the dorsal side of the embryo and by 24hpf; the expression became refined to the brain region, hatching gland, pectoral fin and the tail region (Figure 21B).

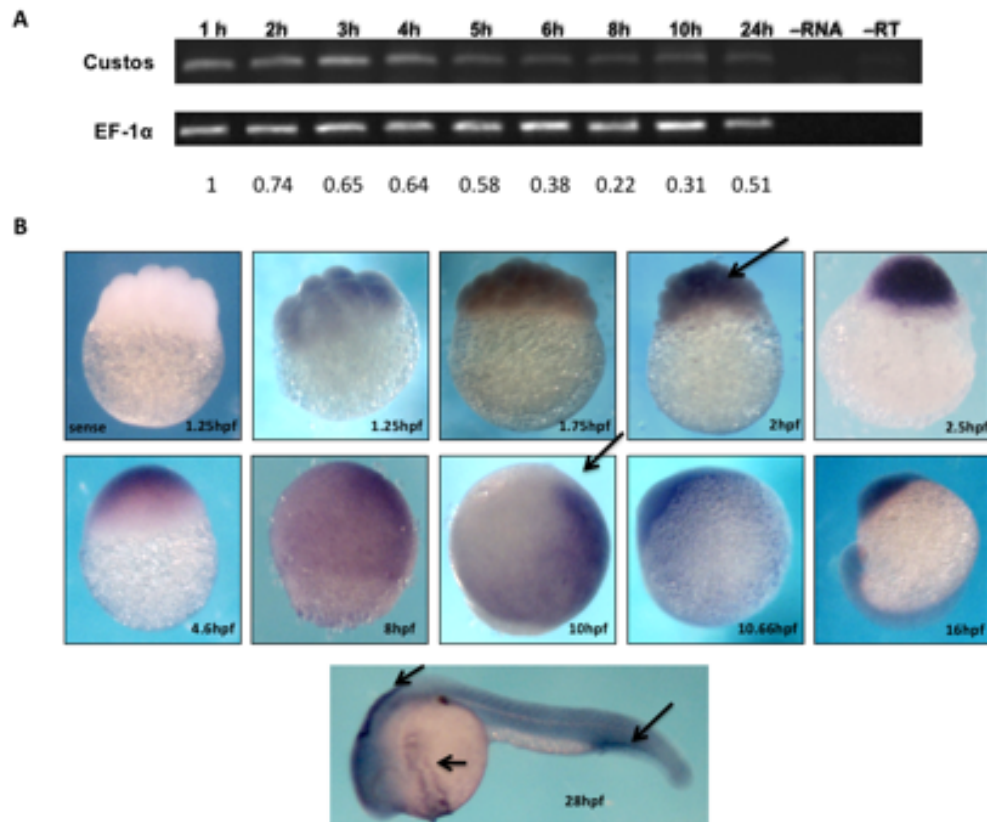


Figure 21: Expression pattern of Custos during zebrafish development. **A.** RT-PCR reveals the temporal expression pattern of Custos as compared to EF-1 α which is used as an internal control. Custos is a maternal gene and is expressed during all stages of development. -RT indicates no reverse transcriptase; -RNA indicates RNA was not used. Numbers indicate expression of Custos normalized to EF-1 α . **B.** *In situ* hybridization reveals the spatial expression pattern of Custos. In early stages, Custos is expressed in the blastomeres during cleavage stage especially in the yolk syncytial layer. During gastrulation, Custos expression becomes refined to the dorsal side of the embryo. By 24hpf, Custos is strongly expressed in the brain, hatching gland, pectoral fin and tail region. Arrows indicate expression of Custos.

Custos is required for anterior development

Zebrafish serves as an outstanding model to study vertebrate development because of its optical clarity and high fecundity. There are two major strategies used to study the *in vivo* function of a gene during development. Overexpression of *in vitro* transcribed mRNA is a commonly used gain-of-function approach in addressing the specific function of a protein during zebrafish development. In the reverse approach, a loss of function of gene can be studied using modified anti-sense oligonucleotides called morpholinos. To uncover the biological role of *Custos in vivo*, we first employed a gain of function strategy. *Custos* mRNA was synthesized using the SP6 mMessage mMachine transcription kit. Zebrafish embryos at 1 cell stage were injected with 25pg, 50pg and 100pg of *Custos* mRNA respectively and incubated at 28°C. Phenotypic assessments of these embryos at 24hpf revealed that *Custos* mRNA dose-dependently produces a ventralization of the injected embryo (Figure 22A and B).

The use of anti-sense oligonucleotides is a commonly used method to knockdown gene expression in various model organisms. Morpholinos (MOs) are synthetic oligonucleotides that bind to complementary RNA *in vivo* and block the initiation of translation of the coding protein of interest. To confirm the specificity of the morpholino approach, rescue experiments are performed, wherein an mRNA is injected in the embryo that codes for the protein of interest, but lacks the morpholino-binding site so that the translation of the rescue mRNA is unaffected. Should the morpholino

microinjection in zebrafish embryos produces a phenotype, that the phenotype produced by the morpholino would be suppressed or rescued by morpholino insensitive mRNA. Another way to confirm that the knockdown phenotype produced by the morpholino is further specific is by using two different morpholinos targeting the same gene. If the phenotype caused by two different morpholinos is the same, one can be more confident about the function of the intended target gene. We used two independent morpholinos for knockdown of Custos RNA translation, Custos MO1 and Custos MO2. Microinjection of either morpholinos produced embryos with small head and reduced eye structures. The embryos were scored using the established V1-V4 scoring system (Figure 23 and 24). The morpholino effects were specific and were rescued by co-injecting either Custos MO1 and Custos MO2 along with the Custos rescue mRNA. Interestingly, both the overexpression and knockdown of Custos generated similar phenotype suggesting optimal levels of Custos may be required for canonical Wnt signaling during development of zebrafish embryo.

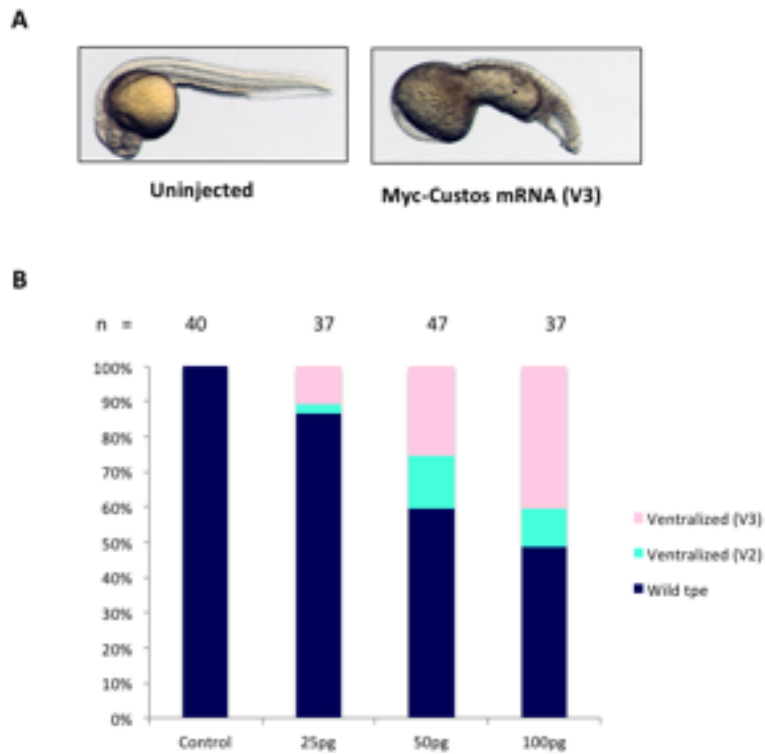


Figure 22: Overexpression of Custos interferes with anterior development. **A** Uninjected fish embryo showing normal zebrafish development, whereas Myc-Custos mRNA injected embryo at 25pg displaying anterior defect, especially ventralization phenotype. **B.** Quantification of Custos RNA injection studies. mRNA injection of zCustos produces a dose-dependent ventralization phenotype. Embryos were scored as V1 if the embryo displayed a mild shortened body axis and/or anterior defect. Embryos were scored as V3 if the embryo was severely shortened and exhibited a completely loss of anterior region. n represents number of embryos used for each injection.

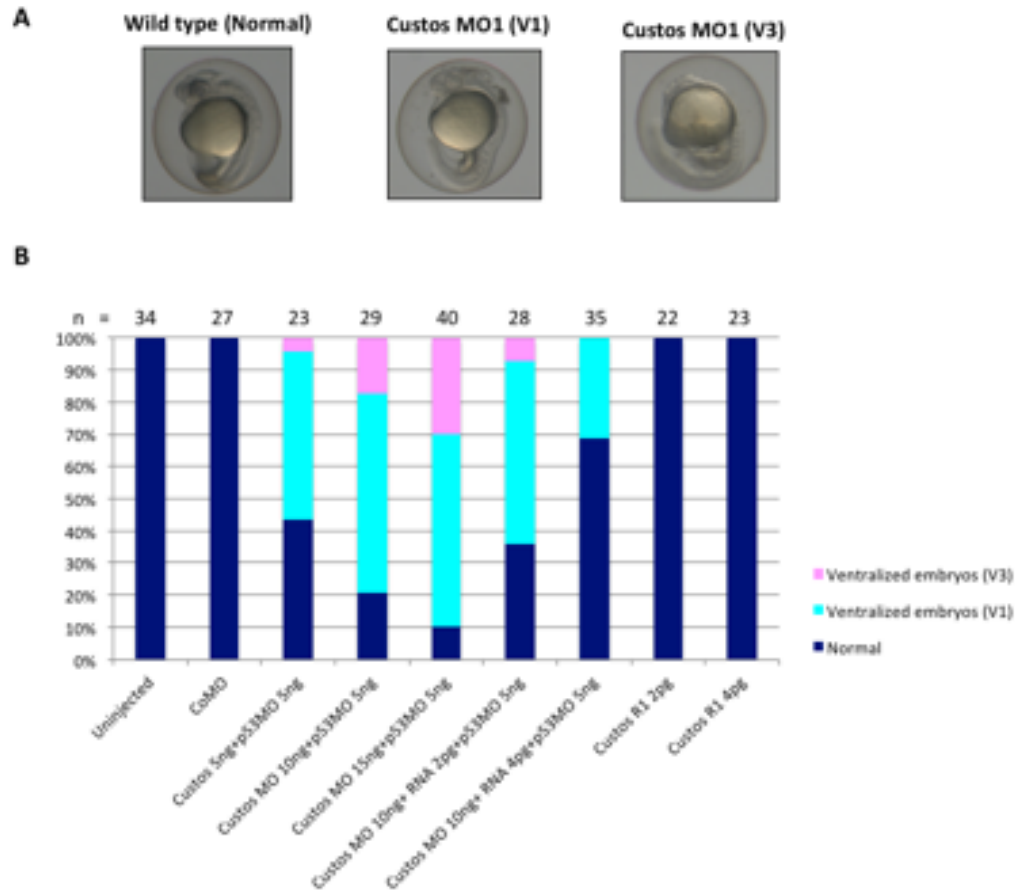


Figure 23: Knockdown of Custos causes ventralization defects. A Uninjected fish embryo shows normal zebrafish development, whereas Custos MO1 injected embryo displays anterior defect, especially ventralization phenotype scored as V1 and V3. **B.** Quantification of Custos MO1 microinjection studies. Uninjected and control morpholino injected embryos show normal development. Knockdown of Custos causes dose-dependent severity of the ventralization phenotype. Embryos were scored as V1 if the embryo displayed a mild shortened body axis and/or anterior defect. Embryos were scored as V3 if the embryo was severely shortened and exhibited a completely loss of anterior region. n represents number of embryos used for each injection. The morphant phenotype was rescued using 4pg of Custos rescue RNA.

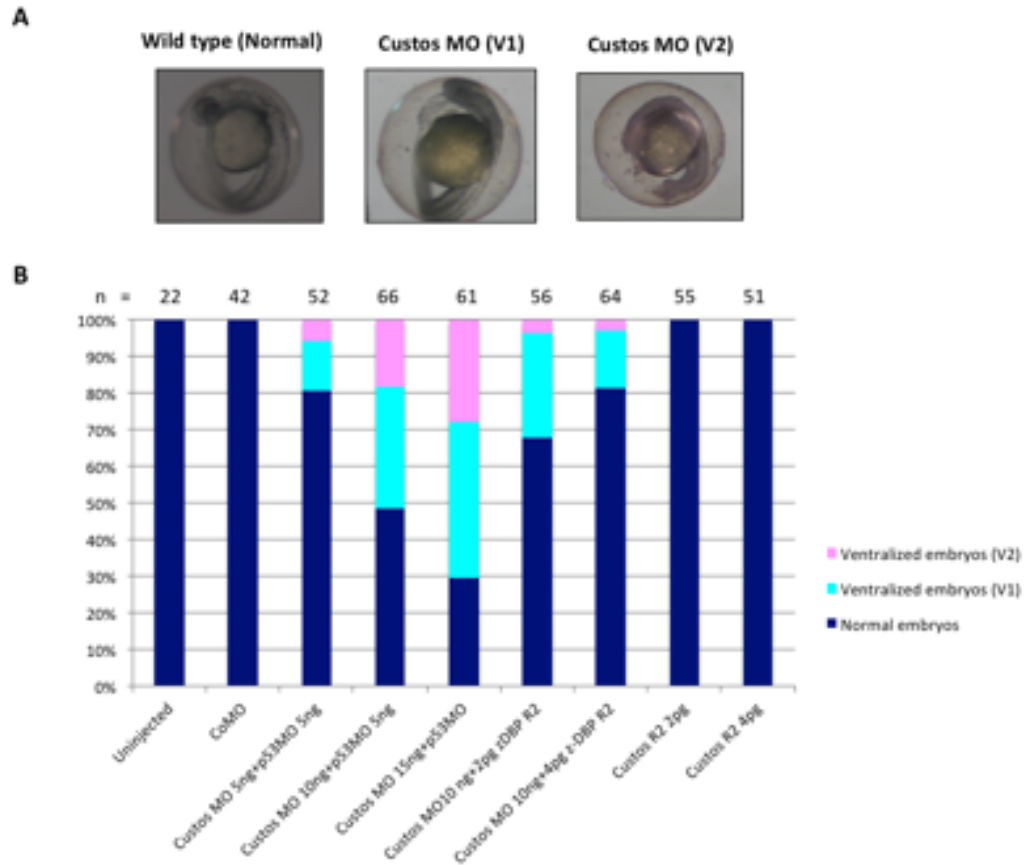


Figure 24: Knockdown of Custos using a second Custos morpholino produces ventralization defects. **A** Uninjected fish embryo shows normal zebrafish development, whereas Custos MO2 injected embryo displays anterior defect, especially ventralization phenotype scored as V1 and V3. **B.** Quantification of Custos MO1 microinjection studies. Uninjected and control morpholino injected embryos show normal development. Knockdown of Custos causes dose-dependent severity of the ventralization phenotype. Embryos were scored as V1 if the embryo displayed a mild shortened body axis and/or anterior defect. Embryos were scored as V2 if the embryo was severely shortened and exhibited a completely loss of anterior region. n represents number of embryos used for each injection.

Knockdown of Custos does not have effect on mesodermal induction

β -catenin is one of the earliest known factor to specify dorsal fate along the dorsal-ventral axis. It is known that prevention of nuclear accumulation of β -catenin produces a ventralized phenotypes in zebrafish embryos. The yolk syncytial layer in zebrafish is essential for induction and patterning of the mesoderm. *In situ* hybridization data suggests that Custos is expressed in the yolk syncytial layer and knockdown experiments reveal that Custos morphants have ventralized phenotype. Hence, we sought to examine whether Custos could be regulating mesodermal induction during zebrafish development. To examine this possibility, we performed RT-PCR on embryos injected with Custos morpholino and on the embryos co-injected with the Custos rescue RNA to analyze the expression levels of two distinct mesodermal markers. We examined the change in the expression levels of mesodermal markers, floating head (*flh*) and goosecoid (*gsc*) and surprisingly found that knockdown or rescue of morphants did not have any effect on the expression of these mesodermal marker genes (Figure 25). However, it is likely that the morpholino may not be sufficient at reducing the maternal store of Custos protein present in the embryos. EF1 α was used as an internal control and did not have any change in expression levels for both the mesodermal markers.

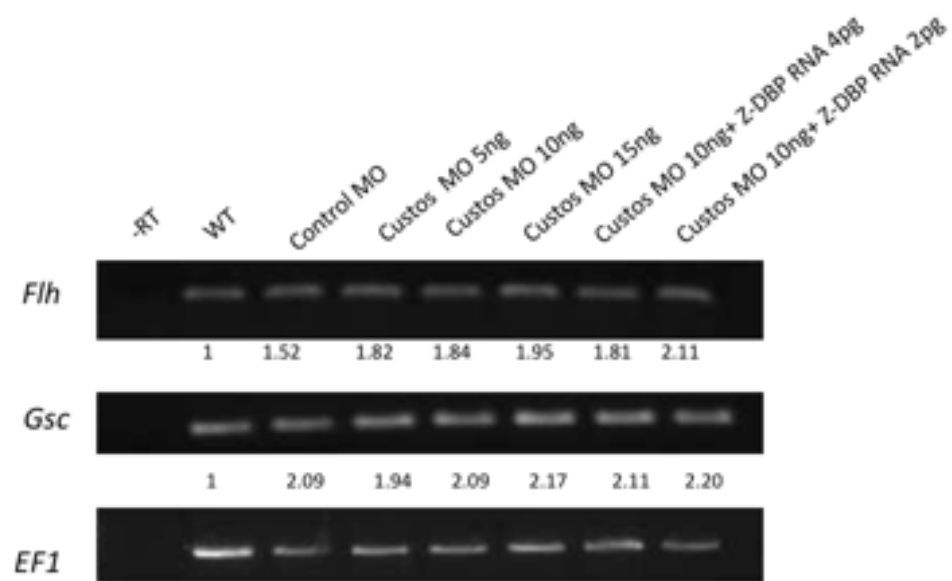


Figure 25: Effect of Custos knockdown on mesodermal induction. The expression of mesodermal markers, *flh* and *Gsc* are not affected by Custos knockdown or rescue as compared to EF1 α . -RT indicates absence reverse transcriptase.

Design and synthesis of CRISPR/Cas9

To further study the requirement for Custos during early development and to eliminate the maternal stores of Custos protein, we employed a genetic approach to stably knockout Custos using CRISPR/Cas9 technology. We designed sgRNA complementary to target sequence in the Custos DNA followed by protospacer adjacent motif (PAM) site. We selected the targets such that the CRISPR will create a disruption in or near a restriction site making it easier for genotyping. Three sgRNAs were designed to target Exon 2 and Exon 3 on the genomic loci; SG11, SG12 and SG13 respectively. We used two different Cas9 vectors, nuclear localized zebrafish codon optimized Cas9 (nls-zCas9-nls)(Jao, Wente et al. 2013) and human Cas9(Hwang, Fu et al. 2013) for our studies. The single guide primers for each target were designed and the respective fragments were amplified using the pDR274 vector. The three single guide RNAs were synthesized from the amplified fragments using the MegaShortscript T7 *in vitro* transcription kit. nls-Cas9-nls RNA was generated using the T7 mMessage mMachine *in vitro* transcription kit.

Custos gene disruption in F0 embryos

Each sgRNA (30pg) was co-injected with nls-Cas9-nls RNA (150pg) at the one cell stage of zebrafish embryo. The following day, 4 normal embryos and 4 deformed embryos from the Exon 2 targeted SG11 injected pool were selected and genomic DNA was isolated from these embryos. Genotyping

primers were used to amplify the respective target and digested with the respective restriction enzymes. For Exon 3 targeted SG12 and SG13 injected embryos, 20 embryos were pooled together and subjected to genotyping and restriction fragment length polymorphism. Partial digestion of the SG11 target site using PflF1enzyme was observed in SG11 CRISPR/Cas9 injected embryos at F0 compared to uninjected samples indicated successful mutagenesis of F0 embryos (Figure 26 A and B). SG12 and SG13 injected embryos did show partial digestion as compared to un-injected fish but most of the sample was digested indicating low mutagenesis efficiency (Figure 27 A, B, C, D and E). These results suggested that the mutagenesis rate in SG11 CRISPR/Cas9 injected fish was much higher than the SG12 and SG13 CRISPR/Cas9 injected fish.

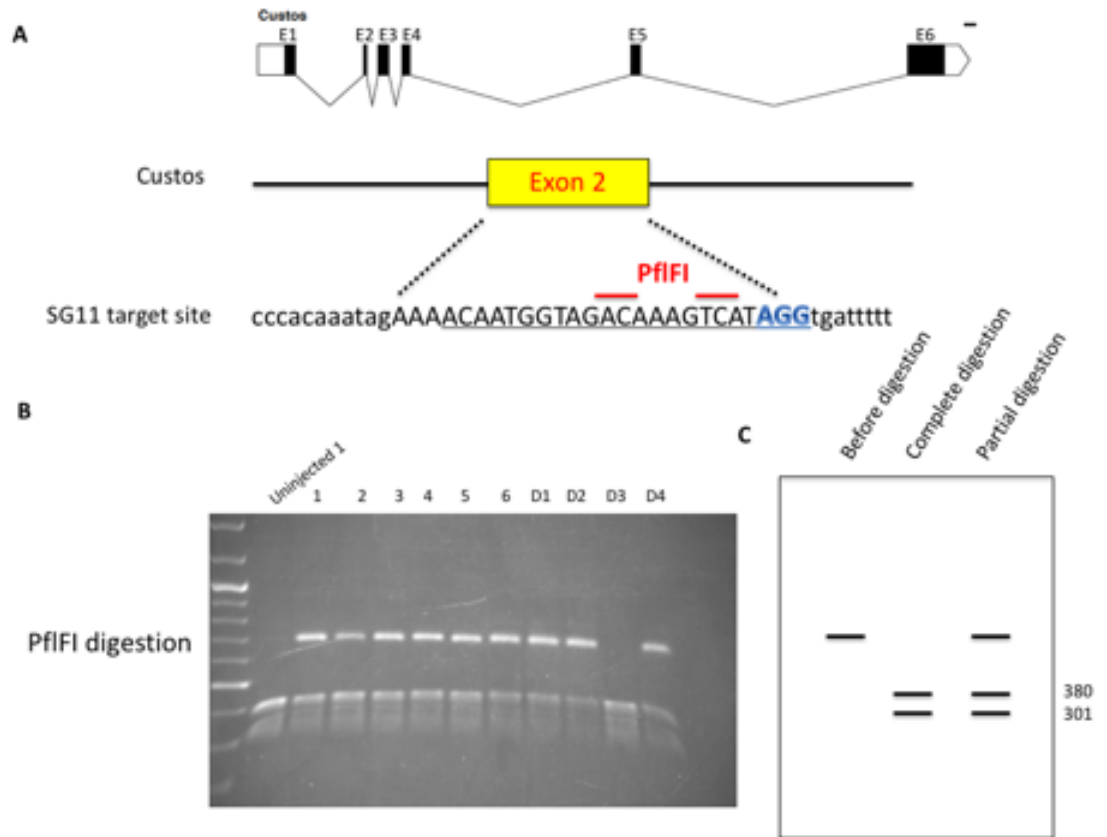


Figure 26: CRISPR/Cas9 gene editing of Custos at target site SG11 **A.** Custos gene showing six exons. CRISPR designed for Exon 2. SG11 target site underlined in black with PflFI restriction site labeled in red. **B.** SG11 uninjected embryos along with 6 normal embryos and 4 deformed embryos, D1-D4 digested with PflF1. **C.** Diagrammatic representation of samples before and after digestion indicating the sizes of the expected fragments.

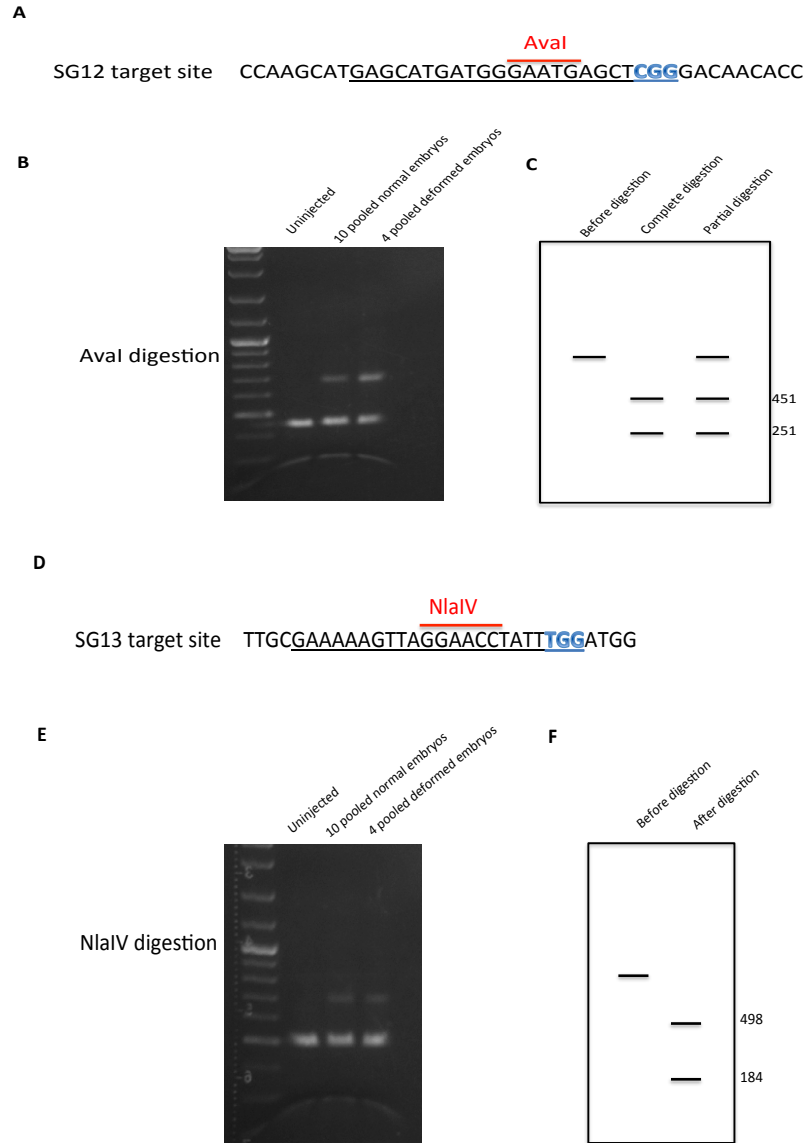


Figure 27: CRISPR/Cas9 gene editing of Custos at target site SG12 and SG13. **A, B.** represent SG12 and SG13 target site underlined with the respective restriction enzymes labeled in red. **B, E** SG12 and SG13 uninjected and injected pool of embryos digested with *AvaI* and *NlaIV* enzymes respectively show partial digestion. **C, F** diagrammatic representation of the samples and the expected fragment sizes before and after digestion with respective restriction enzymes. Blue indicates PAM sequence

Heritable Custos gene modification induced by the CRISPR/Cas9 system

To test whether CRISPR/Cas9 system can induce heritable mutations, we raised the F0 generation to sexual maturity and incrossed the adult fish from SG11 injected embryos. Progeny of six pairs of F0 embryos was analyzed and scored for mutations and phenotypic analysis. Genomic DNA was isolated from a pool of 20 embryos from each incross. Target DNA was amplified and subjected to PflF1 mediated restriction fragment length polymorphism (RFLP). From this screen, we identified 4 out of 6 potential founders for a mutation at the SG11 target site. Sequencing of the amplicon confirmed the presence of mutations in F1 embryos compared to wild type fish.

F1 progeny of Incross 1, incross 2 and incross 3 were next raised to adult hood. Tailclipping was performed on 10 individual fish and isolated DNA was subjected to genotyping and RFLP. Sequencing of all the tailclipped fish amplicons from Incross1 confirmed the presence of a mutation. Surprisingly, we found a frameshift mutation with single base pair insertion resulting in a premature stop codon present in all the sequenced fish (Figure 28A). It was interesting to observe that all the fish in the F1 generation were homozygous for the identical mutation (Figure 28 A and B), but however all the adult fish did not display any phenotype and looked normal.

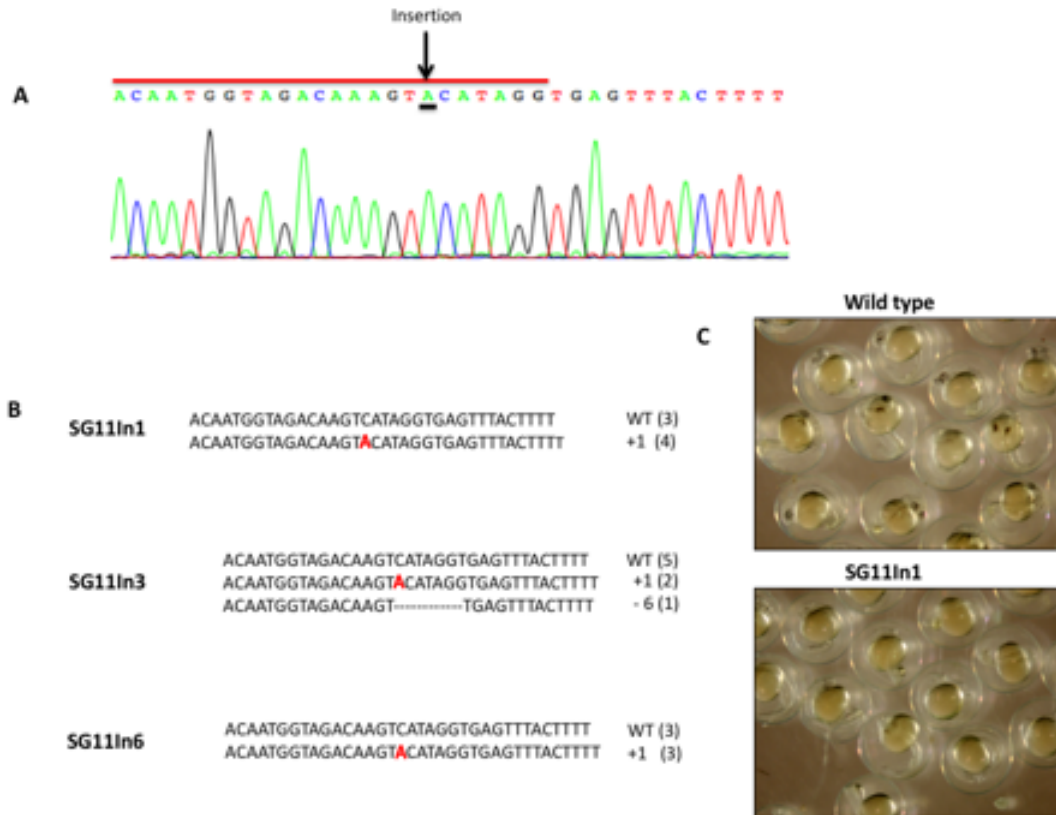


Figure 28: Mutagenesis in F1 fish via Sanger sequencing. A. Sequencing chromatogram-exhibiting insertion of a base pair in both the alleles of Custos target. **B.** Mutants exhibiting an insertion of base pair in all three incrosses of SG11 F0 fish as compared to wild type fish. SG11 Incross 3 displayed a 6 base pair deletion in one fish. A highlighted in red is the inserted base pair. Dotted line indicates deletion of base pairs. **C.** Wild type embryos showing proper development and SG11In1 F2 generation zebrafish embryos showing delayed development and pigmentation defect.

F0 progeny fish homozygous for frameshift mutation

F1 progeny obtained from the F0 incrosses was found to be homozygous for the frameshift mutation. This indicated that the F0 CRISPR/Cas9 injected fish were heterozygous. To confirm the homozygosity of the F1 progeny, the F0 adult fish were outcrossed with the wild type fish. Two separate crosses were set up wherein a female F0 fish was outcrossed with male wildtype fish and F0 male fish was outcrossed with a wild type female fish. Ten random embryos were collected from each cross and subjected to PCR amplification and RFLP. As expected, we observed partial digestion of all the samples with PflF1 enzyme as compared to wildtype (WT) showing complete digestion due to presence of PflF1 restriction site (Figure 29B). The insertion of a single base pair "A" resulted in a new restriction site, RsaI (Figure 29A). To confirm if all the fish contained the same insertion at that position on the target site, we digested the same amplicons with RsaI enzyme. Indeed, all the amplicons showed partial digestion with RsaI enzyme as compared to wildtype (WT) showing no digestion due to absence of RsaI restriction site (Figure 29B). These results clearly indicated that indeed F1 fish were homozygous for the mutation.

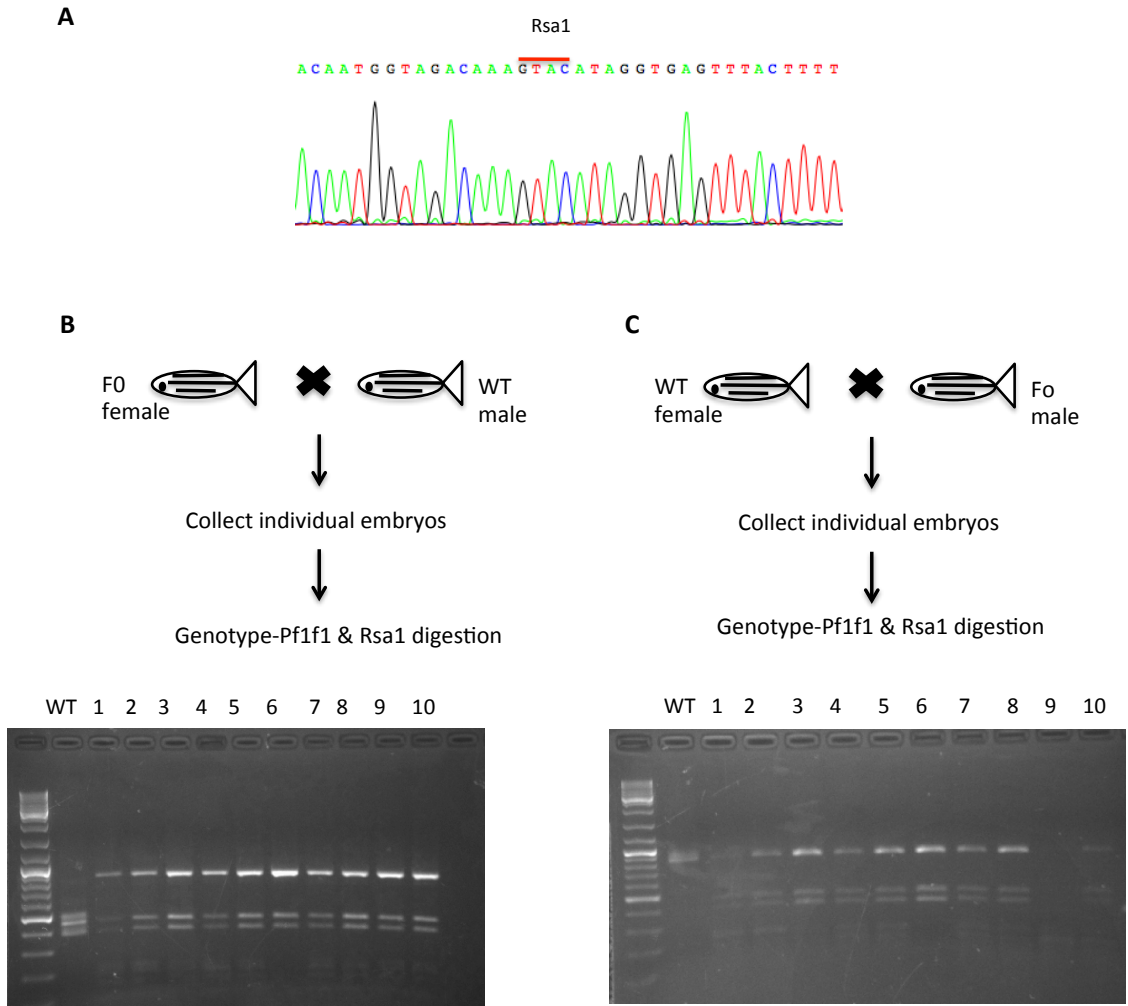


Figure 29: F0 generation is heterozygous. **A.** Sequence chromatogram showing RsaI generated due to the mutation. **B.C.** Embryos obtained from outcross of F0 female and outcross of F0 male subjected to PflF1 digestion. Lanes 1 to 10 exhibit partial digestion as compared to WT showing complete digestion. The same samples subjected to RsaI digestion show partial digestion as compared to WT exhibiting no digestion.

Knockout of Custos gene

The F1 progeny was next incrossed to generate F2 generation fish lines. Phenotypically, all the homozygous fish from the F2 generation displayed a delay in development and pigmentation defect until 30hpf, but however the adult fish did not display any phenotype and looked normal. Genotyping the embryos from the F2 generation revealed that an insertion of a base pair resulted in a premature stop codon. Next, we sought to verify that this generated a complete knockout of Custos by employing RT-PCR assay. Primers were designed spanning exon 1 and exon 6 of Custos gene. Wildtype fish was outcrossed with F2 progeny to generate heterozygous fish. Embryos were collected from wild type, heterozygous and homozygous fish and subjected to RT-PCR analysis. EF1 α was used as an internal control for this study. RT-PCR results revealed that the expression was Custos RNA was completely absent in the homozygous lane whereas the expression levels of Custos were reduced in heterozygous lane as compared to the wild type lane (Figure 30). The gene expression levels in EF1 α lane did not change (Figure 30). These results indicate, that Custos frame shift mutation produced a premature translation termination, thus producing a null mutant. We note, however, we do not have an antibody specific to zebrafish Custos protein and are unable to verify a loss of Custos protein in these fish.

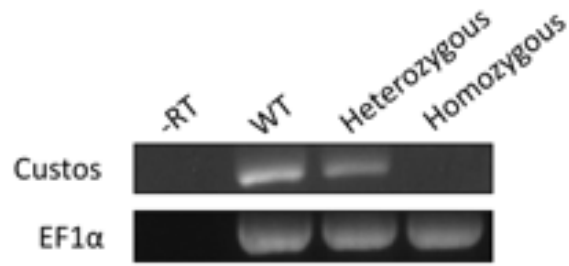


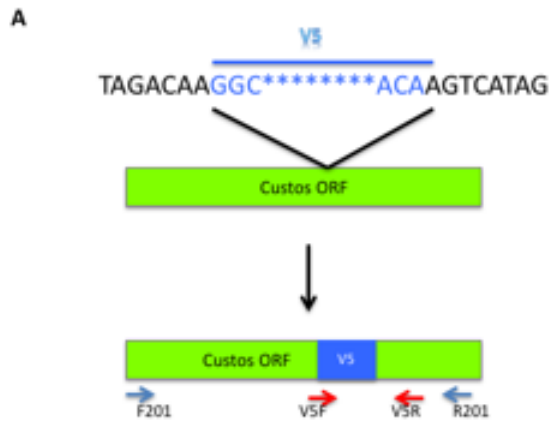
Figure 30: RT-PCR analysis of wildtype, heterozygous and homozygous fish embryos. Custos expression levels were reduced in heterozygous lane as compared to wild type whereas expression of Custos was completely absent in homozygous embryos as compared to WT. EF1 α as the internal control. -RT- no reverse transcriptase present.

Endogenous V5 epitope tagging of Custos using CRISPR/Cas9 system

Tagging an endogenous gene allows to study localization of protein *in vivo*. The simplicity of the CRISPR/Cas9 system allows tagging of endogenous gene in zebrafish. Here, we used this strategy to design a donor oligonucleotide containing a V5 tag with homology arms to introduce the tag in the Custos ORF. The zebrafish embryos were injected with the sgRNA and Cas9mRNA together with the donor oligonucleotide. Two sets of primers were designed for screening of V5 tag (Figure 31A). The embryos post-injection were pooled in a group of 20 and screened for successful CRISPR knockout and tag insertion by PCR.

The F0 embryos were raised and incrossed and outcrossed with wild type fish to produce F1 generation. PCR genotyping revealed potential frameshift mutations in 14 out of 110 fish screened, out of these one fish had an integration of V5 tag (Figure 31B). The F1 potential heterozygous fish were outcrossed with wildtype fish to generate F2 generation heterozygous fish. The CRISPR/Cas9 target site was cloned into pGEM-T-easy vector and sequenced to reveal the frameshift mutants (Figure31B). We next selected the heterozygous fish confirmed as potential mutants from F1 generation and we incrossed two pairs of heterozygous fish to analyze the phenotype and genotype of the potential mutants (Figure 32A). Around 22% and 29% embryos showed delayed development and lack of pigmentation at 30hpf from the respective incrosses (Figure 32B). Five zebrafish embryos from each cross exhibiting the delayed embryogenesis and lack of pigmentation

phenotype were genotyped and five embryos that did not show any phenotypes were subjected to genotyping. The genotyping revealed that the fish that showed phenotype were a combination of both heterozygous and homozygous and wild type fish (Figure 32C). The heterozygous fish from the F2 generation were further incrossed to generate mutants in the F3 generation.



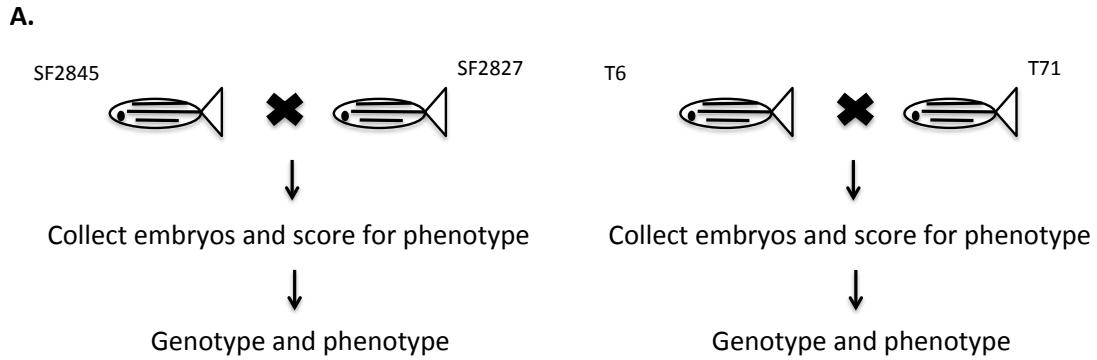
B

```

WT   ACAATGGTAGACAAAGTCATAGGTGAGTTACTTTT
SF2834 ACAATGGTAGACAAAGT---AGGTGAGTTACTTTT (-3) (2)
T71  ACAATGGTAGACAAAGTACATAGGTGAGTTACTTTT (+1) (4)
SF285  ACAATGGTAGACAAAGT-----TTTATACCATGG (-35) (1)
SF2827 ACAATGGTAGACAAAGTGGTAGAAGATTAACATATGTGAGTTACTTTT (+14) (1)
SF2892 ACAATGGTAGACAAAGTGGTAGAAGATTAACATAGGTGAGTTACTTTT (+13) (1)
SF2819 ACAATGGTAGACAAAGTGA-----GTCC-----AGAAT (-36) (1)
SF2845 ACAATGGTAGACAAAGT-----GAGTC-----AAGAATGAA (-35)(1)
SF2881 ACAATGGTAGACAAAGTCAATCCCGAACCCTGCTGAAACCGTACTCCCTGAGTCATAAATGAG (+41)(1)
T110  ACAATGGTAGACAAAGTAAACTCACCTATGACTTGTGGAGTCCAGGCCAGCAGAGGGTTGGGGTAG (+44)(1)
T6    ACAATGGTAGACAAAGTAAACTCACCTATGACTTGTGGAGTCCAGGCCATCATCAGAGGGTTGGGATAGG (+36) (1)

```

Figure 31: Endogenous V5 tagging of Custos **A.** Schematic representation of the donor oligonucleotide and its integration in the Custos ORF. **B.** Sequence of the CRISPR target site of the wildtype fish and different mutants showing indels before the PAM sequence. **NGG-** PAM sequence, WT-wildtype, ---- deletion and red highlighted nucleotides- insertions. F201 and V5R, V5F and R201-V5tag primers.



B.

Crosses	Normal	Delayed/loss of pigmentation
T6 x T71	142 (78.80%)	38 (22%)
SF2845 x SF2827	52 (71%)	21 (29%)

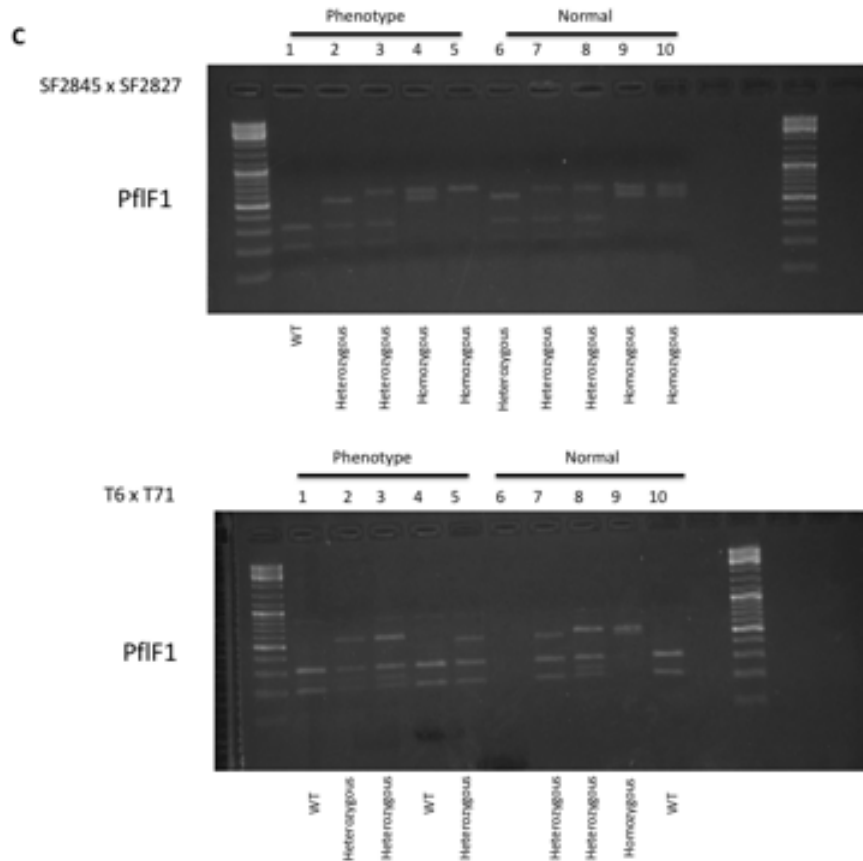


Figure 32: Heterozygous incrosses and genotyping analysis **A.** Schematic representation of the heterozygous fish incross. **B.** Phenotypic analysis of the heterozygous incross. **C.** Genotyping of the fish from each cross with first five (1-5) embryos showing delayed embryogenesis and last five (6-10) wild type.

Characterization of mutants using molecular markers

Custos mutants exhibited delayed development and defects in pigmentation. To understand the Custos mutants at the molecular level, we sought to characterize the mutants using different molecular markers. Signals from the yolk syncytial layer such as Wnt are important for mesodermal induction and maintenance in zebrafish. *In situ* hybridization data reveals Custos expression in the yolk syncytial layer. Hence, we analyzed the expression of mesodermal markers, *gsc* and *flh* in homozygous and wildtype embryos at the bud stage. Interestingly, we observed that the expression of *gsc* was almost absent in the neural plate region as compared to wildtype embryos at this stage. The expression of *flh* was clearly observed in the notochord of the wildtype embryos, but the expression was reduced anteriorly in the homozygous embryos (Figure 33). Embryos hybridized with sense probe did not show any such difference in staining. These results suggested a potential role of Custos in the maintenance of the mesoderm. The Wnt signaling specific marker, *Wnt8a* expression was also reduced in homozygous embryos at the bud stage as compared to wild type embryos.

Next, we also examined the expression of neural markers, *pax2a* in both homozygous and wildtype fish. The expression of early brain specific marker, *pax2a* was reduced in the homozygous embryos at the bud stage as compared to the wild type embryos (Figure 33). We next sought to examine the expression of neural crest markers, *foxd3* and *mitfa* in homozygous as well as wild type embryos. *Foxd3* expression was reduced in homozygous embryos as compared to wild type.

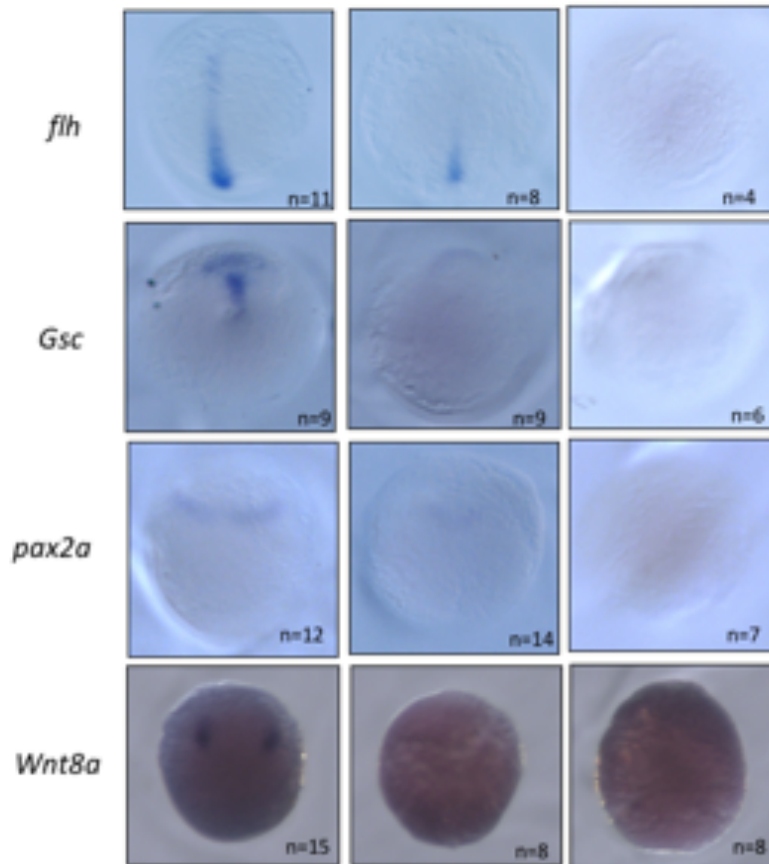
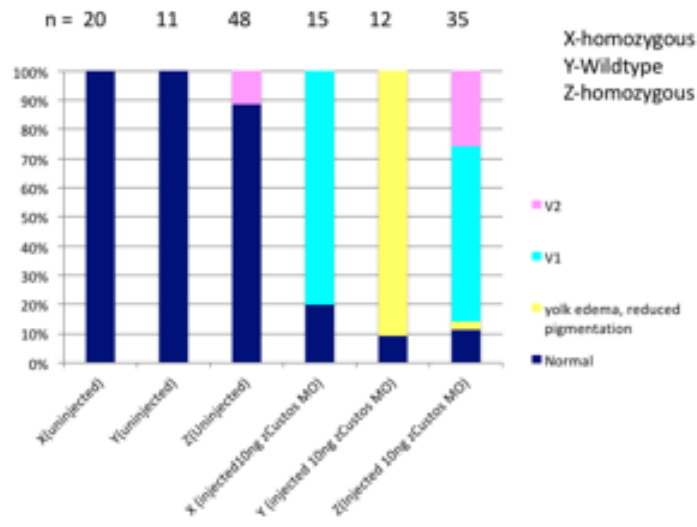


Figure 33: Characterization of homozygous embryos using molecular markers. The expression of molecular markers, *flh*, *Gsc*, *pax2a* and *Wnt8a* were reduced by *Custos* knockout as compared to wildtype embryos at bud stage. Sense indicates no staining.

Custos morpholino effects on mutants

Since we observed discrepancy with the morphant and mutant phenotype, we sought to examine the effects of *Custos* morpholino on wildtype as well as homozygous fish. A blind study was performed by injecting both the *Custos* morpholinos in heterozygous, homozygous and wildtype embryos. The results indicated that both the *Custos* MO1 and *Custos* MO2 injected mutant embryos exhibited a morphant phenotype similar to the wildtype injected embryos, indicating that the morpholinos might have a non-specific effect (Figure 34). However, to validate these results, we need to co-inject the mutant and embryos with *Custos* morpholino and *Custos* rescue RNA.

A Custos morpholino I



B Custos morpholino II

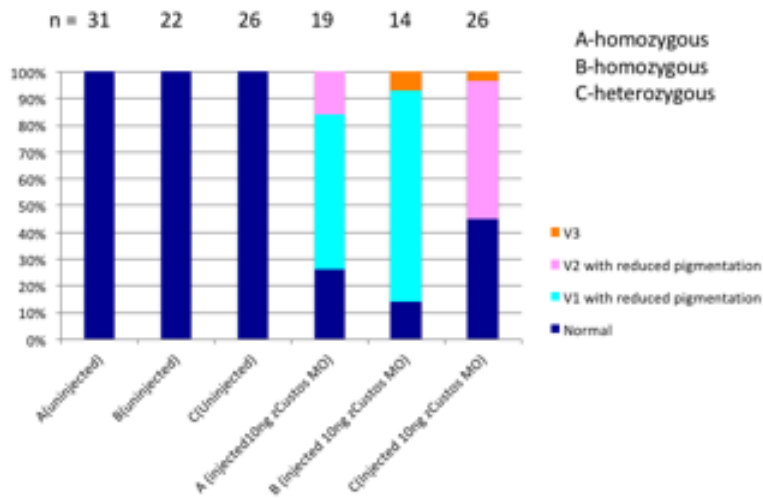


Figure 34: Quantification of Custos morpholino microinjection in mutant embryos **A** Custos MOI injected homozygous embryo displays anterior defect, especially ventralization phenotype scored as V2 and V3. **B**. Quantification of Custos MOII microinjection studies in mutant embryos. Custos MOI injected homozygous embryo displays anterior defect, especially ventralization phenotype scored as V2 and V3 Embryos were scored as V1 if the embryo displayed a mild shortened body axis and/or anterior defect. Embryos were scored as V2 if the embryo was severely shortened and exhibited a completely loss of anterior region. n represents number of embryos used for each injection.

CHAPTER 4
DISCUSSION

Discussion

During vertebrate development, the establishment of a proper body plan involves generation and patterning of the three germ layers, endoderm, mesoderm and ectoderm along the dorsoventral and antero-posterior axes. This requires cell-to-cell interactions along with a number of signaling molecules that are regulated by different signaling pathways. The Wnt signaling pathway is one of the key pathways involved in regulating embryonic patterning. Mutations that disrupt the function of genes involved in Wnt pathway required during patterning have been found to cause numerous birth defects and diseases including cancer and degenerative diseases in humans. Hence, identification and characterization of the molecular components of this pathway is of utmost importance to understand how this pathway regulates embryonic development.

In this thesis, I have characterized a novel protein termed Custos and have shown that this protein is involved in canonical Wnt signaling using mammalian cells and the zebrafish as a model organism. To uncover the functional role of Custos, I have used a number of different genetic, biochemical and embryological studies. The zebrafish Custos is a 236 amino acid protein containing a phosphorylation site at the amino terminal and two nuclear localization signals at the carboxyl terminal. Custos was identified as a binding partner of Dishevelled from a yeast two-hybrid screen in our laboratory. The role of Custos during embryonic development of zebrafish has remained unexplored. Therefore, I characterized this protein in Wnt

signaling and defined its functional role during zebrafish embryonic development.

The Custos protein

The zebrafish Custos is comprised of 236 amino acids consisting of a putative CK1 phosphorylation site and two clusters of nuclear localization signal motifs at its carboxyl terminal. Zebrafish Custos shares 49%, 47%, 45% amino acid sequence identity with humans, mouse and *Xenopus* respectively (Figure 35). All vertebrate Custos proteins except zebrafish Custos consist of two clusters of CK1 sites. Custos is conserved among vertebrates, however, no orthologue was found in invertebrates based on sequence comparison.

Custos interacts with Dishevelled

Since Custos was identified as an interacting partner of Dishevelled in a yeast two-hybrid screen, studies to determine its potential role in canonical Wnt signaling were pursued. I used co-immunoprecipitation and GST pull down studies to confirm the interaction results of yeast two-hybrid screen and found that indeed Custos strongly binds to Dishevelled (figure 10A and figure 11). Dishevelled strongly interacts with carboxyl-terminal region of Custos and more specifically with the fragment consisting of the two nuclear localizing signal motifs. Removal of either of the nuclear localization signal motifs did not have any effect on the interaction of Dishevelled and Custos,

but removal of both the nuclear localization signal motifs impaired the interaction between Dishevelled and Custos (Figure 10D). Therefore, I can conclude that Dishevelled interacts with Custos via its two nuclear localization signal motifs. I propose that the nuclear localization signal motif may play a role in the import or localization of Custos in the nucleus by nuclear transport. Custos itself strongly bound to the fragment consisting the PDZ domain and more specifically between PDZ and the DEP domain of Dishevelled (Figure 10B and C). The fragment consisting of PDZ domain used for the yeast-two hybrid screen ranged from amino acid 238 to 430. The truncated fragment used for co-immunoprecipitation studies, Δ PDZ, which lacks amino acids 241 to 390, bound to Custos, whereas the truncated PDZ fragment that did not bind to Custos had residues ranging from 134 to 432 amino acids of Dishevelled (Figure 9A). This indicated that the Custos binding region on Dishevelled is localized between the 390th and 432nd amino acid. Additional truncated fragments with and without these residues need to be designed and used to further define the precise region of Dishevelled for binding with Custos. This region could be a potential novel functional domain of Dishevelled.


```

Zebrafish 1 M-----SSESSSEEDNTARLKEAVMSFKP-----EDVKIIGKKNNGR
Xenopus 1 MAAPRRGT---OK-SDSDSSDEDFDPREAAWVPPGALDKVS-----DEQNEKIAL
House 1 MVAFSGAMSDSENSSSSSSDAEELAKCREAATPANGLEQRPGAAERPEAGAAQKQAPTPO
Humans 1 MAAPSGTVSDES-SNSSSDAEELRCREAAAMPANGLEQRPHVAGKPRAGAANSQLSTSQ

Zebrafish 37 QSHRADVSRRENDGNELGTTPEFRSIVAKKLGTYLDGCISEVC--SDTVEPAQSENREDE
Xenopus 48 PSLRVRPDCRENDGNELQTTPEFRSIVAKKLAAILDSSIREVVSQNEAVHISAGNGDSED
House 61 PSRRHEVHORENDGNELRITTPEFRSIVAKKLGALLDSSIAIAEVVKKKSOAKKQVAKKE
Humans 60 PSLRHKVRRENDGNELQTTPEFRSIVAKKLGALLDSTFETISEAAKEPAKAKVQKVALED

Zebrafish 95 EGFRLFPSSTPGKWM-EQSPFPFKRNPVPSSESDSDGQENMRFRREAVSLSDILGPVAQN
Xenopus 108 EGFRLFRTSPGKAGIVTSTIPEEK-LASSSESDSDEEQRCREAAVSAQDILRHSTLQ
House 121 DGFRLFFTSIPGQHKKEASPRPKAKKQPPSSSESDSDEEQRCREAAVSASDILQESAIH
Humans 120 DGFRLFFTSIPGQREKEESPQPRKKQPPSSSESDSDEEQRCREAAVSASDILQESAIH

Zebrafish 154 L-----SEKTEKSTKEETEDTVTQKKKKKKKK--TSSEESQDKV-N-HQTEKQSNVVEGN
Xenopus 166 QEPQSTPSKQCDNQP-P-----KQKKKKKKK--DRQDTSQIN-S---V--EETMHIE
House 180 C-----PAKAEK-----KQKKKKKKK--VDSADLAAAP-GLDQV--KQAGVVN
Humans 179 S-----PGTYEKEAK-K-----KQKQKKKAKKVASVDSAVAATTPISMATQKQKSGELN

Zebrafish 205 QEQTTAGERLKKKKKKKKKKKKKLEEDIKKD-----E
Xenopus 209 PGKNELOA---KQKKKKKKKQKQKQKQKDELGN-----E
House 220 GQPVSLGI--QKKKKKKAKKSEAPLQPPAECAAMPEN
Humans 228 GQQVSLGT---KQKKKAKNASQTSFPFPAKSATAIPAN

```

Figure 35: Multiple Sequence alignment of Custos among different vertebrate species. Custos is well conserved among different species. Black boxes indicate complete sequence identity, while gray boxes represent similarity.

Dishevelled promotes dephosphorylation of Custos

Analysis of the primary amino acid sequence of Custos using protein motif comparison suggests that Custos has a consensus CK1 site located amino acids, SxxS. In our studies, we have seen that Custos migrates as two bands in presence of Dishevelled in SDS-PAGE gels. Treatment of Custos with a calf intestinal phosphatase enzyme resulted in a downshifted band to the same position as observed with Dishevelled which suggested that Dishevelled promotes the dephosphorylation of Custos (Figure 14A). Further studies need to be done to study the role of the phosphorylation site by generating truncate constructs and or phosphomimetic substituted mutants (Figure 14B). The phosphomimetic mutants in *Xenopus* did not strongly affect the function of Custos. These studies will shed some light on how this phosphorylation site regulates function of Custos.

Custos strongly binds to β -catenin

The β -catenin protein functions downstream of Dishevelled in the Wnt signaling cascade. As a proposed component of canonical Wnt signaling, the interaction between Custos and β -catenin was investigated and whether this interaction was Wnt-regulated was also examined using co-immunoprecipitation assays. These studies revealed that Custos bound to β -catenin and this interaction was positively regulated by canonical Wnt signaling (figure 13). This study was interesting as it suggested that a small

fraction of Custos bound to β -catenin in control conditions but after Wnt stimulation, the interaction was stronger indicating a likely scaffolding role for Custos in β -catenin nuclear translocation. This data is in concordance with the interaction of Custos homologue in *Xenopus* and β -catenin (Komiya, Mandrekar et al. 2014).

Subcellular localization of Custos

To further delineate the role of Custos in Wnt signaling, I examined the subcellular localization of Custos. Cells transfected with Custos revealed localization of Custos in the perinuclear region and within the nucleus in both control and Wnt treated conditions. The localization of Custos did not appear to significantly change at all after Wnt treatment (figure 15). A time course experiment with live imaging can confirm if the localization of Custos changes or remains unchanged over time. Moreover, transfection of the truncated fragments of Custos revealed that the fragments consisting of the nuclear localization signal motifs were essential for its co-localization to nuclear/perinuclear region as the amino terminal fragment of Custos was localized in the cytoplasm. To confirm this role of nuclear localization signal motifs, an alternative experiment could be performed wherein the nuclear localization signal motif of Custos could be tagged to a non-nuclear protein and if the protein translocated to the nucleus, this would suggest that the nuclear localization signal motif is indeed essential for nuclear localization. The perinuclear localization of Custos suggests that Custos may be located on

the nuclear envelope. Alternative techniques like FRET can give us a better understanding of the location of Custos in the perinuclear region.

Custos does not co-localize with Dishevelled

Custos was identified as a binding partner of Dishevelled from a yeast two-hybrid screen and this interaction was also confirmed by co-immunoprecipitation and GST pull down assays. However, I did not see any co-localization of Custos with Dishevelled in mammalian cell culture. In absence of Wnt stimulation, Dishevelled is found to be localized to the punctate vesicular structures in the cytoplasm, and in response to Wnt ligand, Dishevelled translocates to the perinuclear/nuclear area (Habas and Dawid 2005). It is proposed that Dishevelled can shuttle between the nucleus and cytoplasm (Boutros and Mlodzik 1999). It is also possible that a small pool of Dishevelled may be interacting with Custos at the perinuclear area but immunostaining may not be sufficient to detect this interaction. Alternatively, FRET assay can be employed to study this interaction in detail at the cellular level.

Custos inhibits β -catenin transcriptional activity and modulates canonical Wnt signaling

The hallmark of canonical Wnt signaling is accumulation of β -catenin in the cytoplasm with its subsequent translocation into the nucleus to activate Wnt target genes. We observed that Custos overexpression interfered with

nuclear accumulation of β -catenin in response to Wnt3A stimulation (Figure 15). From this study, I propose that Custos may be interacting with β -catenin at the perinuclear/nuclear region. Here, it may act as a docking protein and hence its overexpression prevents translocation of β -catenin in the nucleus. Luciferase reporter assays revealed that Custos dose-dependently suppressed the transcriptional activation of reporter gene by positive components of canonical Wnt signaling, Dishevelled and β -catenin (Figure 20B). These results suggest that Custos functions downstream of Dishevelled and at the level or downstream of β -catenin (Figure 20B).

Custos co-localizes with lamin

As subcellular localization studies suggested that Custos localized in the perinuclear/nuclear region, I tested if Custos colocalized with a marker localized to the nuclear envelope such as lamin. Lamin is co-localized to the inner surface of nuclear envelope. Custos was found to co-localize with the nuclear envelope marker, lamin (figure 16). This data suggested that Custos may be localized on the nuclear envelope. It is well known that β -catenin translocates into the nucleus by interacting with nuclear pore proteins in an NLS-importin-dependant and independent manner (Henderson and Fagotto 2002). One possibility is that Custos could act as docking protein on the nuclear envelope and regulates the entry of β -catenin into the nucleus. Higher resolution technique such as Fluorescence resonance energy transfer

(FRET) will give us a better understanding of the localization of Custos on the nuclear envelope.

Expression pattern of Custos

To understand the role of Custos during embryogenesis, we first examined its temporal and spatial expression pattern. Expression of Custos was seen throughout zebrafish development and was maternally expressed, as evidenced by *in situ* hybridization as well as RT-PCR. (Figure 21) *In situ* hybridization revealed that Custos was strongly expressed on the dorsal side of the embryo during gastrulation. At this stage the embryo undergoes dramatic morphological changes as the three germ layers are formed. This suggests a potential role of Custos at the start of gastrulation. By 24hpf, the expression of Custos becomes refined to the head region, hatching gland and heart (Figure 21). This expression pattern of Custos was concomitant with the expression pattern of Custos in *Xenopus* (Komiya, Mandrekar et al. 2014).

Custos is required for dorsal-ventral axis formation

To investigate the role of Custos during vertebrate development, we performed gain of function and loss of function studies in zebrafish embryos. Defects in anterior development and patterning of zebrafish axes were seen with both the studies and interestingly, over expression and knockdown of Custos produced the exact same ventralization phenotype (Figure 22, 23 and 24). This suggests that it is not Custos per se but rather optimal levels of

Custos are required during zebrafish development. Importantly, after knockdown of Custos, the phenotype of the morphants could be rescued by co-injecting a Custos rescue RNA that lacks the morpholino-binding site. It is unusual to see a protein involved in canonical Wnt signaling showing the same phenotype after over expression and knockdown. There is only one protein known in literature, WISE that displays a similar outcome. Overexpression and knockdown of WISE resulted in similar defects in eye formation. WISE modulates canonical Wnt signaling pathway by interacting with Lrp6 (Itasaki, Jones et al. 2003, Guidato and Itasaki 2007, Shigetani, Howard et al. 2008, Lintern, Guidato et al. 2009).

The expression of mesodermal genes *Gsc* and *flh* were not affected by knockdown of Custos in zebrafish embryos as compared to EF-1 α , as evidenced by RT-PCR (Figure 25). Custos is a maternal gene, and it is likely that the morpholino did not completely eliminate its maternal store. Hence, this experiment did not give us a clear understanding of the role of Custos in mesoderm development.

Genetic modification to create Custos knockout

Generation of a Custos genetic loss of was essential to eliminate the maternal store of Custos and to understand the function of the protein during zebrafish embryogenesis. Custos knockout using the zebrafish Cas9 produced mutants in the F1 generation and interestingly, the exact frameshift mutation generated using the zebrafish Cas9 was the same in all

the fish (Figure 25). This was an uncommon finding in the field of genetics as this indicated that all the fish were heterozygous for the same mutation in the Fo generation (Figure 29). The mutants displayed delayed development and lack of pigmentation, but by 36hpf the mutant phenotype reverted back to wild type. To validate that the same mutation present in all fish is not an artifact, we outcrossed the mutant fish with wildtype to create heterozygous embryos. The mutation created a new RsaI restriction site. Digestion of the amplified target of the heterozygous fish with RsaI enzyme exhibited partial digestion indicating that the mutation was not an artifact (Figure 29). Loss of Custos expression in homozygous fish of F2 generation as compared to heterozygous and wildtype fish further confirmed that it was indeed a null mutant (Figure 30). But there is still a possibility of a having a splicing event post mid-blastula transition that can give rise to an unknown transcript variant. Hence, additional primers can be employed to detect the transcript variant.

Custos sgRNA target was designed on the second exon of Custos. Hence, loss of Custos expression did not eliminate the possibility of presence of the Custos protein in the homozygous fish. Due to unavailability of zebrafish specific Custos antibody, I was unable to check the endogenous protein levels of Custos. Hence, I employed CRISPR/Cas9 to generate fish with endogenous V5 tag in the Custos open reading frame. Injection of V5 tag along with human Cas9 in zebrafish gave rise to number of putative mutations in different fish (figure 31). The efficiency of mutagenesis was

very low but the mutants derived from this injection in the F2 generation displayed delayed embryogenesis and lack of pigmentation which was similar to the mutant phenotype produced from the zebrafish Cas9 injected embryos. Incross of two pairs of heterozygous fish produced embryos with delayed embryogenesis and pigmentation, but the genotype of these fish did not completely match with the phenotype. The number of embryos genotyped for each incross were ten, hence increasing the number of embryos for genotyping will give us a clear understanding of the genotype-phenotype correlation. Additionally, studies on detecting the protein levels of homozygous and wildtype fish are yet to be performed.

Characterization of the mutants using different molecular markers revealed that the expression of mesodermal markers such as *flh* and *gsc* were did not change at shield stage but a marked reduction was seen at bud stage as compared to wild type embryos. Since, *in situ* hybridization is a qualitative assay, it would be difficult to see if there is any slight reduction in expression of the mesodermal markers at shield stage. A quantitative assay, such as RT-PCR would depict a better picture for the reduction of expression of mesodermal markers and Wnt8a. Wnt signaling plays an important role in induction of the mesoderm. In zebrafish embryos, β -catenin is found to be accumulated in the nuclei of the dorsal yolk syncytial and dorsal marginal blastomeres at the mid blastula stage (Schneider, Steinbeisser et al. 1996). Maternal effect mutation in the gene *Ichabod* in zebrafish, produce embryos with severe axis defects and the embryos also display low levels of β -catenin

in the dorsal nuclei, implicating that β -catenin nuclear accumulation is essential for axis induction(Kelly, Chin et al. 2000). Based on *in situ* hybridization data, Custos is expressed in the yolk syncytial layer (Figure 21) and loss of Custos shows reduced expression of mesodermal and Wnt markers implicating that it could play a major role in mesoderm induction(Figure 33). I propose that Custos might also play a role in neurulation as loss of maternal Custos resulted in reduction of brain specific marker (Figure 33). The reversion of the mutant phenotype to the wild type by 36hpf, suggests that there could be another unknown protein present. Additionally, I need to examine the expression of these markers at later stages of zebrafish development. Continued characterization studies using more molecular markers will provide a better understanding of the role of Custos during zebrafish development.

My knockdown studies were not in concordance with my knockout studies, the morphant phenotype was different from the mutant phenotype. One major disadvantage of morpholino is that it can have off targets effects. To eliminate the possibility of non-specific effects, I performed two blind studies by injecting Custos morpholino I and morpholino II in wildtype, heterozygous and homozygous embryos. It was surprising to see that the homozygous embryos injected with morpholino I and morpholino II exhibited a morphant phenotype indicating that the Custos morpholino might be non-specific or the mutant may have some residual Custos protein present (Figure 34). From previous studies done in our laboratory, we have

seen that Custos morphant in *Xenopus laevis* exhibits small head and shortened axis (Komiya, Mandrekar et al. 2014) which is similar to the morphant phenotype seen in zebrafish embryos. Since, we performed the blind study only once using each of these morpholinos, we need to repeat these studies and additional experiments need to be performed such as co-injection of morpholino and Custos rescue RNA, lacking the morpholino binding site in mutants. If we see rescue of the phenotype that will indicate that the mutant still has some residual protein present.

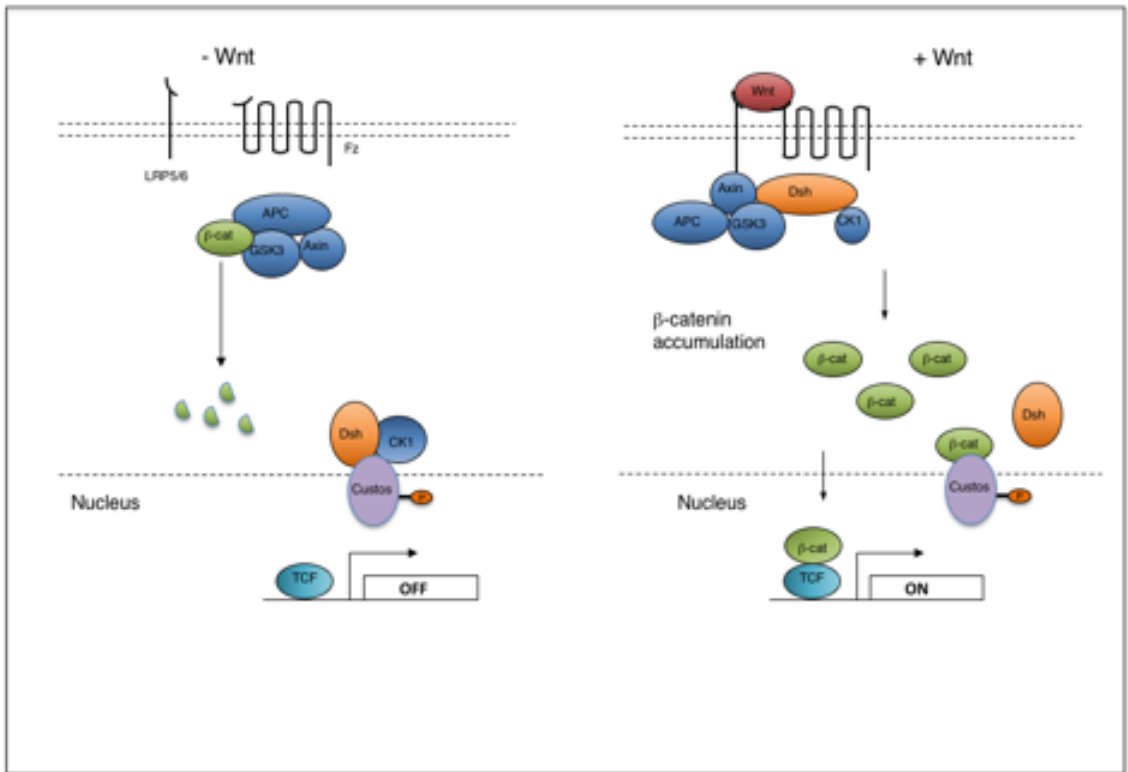


Figure 36: Schematic model of how Custos is involved in the canonical Wnt signaling pathway. Custos may be present on the nuclear envelope and work as a docking protein by interacting with β -catenin and inhibiting its translocation in the nucleus.

Summary and Conclusions:

In summary, I propose that Custos is a novel component of canonical Wnt signaling cascade and a binding partner of Dishevelled. Custos functions downstream of Dishevelled and interacts with β -catenin to modulate canonical Wnt signaling. I propose that Custos at the perinuclear area interacts with Dishevelled in the cytoplasm closer to the perinuclear region. On activation of the Wnt signaling pathway, β -catenin on the way to its entry into the nucleus gets exchanged for Dishevelled and strongly binds to Custos. Custos, then serves as a docking protein to prevent β -catenin entry in the nucleus(Figure 36). During development, Custos is required early in development, prior to gastrulation for axis induction of axis formation and later in development for brain development, and this is evident from knockout/knockdown and overexpression studies where the morphant embryos display anterior defect. Further characterization of this protein will illuminate key insights into the function of this protein in zebrafish development.

Bibliography

Aberle, H., A. Bauer, J. Stappert, A. Kispert and R. Kemler (1997). "beta-catenin is a target for the ubiquitin-proteasome pathway." EMBO J **16**(13): 3797-3804.

Axelrod, J. D. (2001). "Unipolar membrane association of Dishevelled mediates Frizzled planar cell polarity signaling." Genes Dev **15**(10): 1182-1187.

Axelrod, J. D., J. R. Miller, J. M. Shulman, R. T. Moon and N. Perrimon (1998). "Differential recruitment of Dishevelled provides signaling specificity in the planar cell polarity and Wingless signaling pathways." Genes Dev **12**(16): 2610-2622.

Banziger, C., D. Soldini, C. Schutt, P. Zipperlen, G. Hausmann and K. Basler (2006). "Wntless, a conserved membrane protein dedicated to the secretion of Wnt proteins from signaling cells." Cell **125**(3): 509-522.

Bartscherer, K., N. Pelte, D. Ingelfinger and M. Boutros (2006). "Secretion of Wnt ligands requires Evi, a conserved transmembrane protein." Cell **125**(3): 523-533.

Behrens, J., B. A. Jerchow, M. Wurtele, J. Grimm, C. Asbrand, R. Wirtz, M. Kuhl, D. Wedlich and W. Birchmeier (1998). "Functional interaction of an axin homolog, conductin, with beta-catenin, APC, and GSK3beta." Science **280**(5363): 596-599.

Belenkaya, T. Y., Y. Wu, X. Tang, B. Zhou, L. Cheng, Y. V. Sharma, D. Yan, E. M. Selva and X. Lin (2008). "The retromer complex influences Wnt secretion by recycling wntless from endosomes to the trans-Golgi network." Dev Cell **14**(1): 120-131.

Bellipanni, G., M. Varga, S. Maegawa, Y. Imai, C. Kelly, A. P. Myers, F. Chu, W. S. Talbot and E. S. Weinberg (2006). "Essential and opposing roles of zebrafish beta-catenins in the formation of dorsal axial structures and neurectoderm." Development **133**(7): 1299-1309.

Bhanot, P., M. Brink, C. H. Samos, J. C. Hsieh, Y. Wang, J. P. Macke, D. Andrew, J. Nathans and R. Nusse (1996). "A new member of the frizzled family from *Drosophila* functions as a Wingless receptor." Nature **382**(6588): 225-230.

Bilic, J., Y. L. Huang, G. Davidson, T. Zimmermann, C. M. Cruciat, M. Bienz and C. Niehrs (2007). "Wnt induces LRP6 signalosomes and promotes dishevelled-dependent LRP6 phosphorylation." Science **316**(5831): 1619-1622.

Bill, B. R., A. M. Petzold, K. J. Clark, L. A. Schimmenti and S. C. Ekker (2009). "A primer for morpholino use in zebrafish." Zebrafish **6**(1): 69-77.

Boutros, M. and M. Mlodzik (1999). "Dishevelled: at the crossroads of divergent intracellular signaling pathways." Mech Dev **83**(1-2): 27-37.

Breitman, M., A. Zilberberg, M. Caspi and R. Rosin-Arbesfeld (2008). "The armadillo repeat domain of the APC tumor suppressor protein interacts with Striatin family members." Biochim Biophys Acta **1783**(10): 1792-1802.

Cadigan, K. M. and R. Nusse (1997). "Wnt signaling: a common theme in animal development." Genes Dev **11**(24): 3286-3305.

Casagolda, D., B. Del Valle-Perez, G. Valls, E. Lugalde, M. Vinyoles, J. Casado-Vela, G. Solanas, E. Batlle, A. B. Reynolds, J. I. Casal, A. G. de Herreros and M. Dunach (2010). "A p120-catenin-CK1epsilon complex regulates Wnt signaling." J Cell Sci **123**(Pt 15): 2621-2631.

Chakrabarti, S., G. Streisinger, F. Singer and C. Walker (1983). "Frequency of gamma-Ray Induced Specific Locus and Recessive Lethal Mutations in Mature Germ Cells of the Zebrafish, *BRACHYDANIO RERIO*." Genetics **103**(1): 109-123.

Cheong, J. K. and D. M. Virshup (2011). "Casein kinase 1: Complexity in the family." Int J Biochem Cell Biol **43**(4): 465-469.

Cheyette, B. N., J. S. Waxman, J. R. Miller, K. Takemaru, L. C. Sheldahl, N. Khlebtsova, E. P. Fox, T. Earnest and R. T. Moon (2002). "Dapper, a Dishevelled-associated antagonist of beta-catenin and JNK signaling, is required for notochord formation." Dev Cell **2**(4): 449-461.

Clements, D., R. V. Friday and H. R. Woodland (1999). "Mode of action of VegT in mesoderm and endoderm formation." Development **126**(21): 4903-4911.

Clevers, H. (2006). "Wnt/beta-catenin signaling in development and disease." Cell **127**(3): 469-480.

Cong, F., L. Schweizer and H. Varmus (2004). "Wnt signals across the plasma membrane to activate the beta-catenin pathway by forming oligomers containing its receptors, Frizzled and LRP." Development **131**(20): 5103-5115.

Coombs, G. S., J. Yu, C. A. Canning, C. A. Veltri, T. M. Covey, J. K. Cheong, V. Utomo, N. Banerjee, Z. H. Zhang, R. C. Jadulco, G. P. Concepcion, T. S. Bugni, M. K. Harper, I. Mihalek, C. M. Jones, C. M. Ireland and D. M. Virshup (2010). "WLS-dependent secretion of WNT3A requires Ser209 acylation and vacuolar acidification." J Cell Sci **123**(Pt 19): 3357-3367.

Coudreuse, D. Y., G. Roel, M. C. Betist, O. Destree and H. C. Korswagen (2006). "Wnt gradient formation requires retromer function in Wnt-producing cells." Science **312**(5775): 921-924.

Dajani, R., E. Fraser, S. M. Roe, M. Yeo, V. M. Good, V. Thompson, T. C. Dale and L. H. Pearl (2003). "Structural basis for recruitment of glycogen synthase kinase 3beta to the axin-APC scaffold complex." EMBO J **22**(3): 494-501.

Davidson, G., W. Wu, J. Shen, J. Bilic, U. Fenger, P. Stannek, A. Glinka and C. Niehrs (2005). "Casein kinase 1 gamma couples Wnt receptor activation to cytoplasmic signal transduction." Nature **438**(7069): 867-872.

Doubravaska, L., M. Krausova, D. Gradl, M. Vojtechova, L. Tumova, J. Lukas, T. Valenta, V. Pospichalova, B. Fafilek, J. Plachy, O. Sebesta and V. Korinek (2011). "Fatty acid modification of Wnt1 and Wnt3a at serine is prerequisite for lipidation at cysteine and is essential for Wnt signalling." Cell Signal **23**(5): 837-848.

Driever, W., L. Solnica-Krezel, A. F. Schier, S. C. Neuhauss, J. Malicki, D. L. Stemple, D. Y. Stainier, F. Zwartkruis, S. Abdelilah, Z. Rangini, J. Belak and C. Boggs (1996). "A genetic screen for mutations affecting embryogenesis in zebrafish." Development **123**: 37-46.

Eklöf Spink, K., S. G. Fridman and W. I. Weis (2001). "Molecular mechanisms of beta-catenin recognition by adenomatous polyposis coli revealed by the structure of an APC-beta-catenin complex." EMBO J **20**(22): 6203-6212.

Fahmy, O. G. and M. J. Fahmy (1959). "Complementation among the subgenic mutants in the r-locus of *Drosophila melanogaster*." Nature **184**: 1927-1929.

Fan, S., S. H. Ramirez, T. M. Garcia and S. Dewhurst (2004). "Dishevelled promotes neurite outgrowth in neuronal differentiating neuroblastoma 2A cells, via a DIX-domain dependent pathway." Brain Res Mol Brain Res **132**(1): 38-50.

Franch-Marro, X., F. Wendler, S. Guidato, J. Griffith, A. Baena-Lopez, N. Itasaki, M. M. Maurice and J. P. Vincent (2008). "Wingless secretion requires endosome-to-Golgi retrieval of Wntless/Evi/Sprinter by the retromer complex." Nat Cell Biol **10**(2): 170-177.

Gan, X. Q., J. Y. Wang, Y. Xi, Z. L. Wu, Y. P. Li and L. Li (2008). "Nuclear Dvl, c-Jun, beta-catenin, and TCF form a complex leading to stabilization of beta-catenin-TCF interaction." J Cell Biol **180**(6): 1087-1100.

Gasnereau, I., P. Herr, P. Z. Chia, K. Basler and P. A. Gleeson (2011). "Identification of an endocytosis motif in an intracellular loop of Wntless protein, essential for its recycling and the control of Wnt protein signaling." J Biol Chem **286**(50): 43324-43333.

Giraldez, A. J., R. R. Copley and S. M. Cohen (2002). "HSPG modification by the secreted enzyme Notum shapes the Wingless morphogen gradient." Dev Cell **2**(5): 667-676.

Gong, Y., C. Mo and S. E. Fraser (2004). "Planar cell polarity signalling controls cell division orientation during zebrafish gastrulation." Nature **430**(7000): 689-693.

Gonzalez, F., L. Swales, A. Bejsovec, H. Skaer and A. Martinez Arias (1991). "Secretion and movement of wingless protein in the epidermis of the Drosophila embryo." Mech Dev **35**(1): 43-54.

Gray, R. S., I. Roszko and L. Solnica-Krezel (2011). "Planar cell polarity: coordinating morphogenetic cell behaviors with embryonic polarity." Dev Cell **21**(1): 120-133.

Griffin, K. J., S. L. Amacher, C. B. Kimmel and D. Kimelman (1998). "Molecular identification of spadetail: regulation of zebrafish trunk and tail mesoderm formation by T-box genes." Development **125**(17): 3379-3388.

Guidato, S. and N. Itasaki (2007). "Wise retained in the endoplasmic reticulum inhibits Wnt signaling by reducing cell surface LRP6." Dev Biol **310**(2): 250-263.

Habas, R. and I. B. Dawid (2005). "Dishevelled and Wnt signaling: is the nucleus the final frontier?" J Biol **4**(1): 2.

Habas, R., Y. Kato and X. He (2001). "Wnt/Frizzled activation of Rho regulates vertebrate gastrulation and requires a novel Formin homology protein Daam1." Cell **107**(7): 843-854.

Haffter, P., M. Granato, M. Brand, M. C. Mullins, M. Hammerschmidt, D. A. Kane, J. Odenthal, F. J. van Eeden, Y. J. Jiang, C. P. Heisenberg, R. N. Kelsh, M. Furutani-Seiki, E. Vogelsang, D. Beuchle, U. Schach, C. Fabian and C. Nusslein-Volhard (1996). "The identification of genes with unique and essential functions in the development of the zebrafish, *Danio rerio*." Development **123**: 1-36.

Hamblet, N. S., N. Lijam, P. Ruiz-Lozano, J. Wang, Y. Yang, Z. Luo, L. Mei, K. R. Chien, D. J. Sussman and A. Wynshaw-Boris (2002). "Dishevelled 2 is essential for cardiac outflow tract development, somite segmentation and neural tube closure." Development **129**(24): 5827-5838.

Hart, M. J., R. de los Santos, I. N. Albert, B. Rubinfeld and P. Polakis (1998). "Downregulation of beta-catenin by human Axin and its association with the APC tumor suppressor, beta-catenin and GSK3 beta." Curr Biol **8**(10): 573-581.

He, X., M. Semenov, K. Tamai and X. Zeng (2004). "LDL receptor-related proteins 5 and 6 in Wnt/beta-catenin signaling: arrows point the way." Development **131**(8): 1663-1677.

Heisenberg, C. P., C. Houart, M. Take-Uchi, G. J. Rauch, N. Young, P. Coutinho, I. Masai, L. Caneparo, M. L. Concha, R. Geisler, T. C. Dale, S. W. Wilson and D. L. Stemple (2001). "A mutation in the Gsk3-binding domain of zebrafish Masterblind/Axin1 leads to a fate transformation of telencephalon and eyes to diencephalon." Genes Dev **15**(11): 1427-1434.

Henderson, B. R. and F. Fagotto (2002). "The ins and outs of APC and beta-catenin nuclear transport." EMBO Rep **3**(9): 834-839.

Herr, P. and K. Basler (2012). "Porcupine-mediated lipidation is required for Wnt recognition by Wls." Dev Biol **361**(2): 392-402.

Horvath, P. and R. Barrangou (2010). "CRISPR/Cas, the immune system of bacteria and archaea." Science **327**(5962): 167-170.

Hwang, W. Y., Y. Fu, D. Reyon, M. L. Maeder, P. Kaini, J. D. Sander, J. K. Joung, R. T. Peterson and J. R. Yeh (2013). "Heritable and precise zebrafish genome editing using a CRISPR-Cas system." PLoS One **8**(7): e68708.

Hyde, C. E. and R. W. Old (2000). "Regulation of the early expression of the Xenopus nodal-related 1 gene, Xnr1." Development **127**(6): 1221-1229.

Ikeda, S., M. Kishida, Y. Matsuura, H. Usui and A. Kikuchi (2000). "GSK-3beta-dependent phosphorylation of adenomatous polyposis coli gene product can be modulated by beta-catenin and protein phosphatase 2A complexed with Axin." Oncogene **19**(4): 537-545.

Ishida-Takagishi, M., A. Enomoto, N. Asai, K. Ushida, T. Watanabe, T. Hashimoto, T. Kato, L. Weng, S. Matsumoto, M. Asai, Y. Murakumo, K. Kaibuchi, A. Kikuchi and M. Takahashi (2012). "The Dishevelled-associating protein Daple controls the non-canonical Wnt/Rac pathway and cell motility." Nat Commun **3**: 859.

Itasaki, N., C. M. Jones, S. Mercurio, A. Rowe, P. M. Domingos, J. C. Smith and R. Krumlauf (2003). "Wise, a context-dependent activator and inhibitor of Wnt signalling." Development **130**(18): 4295-4305.

Janda, C. Y., D. Waghray, A. M. Levin, C. Thomas and K. C. Garcia (2012). "Structural basis of Wnt recognition by Frizzled." Science **337**(6090): 59-64.

Jao, L. E., S. R. Wentz and W. Chen (2013). "Efficient multiplex biallelic zebrafish genome editing using a CRISPR nuclease system." Proc Natl Acad Sci U S A **110**(34): 13904-13909.

Jessen, J. R. (2012). "Analyzing planar cell polarity during zebrafish gastrulation." Methods Mol Biol **839**: 69-78.

Jesuthasan, S. and U. Stahle (1997). "Dynamic microtubules and specification of the zebrafish embryonic axis." Curr Biol **7**(1): 31-42.

Jinek, M., K. Chylinski, I. Fonfara, M. Hauer, J. A. Doudna and E. Charpentier (2012). "A programmable dual-RNA-guided DNA endonuclease in adaptive bacterial immunity." Science **337**(6096): 816-821.

Kakugawa, S., P. F. Langton, M. Zebisch, S. A. Howell, T. H. Chang, Y. Liu, T. Feizi, G. Bineva, N. O'Reilly, A. P. Snijders, E. Y. Jones and J. P. Vincent (2015). "Notum

deacylates Wnt proteins to suppress signalling activity." Nature **519**(7542): 187-192.

Katanaev, V. L., G. P. Solis, G. Hausmann, S. Buestorf, N. Katanayeva, Y. Schrock, C. A. Stuermer and K. Basler (2008). "Reggie-1/flotillin-2 promotes secretion of the long-range signalling forms of Wingless and Hedgehog in *Drosophila*." EMBO J **27**(3): 509-521.

Kawasaki, Y., T. Senda, T. Ishidate, R. Koyama, T. Morishita, Y. Iwayama, O. Higuchi and T. Akiyama (2000). "Asef, a link between the tumor suppressor APC and G-protein signaling." Science **289**(5482): 1194-1197.

Keller, R., L. A. Davidson and D. R. Shook (2003). "How we are shaped: the biomechanics of gastrulation." Differentiation **71**(3): 171-205.

Kelly, C., A. J. Chin, J. L. Leatherman, D. J. Kozlowski and E. S. Weinberg (2000). "Maternally controlled (beta)-catenin-mediated signaling is required for organizer formation in the zebrafish." Development **127**(18): 3899-3911.

Kim, C. H., T. Oda, M. Itoh, D. Jiang, K. B. Artinger, S. C. Chandrasekharappa, W. Driever and A. B. Chitnis (2000). "Repressor activity of Headless/Tcf3 is essential for vertebrate head formation." Nature **407**(6806): 913-916.

Kim, H. J., H. J. Lee, H. Kim, S. W. Cho and J. S. Kim (2009). "Targeted genome editing in human cells with zinc finger nucleases constructed via modular assembly." Genome Res **19**(7): 1279-1288.

Kimelman, D. (2006). "Mesoderm induction: from caps to chips." Nat Rev Genet **7**(5): 360-372.

Kimmel, C. B., W. W. Ballard, S. R. Kimmel, B. Ullmann and T. F. Schilling (1995). "Stages of embryonic development of the zebrafish." Dev Dyn **203**(3): 253-310.

- Kishida, S., H. Yamamoto and A. Kikuchi (2004). "Wnt-3a and Dvl induce neurite retraction by activating Rho-associated kinase." Mol Cell Biol **24**(10): 4487-4501.
- Kohler, E. M., K. Brauburger, J. Behrens and J. Schneikert (2010). "Contribution of the 15 amino acid repeats of truncated APC to beta-catenin degradation and selection of APC mutations in colorectal tumours from FAP patients." Oncogene **29**(11): 1663-1671.
- Komekado, H., H. Yamamoto, T. Chiba and A. Kikuchi (2007). "Glycosylation and palmitoylation of Wnt-3a are coupled to produce an active form of Wnt-3a." Genes Cells **12**(4): 521-534.
- Komiya, Y. and R. Habas (2008). "Wnt signal transduction pathways." Organogenesis **4**(2): 68-75.
- Komiya, Y., N. Mandrekar, A. Sato, I. B. Dawid and R. Habas (2014). "Custos controls beta-catenin to regulate head development during vertebrate embryogenesis." Proc Natl Acad Sci U S A **111**(36): 13099-13104.
- Korinek, V., N. Barker, P. Moerer, E. van Donselaar, G. Huls, P. J. Peters and H. Clevers (1998). "Depletion of epithelial stem-cell compartments in the small intestine of mice lacking Tcf-4." Nat Genet **19**(4): 379-383.
- Kurayoshi, M., H. Yamamoto, S. Izumi and A. Kikuchi (2007). "Post-translational palmitoylation and glycosylation of Wnt-5a are necessary for its signalling." Biochem J **402**(3): 515-523.
- Lawson, N. D. and S. A. Wolfe (2011). "Forward and reverse genetic approaches for the analysis of vertebrate development in the zebrafish." Dev Cell **21**(1): 48-64.
- Lee, E., A. Salic and M. W. Kirschner (2001). "Physiological regulation of [beta]-catenin stability by Tcf3 and CK1epsilon." J Cell Biol **154**(5): 983-993.

Li, L., H. Yuan, W. Xie, J. Mao, A. M. Caruso, A. McMahon, D. J. Sussman and D. Wu (1999). "Dishevelled proteins lead to two signaling pathways. Regulation of LEF-1 and c-Jun N-terminal kinase in mammalian cells." J Biol Chem **274**(1): 129-134.

Lijam, N., R. Paylor, M. P. McDonald, J. N. Crawley, C. X. Deng, K. Herrup, K. E. Stevens, G. Maccaferri, C. J. McBain, D. J. Sussman and A. Wynshaw-Boris (1997). "Social interaction and sensorimotor gating abnormalities in mice lacking Dvl1." Cell **90**(5): 895-905.

Lin, X. (2004). "Functions of heparan sulfate proteoglycans in cell signaling during development." Development **131**(24): 6009-6021.

Lintern, K. B., S. Guidato, A. Rowe, J. W. Saldanha and N. Itasaki (2009). "Characterization of wise protein and its molecular mechanism to interact with both Wnt and BMP signals." J Biol Chem **284**(34): 23159-23168.

Lu, W., V. Yamamoto, B. Ortega and D. Baltimore (2004). "Mammalian Ryk is a Wnt coreceptor required for stimulation of neurite outgrowth." Cell **119**(1): 97-108.

Lu, X., A. G. Borchers, C. Jolicœur, H. Rayburn, J. C. Baker and M. Tessier-Lavigne (2004). "PTK7/CCK-4 is a novel regulator of planar cell polarity in vertebrates." Nature **430**(6995): 93-98.

Luo, W. and S. C. Lin (2004). "Axin: a master scaffold for multiple signaling pathways." Neurosignals **13**(3): 99-113.

Makarova, K. S., D. H. Haft, R. Barrangou, S. J. Brouns, E. Charpentier, P. Horvath, S. Moineau, F. J. Mojica, Y. I. Wolf, A. F. Yakunin, J. van der Oost and E. V. Koonin (2011). "Evolution and classification of the CRISPR-Cas systems." Nat Rev Microbiol **9**(6): 467-477.

Makarova, K. S., Y. I. Wolf, O. S. Alkhnbashi, F. Costa, S. A. Shah, S. J. Saunders, R. Barrangou, S. J. Brouns, E. Charpentier, D. H. Haft, P. Horvath, S. Moineau, F. J. Mojica, R. M. Terns, M. P. Terns, M. F. White, A. F. Yakunin, R. A. Garrett, J. van der Oost, R.

- Backofen and E. V. Koonin (2015). "An updated evolutionary classification of CRISPR-Cas systems." Nat Rev Microbiol **13**(11): 722-736.
- Mandrekar, N. and N. L. Thakur (2009). "Significance of the zebrafish model in the discovery of bioactive molecules from nature." Biotechnol Lett **31**(2): 171-179.
- Mao, J., J. Wang, B. Liu, W. Pan, G. H. Farr, 3rd, C. Flynn, H. Yuan, S. Takada, D. Kimelman, L. Li and D. Wu (2001). "Low-density lipoprotein receptor-related protein-5 binds to Axin and regulates the canonical Wnt signaling pathway." Mol Cell **7**(4): 801-809.
- Marin, O., V. H. Bustos, L. Cesaro, F. Meggio, M. A. Pagano, M. Antonelli, C. C. Allende, L. A. Pinna and J. E. Allende (2003). "A noncanonical sequence phosphorylated by casein kinase 1 in beta-catenin may play a role in casein kinase 1 targeting of important signaling proteins." Proc Natl Acad Sci U S A **100**(18): 10193-10200.
- Marlow, F., J. Topczewski, D. Sepich and L. Solnica-Krezel (2002). "Zebrafish Rho kinase 2 acts downstream of Wnt11 to mediate cell polarity and effective convergence and extension movements." Curr Biol **12**(11): 876-884.
- McCartney, B. M. and I. S. Nathke (2008). "Cell regulation by the Apc protein Apc as master regulator of epithelia." Curr Opin Cell Biol **20**(2): 186-193.
- McMahon, A. P. and R. T. Moon (1989). "Ectopic expression of the proto-oncogene int-1 in *Xenopus* embryos leads to duplication of the embryonic axis." Cell **58**(6): 1075-1084.
- Melby, A. E., C. Beach, M. Mullins and D. Kimelman (2000). "Patterning the early zebrafish by the opposing actions of bozozok and vox/vent." Dev Biol **224**(2): 275-285.
- Moens, C. B., T. M. Donn, E. R. Wolf-Saxon and T. P. Ma (2008). "Reverse genetics in zebrafish by TILLING." Brief Funct Genomic Proteomic **7**(6): 454-459.

Mullins, M. C., M. Hammerschmidt, P. Haffter and C. Nusslein-Volhard (1994). "Large-scale mutagenesis in the zebrafish: in search of genes controlling development in a vertebrate." Curr Biol **4**(3): 189-202.

Nasevicius, A. and S. C. Ekker (2000). "Effective targeted gene 'knockdown' in zebrafish." Nat Genet **26**(2): 216-220.

Nishita, M., S. K. Yoo, A. Nomachi, S. Kani, N. Sougawa, Y. Ohta, S. Takada, A. Kikuchi and Y. Minami (2006). "Filopodia formation mediated by receptor tyrosine kinase Ror2 is required for Wnt5a-induced cell migration." J Cell Biol **175**(4): 555-562.

Nusse, R. (2015). "Cell signalling: Disarming Wnt." Nature **519**(7542): 163-164.

Nusse, R. and H. E. Varmus (1982). "Many tumors induced by the mouse mammary tumor virus contain a provirus integrated in the same region of the host genome." Cell **31**(1): 99-109.

Panakova, D., H. Sprong, E. Marois, C. Thiele and S. Eaton (2005). "Lipoprotein particles are required for Hedgehog and Wingless signalling." Nature **435**(7038): 58-65.

Peterson-Nedry, W., N. Erdeniz, S. Kremer, J. Yu, S. Baig-Lewis and M. Wehrli (2008). "Unexpectedly robust assembly of the Axin destruction complex regulates Wnt/Wg signaling in *Drosophila* as revealed by analysis in vivo." Dev Biol **320**(1): 226-241.

Pfeiffer, S., S. Ricardo, J. B. Manneville, C. Alexandre and J. P. Vincent (2002). "Producing cells retain and recycle Wingless in *Drosophila* embryos." Curr Biol **12**(11): 957-962.

Pinson, K. I., J. Brennan, S. Monkley, B. J. Avery and W. C. Skarnes (2000). "An LDL-receptor-related protein mediates Wnt signalling in mice." Nature **407**(6803): 535-538.

Port, F., G. Hausmann and K. Basler (2011). "A genome-wide RNA interference screen uncovers two p24 proteins as regulators of Wingless secretion." EMBO Rep **12**(11): 1144-1152.

Port, F., M. Kuster, P. Herr, E. Furger, C. Banziger, G. Hausmann and K. Basler (2008). "Wingless secretion promotes and requires retromer-dependent cycling of Wntless." Nat Cell Biol **10**(2): 178-185.

Prasad, B. C. and S. G. Clark (2006). "Wnt signaling establishes anteroposterior neuronal polarity and requires retromer in *C. elegans*." Development **133**(9): 1757-1766.

Rijsewijk, F., M. Schuermann, E. Wagenaar, P. Parren, D. Weigel and R. Nusse (1987). "The *Drosophila* homolog of the mouse mammary oncogene *int-1* is identical to the segment polarity gene *wingless*." Cell **50**(4): 649-657.

Sander, J. D. and J. K. Joung (2014). "CRISPR-Cas systems for editing, regulating and targeting genomes." Nat Biotechnol **32**(4): 347-355.

Sasai, N., Y. Nakazawa, T. Haraguchi and Y. Sasai (2004). "The neurotrophin-receptor-related protein NRH1 is essential for convergent extension movements." Nat Cell Biol **6**(8): 741-748.

Sato, T., J. H. van Es, H. J. Snippert, D. E. Stange, R. G. Vries, M. van den Born, N. Barker, N. F. Shroyer, M. van de Wetering and H. Clevers (2011). "Paneth cells constitute the niche for Lgr5 stem cells in intestinal crypts." Nature **469**(7330): 415-418.

Schier, A. F. and W. S. Talbot (2005). "Molecular genetics of axis formation in zebrafish." Annu Rev Genet **39**: 561-613.

Schneider, S., H. Steinbeisser, R. M. Warga and P. Hausen (1996). "Beta-catenin translocation into nuclei demarcates the dorsalizing centers in frog and fish embryos." Mech Dev **57**(2): 191-198.

- Schohl, A. and F. Fagotto (2003). "A role for maternal beta-catenin in early mesoderm induction in *Xenopus*." EMBO J **22**(13): 3303-3313.
- Schulte-Merker, S., K. J. Lee, A. P. McMahon and M. Hammerschmidt (1997). "The zebrafish organizer requires chordin." Nature **387**(6636): 862-863.
- Schwarz-Romond, T., M. Fiedler, N. Shibata, P. J. Butler, A. Kikuchi, Y. Higuchi and M. Bienz (2007). "The DIX domain of Dishevelled confers Wnt signaling by dynamic polymerization." Nat Struct Mol Biol **14**(6): 484-492.
- Seifert, J. R. and M. Mlodzik (2007). "Frizzled/PCP signalling: a conserved mechanism regulating cell polarity and directed motility." Nat Rev Genet **8**(2): 126-138.
- Semenov, M. V., R. Habas, B. T. Macdonald and X. He (2007). "SnapShot: Noncanonical Wnt Signaling Pathways." Cell **131**(7): 1378.
- Shigetani, Y., S. Howard, S. Guidato, K. Furushima, T. Abe and N. Itasaki (2008). "Wise promotes coalescence of cells of neural crest and placode origins in the trigeminal region during head development." Dev Biol **319**(2): 346-358.
- Slusarski, D. C. and F. Pelegri (2007). "Calcium signaling in vertebrate embryonic patterning and morphogenesis." Dev Biol **307**(1): 1-13.
- Slusarski, D. C., J. Yang-Snyder, W. B. Busa and R. T. Moon (1997). "Modulation of embryonic intracellular Ca²⁺ signaling by Wnt-5A." Dev Biol **182**(1): 114-120.
- Sobrado, P., A. Jedlicki, V. H. Bustos, C. C. Allende and J. E. Allende (2005). "Basic region of residues 228-231 of protein kinase CK1alpha is involved in its interaction with axin: binding to axin does not affect the kinase activity." J Cell Biochem **94**(2): 217-224.

Stachel, S. E., D. J. Grunwald and P. Z. Myers (1993). "Lithium perturbation and gooseoid expression identify a dorsal specification pathway in the pregastrula zebrafish." Development **117**(4): 1261-1274.

Stamos, J. L. and W. I. Weis (2013). "The beta-catenin destruction complex." Cold Spring Harb Perspect Biol **5**(1): a007898.

Strutt, D. I. (2001). "Asymmetric localization of frizzled and the establishment of cell polarity in the Drosophila wing." Mol Cell **7**(2): 367-375.

Tada, M. and C. P. Heisenberg (2012). "Convergent extension: using collective cell migration and cell intercalation to shape embryos." Development **139**(21): 3897-3904.

Tahinci, E., C. A. Thorne, J. L. Franklin, A. Salic, K. M. Christian, L. A. Lee, R. J. Coffey and E. Lee (2007). "Lrp6 is required for convergent extension during Xenopus gastrulation." Development **134**(22): 4095-4106.

Tamai, K., X. Zeng, C. Liu, X. Zhang, Y. Harada, Z. Chang and X. He (2004). "A mechanism for Wnt coreceptor activation." Mol Cell **13**(1): 149-156.

Tanaka, K., Y. Kitagawa and T. Kadowaki (2002). "Drosophila segment polarity gene product porcupine stimulates the posttranslational N-glycosylation of wingless in the endoplasmic reticulum." J Biol Chem **277**(15): 12816-12823.

Teran, E., A. D. Branscomb and J. M. Seeling (2009). "Dpr Acts as a molecular switch, inhibiting Wnt signaling when unphosphorylated, but promoting Wnt signaling when phosphorylated by casein kinase Idelta/epsilon." PLoS One **4**(5): e5522.

Theisen, H., J. Purcell, M. Bennett, D. Kansagara, A. Syed and J. L. Marsh (1994). "dishevelled is required during wingless signaling to establish both cell polarity and cell identity." Development **120**(2): 347-360.

Tolwinski, N. S., M. Wehrli, A. Rives, N. Erdeniz, S. DiNardo and E. Wieschaus (2003). "Wg/Wnt signal can be transmitted through arrow/LRP5,6 and Axin independently of Zw3/Gsk3beta activity." Dev Cell **4**(3): 407-418.

Toomes, C., H. M. Bottomley, R. M. Jackson, K. V. Towns, S. Scott, D. A. Mackey, J. E. Craig, L. Jiang, Z. Yang, R. Trembath, G. Woodruff, C. Y. Gregory-Evans, K. Gregory-Evans, M. J. Parker, G. C. Black, L. M. Downey, K. Zhang and C. F. Inglehearn (2004). "Mutations in LRP5 or FZD4 underlie the common familial exudative vitreoretinopathy locus on chromosome 11q." Am J Hum Genet **74**(4): 721-730.

Tree, D. R., J. M. Shulman, R. Rousset, M. P. Scott, D. Gubb and J. D. Axelrod (2002). "Prickle mediates feedback amplification to generate asymmetric planar cell polarity signaling." Cell **109**(3): 371-381.

van Amerongen, R. and R. Nusse (2009). "Towards an integrated view of Wnt signaling in development." Development **136**(19): 3205-3214.

van Impel, A., Z. Zhao, D. M. Hermkens, M. G. Roukens, J. C. Fischer, J. Peterson-Maduro, H. Duckers, E. A. Ober, P. W. Ingham and S. Schulte-Merker (2014). "Divergence of zebrafish and mouse lymphatic cell fate specification pathways." Development **141**(6): 1228-1238.

Wallingford, J. B., S. E. Fraser and R. M. Harland (2002). "Convergent extension: the molecular control of polarized cell movement during embryonic development." Dev Cell **2**(6): 695-706.

Wallingford, J. B. and R. Habas (2005). "The developmental biology of Dishevelled: an enigmatic protein governing cell fate and cell polarity." Development **132**(20): 4421-4436.

Wang, Y., D. Huso, H. Cahill, D. Ryugo and J. Nathans (2001). "Progressive cerebellar, auditory, and esophageal dysfunction caused by targeted disruption of the frizzled-4 gene." J Neurosci **21**(13): 4761-4771.

- Weng, W. and D. L. Stemple (2003). "Nodal signaling and vertebrate germ layer formation." Birth Defects Res C Embryo Today **69**(4): 325-332.
- Weyer, C. J., P. D. Nieuwkoop and A. Lindenmayer (1977). "A diffusion model for mesoderm induction in amphibian embryos." Acta Biotheor **26**(3): 164-180.
- Wharton, K. A., Jr. (2003). "Runnin' with the Dvl: proteins that associate with Dsh/Dvl and their significance to Wnt signal transduction." Dev Biol **253**(1): 1-17.
- Willert, K., J. D. Brown, E. Danenberg, A. W. Duncan, I. L. Weissman, T. Reya, J. R. Yates, 3rd and R. Nusse (2003). "Wnt proteins are lipid-modified and can act as stem cell growth factors." Nature **423**(6938): 448-452.
- Willert, K. and K. A. Jones (2006). "Wnt signaling: is the party in the nucleus?" Genes Dev **20**(11): 1394-1404.
- Winklbauer, R. and O. Luu (2008). "Frizzled-7-dependent tissue separation in the *Xenopus* gastrula." Methods Mol Biol **469**: 485-492.
- Winklbauer, R., A. Medina, R. K. Swain and H. Steinbeisser (2001). "Frizzled-7 signalling controls tissue separation during *Xenopus* gastrulation." Nature **413**(6858): 856-860.
- Wong, H. C., A. Bourdelas, A. Krauss, H. J. Lee, Y. Shao, D. Wu, M. Mlodzik, D. L. Shi and J. Zheng (2003). "Direct binding of the PDZ domain of Dishevelled to a conserved internal sequence in the C-terminal region of Frizzled." Mol Cell **12**(5): 1251-1260.
- Wong, L. L. and P. N. Adler (1993). "Tissue polarity genes of *Drosophila* regulate the subcellular location for prehair initiation in pupal wing cells." J Cell Biol **123**(1): 209-221.

- Wu, J., T. J. Klein and M. Mlodzik (2004). "Subcellular localization of frizzled receptors, mediated by their cytoplasmic tails, regulates signaling pathway specificity." PLoS Biol **2**(7): E158.
- Yamaguchi, T. P. (2001). "Heads or tails: Wnts and anterior-posterior patterning." Curr Biol **11**(17): R713-724.
- Yang, P. T., M. J. Lorenowicz, M. Silhankova, D. Y. Coudreuse, M. C. Betist and H. C. Korswagen (2008). "Wnt signaling requires retromer-dependent recycling of MIG-14/Wntless in Wnt-producing cells." Dev Cell **14**(1): 140-147.
- Yang-Snyder, J., J. R. Miller, J. D. Brown, C. J. Lai and R. T. Moon (1996). "A frizzled homolog functions in a vertebrate Wnt signaling pathway." Curr Biol **6**(10): 1302-1306.
- Yost, C., M. Torres, J. R. Miller, E. Huang, D. Kimelman and R. T. Moon (1996). "The axis-inducing activity, stability, and subcellular distribution of beta-catenin is regulated in *Xenopus* embryos by glycogen synthase kinase 3." Genes Dev **10**(12): 1443-1454.
- Zeng, X., H. Huang, K. Tamai, X. Zhang, Y. Harada, C. Yokota, K. Almeida, J. Wang, B. Doble, J. Woodgett, A. Wynshaw-Boris, J. C. Hsieh and X. He (2008). "Initiation of Wnt signaling: control of Wnt coreceptor Lrp6 phosphorylation/activation via frizzled, dishevelled and axin functions." Development **135**(2): 367-375.
- Zhai, L., D. Chaturvedi and S. Cumberledge (2004). "Drosophila wnt-1 undergoes a hydrophobic modification and is targeted to lipid rafts, a process that requires porcupine." J Biol Chem **279**(32): 33220-33227.
- Zhang, J., D. W. Houston, M. L. King, C. Payne, C. Wylie and J. Heasman (1998). "The role of maternal VegT in establishing the primary germ layers in *Xenopus* embryos." Cell **94**(4): 515-524.